Evolution of and processes acting on inner continental shelf areas, resolved with hydroacoustic and sedimentological methods: Case studies from the Baltic Sea and the Andaman Sea

Dissertation
zur Erlangung des Doktorgrades
der Mathematisch-Naturwissenschaftlichen Fakultät
der Christian-Albrechts Universität
Kiel

vorgelegt von
Peter Feldens

Kiel, 2011

Referent:	Prof. Dr. Karl Stattegger
Koreferent:	Prof. Dr. Sebastian Krastel-Gudegast

Tag der mündlichen Prüfung:	29.06.2011
Zum Druck genehmigt:	30.06.2011

gez. Prof. Dr. Lutz Kipp, Dekan

Ich versichere an Eides statt, dass:

1) Ich bis zum heutigen Tage weder an der Christian-Albrechts-Universität zu Kiel noch an einer anderen Hochschule ein Promotionsverfahren endgültig nicht bestanden habe oder mich in einem entsprechenden Verfahren befinde oder befunden habe.
2) Ich die Inanspruchnahme fremder Hilfen aufgeführt habe, sowie, dass ich die wörtlich oder inhaltlich aus anderen Quellen entnommenen Stellen als solche gekennzeichnet habe.
3) Die Arbeit unter Einhaltung der Regeln guter wissenschaftlicher Praxis der Deutschen Forschungsgemeinschaft entstanden ist.

Kiel, Unterschrift:

Abstract

Shallow seas are influenced by a magnitude of processes, acting on- and offshore. Therefore, most shallow sea areas have a unique appearance, preserving information both about their geologic history and processes acting on them. For this study, extensive hydroacoustic surveys, including side scan sonar, multibeam echo sounder, and reflection seismic, as well as sedimentological analysis were carried out in the Fehmarn Belt (SW Baltic Sea) and offshore Khao Lak (Andaman Sea, Thailand) between 2007 and 2011. The geologic evolution since the last glacial as well as recent sediment dynamics were investigated in Fehmarn Belt, while offshore impacts of the 2004 Indian Ocean Tsunami where evaluated off Khao Lak.

The development of the Baltic Sea since the last glacial period was controlled by several regression and transgression events during the phases Baltic Ice Lake, Yoldia Sea, Ancylus Lake and Littorina Sea. Many details regarding the development of these stages are unsolved, one question being whether, and to what extent, the regression of the Ancylus Lake at 9,200 to 9,000 ^{14}C yr BP took place over the Darss Sill. Next to the general geological evolution of Fehmarn Belt since the last glacial, this study addresses the question whether a drowned river system in Fehmarn Belt (SW Baltic Sea) can be related to the drainage of the Ancylus Lake. The river channel is cut into glacial till in the western Fehmarn Belt, reaching an incision depth of up to 12 m at a base level of 40 m b.s.l. (below sea level). Its continuation towards west can be recognized in bathymetric data, while the channel is buried towards Mecklenburg Bay. According to seismic images, it is rapidly widening from several hundred meters to more than 1 kilometre and seems to fade towards east. Sediment thickness above the glacial till can exceed 30 m in the buried section of the channel. It is proposed that the channel was mainly shaped as part of a glacial meltwater system at a water level of 30 m b.s.l., although it was eventually incised subglacially. During the lowstand of the Baltic Ice Lake, local, shallow water bodies covered the study area and calm conditions prevailed. A previously reported westward directed drainage of a lake in the eastern Fehmarn Belt could be restricted to a time interval following the highstand of the Ancylus Lake, and prior to the Littorina transgression. Timing, water level and potential water discharge of this event suggest its connection to the partial drainage of the Ancylus Lake over the Darss Sill. Subsequently to the regression, cliffs and lake deposits point to a local water level between 24 to 26 m b.s.l. However, finding of a channel system filled with sediment deposited during the early Littorina Transgression might indicate a short phase with a water level down to 30 m b.s.l. With rising water level during the Littorina transgression, a large subaqueous dune field was formed in the central Fehmarn Belt. It is situated in water depths between 11 and 25 m, with an extension of about 8.1 km E – W and 1.8 km N - S. It consists of asymmetric dunes, indicating a W to E directed current, with crest heights of up to 2.5 m. The dunes are composed of allochthonous, well-sorted medium to coarse sand. Sand ribbons, connected to the subaqueous dune-field and protruding towards the southwest, are supposed to be sediment-conduits. Only minor movements of the field over the annual cycle could be observed, but comparisons with older maps show an increase in spatial extension over the course of decades. It is assumed that sediment movements in the subaqueous dune field occur mainly during west-storm conditions, when salt water infrequently intrudes from the North Sea into the Baltic Sea.

The aim of the second case study was to resolve impact of the 2004 Indian Ocean Tsunami on offshore areas. The coastal area of Khao Lak (Thailand) was heavily damaged by the 2004 Indian Ocean tsunami. Meanwhile, its impact on offshore areas is mostly unknown, although offshore tsunami deposits were speculated to be widespread in the geological record. The 2004 tsunami offered the unique opportunity to catalogue its offshore effects from a well-recorded series of events. In Thailand, reported onshore tsunami deposits, containing marine

sediments, as well as satellite images, showing large amounts of sediment transported offshore, indicate that the seafloor was impacted by tsunami run-up and backwash. Offshore Khao Lak, paleoreefs with associated boulder fields and sandy sediments dominate the inner continental shelf. Patches of fine-grained (silt to fine sand) sediments exist in water depths of less than 15 m. The sediment distribution pattern is stable between 2007 and 2010, apart from small shifts regarding the boundaries of the fine-grained sediment patches. In sediment cores and grab samples an event layer was documented, situated below a cover of modern sediments that is only a few cm thick. The event-layer can be securely traced down to 18 m water depth. It consists mostly of sand, including coral fragments, but contains compounds of terrigenous origin as well. It is interpreted as a 2004 Indian Ocean tsunami deposit, which was the last major event in the area. Beneath 18 m water depth, indications of potential tsunami influence on a system of sand ridges are found, including erosion of app. 1 m deep channels at the NW-flank of the sand ridges and the deposition of silty material sandwiched by sandy sediments. On wide areas of the study-site an impact of the tsunami is hardly identifiable by seafloor morphology or sediment distribution five year after the event, pointing towards a tsunami impact focussed to some areas and a rapid return of the seafloor to equilibrium conditions.

Zusammenfassung

Flache Bereiche von Schelfmeeren werden von einer Vielzahl von Faktoren geformt. Ihr gegenwärtiges Erscheinungsbild ist daher meist einzigartig, und erhält Informationen über die geologische Geschichte sowie über einwirkende Prozesse. Diese Arbeit präsentiert die Ergebnisse umfangreicher hydroakustischer (Seitensichtsonar, Fächerecholot, seismische Messmethoden) und sedimentologischer Untersuchungen in zwei Arbeitsgebieten, gelegen im Fehmarn Belt (SW Ostsee, Deutschland) und seewärts von Khao Lak (Andaman See, Thailand). Die geologische Entwicklung seit dem letzten Glazial sowie die rezente Sedimentdynamik sind Schwerpunkte der Arbeit im Fehmarn Belt. Im Arbeitsgebiet vor Thailand liegt der Fokus auf der Identifikation von Sediment- und morphologischen Strukturen, die durch einen Tsunami, der am 26.12.2004 die Küsten entlang des Indischen Ozeans traf, entstanden sind.

Die geologische Entwicklung im Bereich des Fehmarn Belt sowie der östlich anschließenden Mecklenburger Bucht wurde seit dem letzten Glazial durch starke Schwankungen des Wasserspiegels im Rahmen der Entwicklung der heutigen Ostsee durch die Phasen des Baltischen Eistausees, des Yoldia Meeres, des Ancylus Sees und der Littorina Meeres geprägt. Sowohl Fehmarn Belt als auch Mecklenburger Bucht sind vom Hauptteil des Ostseeraumes durch Schwellen isoliert, die einen Wassertausch unterhalb eines Niveaus von 24 Metern seit dem letzten Glazial verhindert haben. Im westlichen Fehmarn Belt ist ein ertrunkener Flusslauf bis zu 12 Meter tief in glaziale Ablagerungen eingeschnitten. Die heutige Basis des Flusslaufes liegt maximal 42 Meter unterhalb des Meeresspiegels. Die Fortsetzung des Flusslaufes nach Westen ist in bathymetrischen Karten deutlich erkennbar, wogegen er nach Osten, Richtung Mecklenburger Bucht, mit Sediment verfüllt ist. Anhand von seismischen Aufnahmen lässt sich zeigen, dass die Breite des verfüllten Flusslaufes von wenigen hundert Metern auf mehr als einen Kilometer im zentralen Teil des Fehmarn Belt zunimmt, und er dort auszulaufen scheint. Die Sedimentmächtigkeit über den glazialen Sedimenten im verfüllten Abschnitt des Flusslaufes beträgt maximal etwa 30 Meter. Der Flusslauf war Bestandteil eines glazialen Entwässerungssystems, mit einem Wasserstand von etwa 30 Metern unter dem heutigen Meeresspiegel. Auf Grund des auf kurzer Distanz stark wechselnden morphologischen Erscheinungsbildes lässt sich vermuten, dass der Flusslauf ursprünglich subglazial angelegt und später reaktiviert wurde. Während beider Tiefstände des

Baltischen Eistausees war der westliche Fehmarn Belt Teil einer lokalen Seenlandschaft. Eine bereits beschriebene ausgeprägte Regression eines Sees im östlichen Fehmarn Belt konnte auf den Zeitraum zwischen dem Hochstand des Ancylus-Sees und dem Beginn der Littorina-Transgression eingegrenzt werden. Der Zeitraum, der Wasserstand nach der Regression sowie das berechnete Durchflussvolumen legen nahe, dass diese Regression kein lokales Ereignis war, sondern mit der partiellen Regression des Ancylus-Sees hinter der Darßer Schwelle in Verbindung stand. Fossile Kliffs und im lakustrinen Milieu abgelagerte Sedimente weisen auf einen Wasserstand zwischen 24 und 26 m unterhalb des heutigen Meeresspiegels im Anschluss an diese Regression hin, auch wenn ein kurzfristig niedrigerer Wasserstand um 30 m nicht ausgeschlossen werden kann. Während der anschließenden Littorina-Transgression bildete sich ein in Ost-West Richtung 8.1 km ausgedehntes Riesenrippelfeld zwischen 11 und 25 Meter Wassertiefe im zentralen Bereich des Fehmarn Belt. Die asymmetrischen Strömungsrippeln zeigen eine West-Ost gerichtete Strömung an und haben ein Kammhöhe von bis zu 2.5 Metern. Sie bestehen aus allochthonen Mittel- bis Grobsanden. Der Sedimenttransport in das Rippelfeld erfolgt vermutlich über Sandbänder, die aus dem Feld zu einer Abrasionplattform westlich von Fehmarn reichen. Während nur minimale Bewegung der Riesenrippeln über einen Jahreszyklus festzustellen waren, zeigt der Vergleich mit älteren Aufnahmen deutlich eine Ausdehnung des Feldes über den Zeitraum von Jahrzehnten. Die Bewegungen des Feldes hängen vermutlich mit unregelmäßig auftretenden Salzwassereinbrüchen aus der Nordsee in die Ostsee zusammen, die entlang der Südseite des Fehmarn Belt strömen.

Vor den Küsten von Thailand lag der Schwerpunkt der Arbeit auf der Identifikation von Einwirkungen des Tsunami von 2004 auf den Flachwasserbereich. Die Küsten von Khao Lak gehörten dabei zu den am schwersten betroffenen Gebieten. Der Einfluss von Tsunami auf den Meeresboden ist allerdings weitgehend unverstanden, obwohl vermutet wurde, dass Paläo-Tsunamis in der geologischen Vergangenheit großen Einfluss auf Schelfbereiche hatten. Der Tsunami von 2004 ermöglichte es, dessen Auswirkungen auf den Meeresboden gezielt zu untersuchen. Marine Komponenten, die in Tsunamiablagerungen an Land gefunden wurden sowie Satellitenaufnahmen, die deutlich den seewärtigen Transport von Sediment zeigen, weisen auf einen Beeinflussung des Meeresbodens vor Thailand durch die auflaufende und ablaufende Tsunamiwelle hin. Der Meeresboden seewärts von Khao Lak wird durch eine ertrunkene Riffplattform und daran anschließende ausgedehnte Sandflächen geprägt. In lokal scharf abgegrenzten Gebieten findet sich feinkörnigeres, siltig bis maximal feinsandiges Sediment bis in eine Wassertiefe von 15 m. Die großräumige Sedimentverteilung war während des Untersuchungszeitraumes zwischen 2007 und 2010 stabil, allerdings wurden kleinräumige Verschiebungen der Sedimentgrenzen des siltig-feinsandigen Meeresbodens beobachtet. In verschiedenen Sedimentkernen und Greiferproben konnte eine Event-Lage nachgewiesen werden, die aus überwiegend sandigem Sediment besteht, terrigene Bestandteile enthält und von einer wenige Zentimeter mächtigen Sedimentschicht bedeckt ist, die nach 2004 abgelagert worden ist. Diese Event-Lage wird als Ablagerung des Tsunami von 2004 interpretiert und kann bis in eine Wassertiefe von 18 m nachgewiesen werden. In Wassertiefen unterhalb von 18 m finden sich Hinweise auf die Beeinflussung eines Sandrückensystem durch den Tsunami. Sowohl etwa 1 Meter tief erodierte Kanäle als auch Ablagerungen von überwiegend siltigem Material zwischen Sandlagen könnten auf den Tsunami von 2004 zurückzuführen sein; dies lässt sich mit den vorhandenen Daten allerdings nicht zweifelsfrei nachweisen. Über weite Teile des Untersuchungsgebietes lassen sich keine Sedimente oder morphologische Strukturen nachweisen, die auf den Tsunami von 2004 zurückzuführen sind. Dies deutet sowohl auf einen örtlich begrenzten Einfluss des Tsunami im Untersuchungsgebiet, als auch auf eine schnelle Regeneration des Meeresbodens nach einem Tsunami hin.

Table of Content

Chapter I
General Introduction

The importance of shallow coastal seas is without doubt increasing, especially in densely populated coastal areas. This includes their importance as a resource, e.g. for mining, energy production (e.g. windparks), fishery and aquaculture, as well as their conservation by the designation of protected areas. On the other hand, the increasing population density in the coastal zone goes along with a growing vulnerability against extreme events like heavy storms and tsunamis, such as the 2004 Indian Ocean Tsunami, or the tsunami that struck Japan in 2011.

Besides anthropogenic impacts, shallow seas – here including both continental shelf seas and intracontinental water bodies (e.g. the Baltic Sea) – are influenced by a multitude of natural processes, acting on different time scales. The overall geometry of continental shelf seas is driven by long term processes, such as plate movements and mountain building processes (Nittrouer 2007). Today, their appearance has been further shaped by the change of sea level, especially since the last glaciation. The glaciation was also the dominant process responsible for the formation of intracontintenal water bodies in high latitudes, such as the Baltic Sea or the North-American Great Lakes (Björck 1995, Larson and Schaetzl 2001). Besides continuous processes like wave action over the annual cycle, especially short term events such as heavy storms or tsunamis have a major impact on the continental shelf (Einsele et al. 1994), which is in particular the case in shallow waters. The setting of onshore areas has also a strong impact on the appearance of the adjacent continental shelf sea. Notable examples are the formation of deltas in areas with strong fluvial sediment discharge, but also flooding events of small, local rivers, observed for example during monsoonal phases in low latitudes have profound effects on the shelf.

Due to the magnitude of different processes, shallow water areas are complex systems, and most inner shelf areas are unique and cannot be easily compared. However, in every shallow sea, the sediments deposited on the seafloor as well as morphological features are a rich source of information about past and present processes and events. Furthermore, they preserve information about recent anthropogenic impact.

Basic geologic data – among other data - are necessary to make informed decisions about sustainable use of the shallow sea areas. A combination of different approaches is generally used to derive the necessary data. Highly sophisticated models give insights on individual processes, but the combination of different models in order to explain the complex shallow sea system is still under development (Syvitski et al. 2007). Models also form the foundation for planning of mitigation efforts against natural disasters. However, modelling efforts have to be necessarily combined with detailed case studies. Case studies provide knowledge on the impact of individual processes, deliver highly important information about recurrence rates of events, provide a data-base for general validation of models and give information about regional geology as well as geologic evolution.

In this thesis, two case studies from two wave-dominated shallow sea settings are presented. The first is dealing with the Baltic Sea, a semi-enclosed intracontinental sea (Bobertz and Harff 2004). The case study is concerned with the complex geologic evolution of the Baltic Sea. The focus is laid on the development of the Fehmarn Belt and Mecklenburg Bay area during the Baltic Ice Lake and Ancylus Lake phases, which is under heavy debate since decades (e.g. Björck et al. 2008). Additionally, information about sediment dynamics over the last decades in an area north of the island Fehmarn is given (chapter III).

The second case study aims to identify offshore deposits of the 2004 Indian Ocean Tsunami, and to identify their preservation potential. Offshore effects of tsunami are poorly understood, especially compared to onshore influences. Well-described modern offshore tsunami deposits of unquestionable origin would be of great use in the search for offshore deposits of paleo-tsunamis, which might comprise a large percentage of the preserved tsunami record (Dawson and Stewart 2007). The chosen study site is situated in the Andaman Sea off Thailand, heavily damaged during the 2004 Indian Ocean Tsunami (Siripong 2006). Additionally, insights on anthropogenic impacts and the geological built-up of this previously poorly investigated area were obtained during the efforts to identify the offshore tsunami impacts (chapter IV).

A combination of hydroacoustic and sedimentological methods was used in this study in order to achieve the aims. The fundamental principles of those methods are described in chapter II. Hydroacoustic methods, specifically side scan sonar and multibeam echo sounder measurements, deliver full-coverage information about local bathymetry and sediment properties, while repeated measurements give information about local sediment dynamics. Seismic systems give information on the built-up of the shallow subsurface structure. Based on such data, surface sediment samples and sediment cores can be specifically retrieved even from small-scale seafloor features. While all these methods have been available for several decades, only the advances of computing power and GIS-technology over the last ten years allowed for the combined use of high-resolution datasets over large areas.

Chapter II
Methods

1. Hydroacoustic methods

1.1 Side Scan Sonar

Side Scan sonar systems saw their first military use during World War II for object detection on the sea floor (Jones 1999), although their development in Great Britain already started in the 1920's (Fish and Carr 2001). Since the 1950's the system developed into a valuable tool for civilian purposes, including the marine geosciences.

Side scan sonar use acoustic signals to create representative images of the seafloor. It comprises a work station, power supply, and normally two transducers towed behind a ship above the seafloor, each capable of sending and receiving acoustic signals. The transducers insonify an area of the seafloor perpendicular to the tow direction, with narrow horizontal directivity and wide vertical directivity (Lurton 2002), and record the intensity and travel time of return signals backscattered from the seafloor (Fig. 1). The intensity of the backscattered signal is dependent on different factors: Primarily, it is related to physical properties of the sediment forming the seafloor surface, including grain size distribution and roughness in the scale of the used wavelength (Blondel 2009). Additionally, the inclination of small-scale morphology to the side scan sonar towfish is important. If the morphology is inclined towards the towfish, return signal strength increases, if the morphology is inclined away from the towfish, it decreases. This allows for the easy identification of e.g. ripple structures. Objects elevated from the seafloor (boulders or artificial objects) are easily identified, as an acoustic shadow is forming behind them. Steep depressions can also cause an acoustic shadow. Objects in the water column (e.g. fish swarms) return parts of the emitted signal, and are visible in the resulting side scan sonar image (Fig. 1).

Typically, side scan sonar systems used on continental shelf areas utilize frequencies of one hundred to several hundred kHz. Their maximal range is limited due to the continuous absorption of the signal, which eventually leads to background noise intensity exceeding the intensity of the backscattered signal.

The maximum resolution (ability to resolve two distinct objects) in the across-track direction depends on the footprint of the signal pulse on the seafloor. Generally, higher frequency sonar systems employ shorter pulse durations - typically around 0.1 ms for 100 kHz continuous wave systems (Fish and Carr 2001) - and therefore produce higher resolution images. This comes at the cost of reduced range due to higher absorption of the acoustic signal. Generally, the footprint size is at maximum close to the nadir, beneath the side scan sonar towfish, therefore across-track resolution is poor here. With increasing distance from the towfish, the acoustic signal approaches grazing angles (i.e. becomes increasingly oblique to the seafloor), and across track resolution increases.

Quantitatively, the maximal resolution in the across-track direction is (Jones 1999):

$$R_x = \frac{cT}{2 \sin \theta}$$

with: R_x across track resolution, c sound velocity, T pulse duration, θ grazing angle.

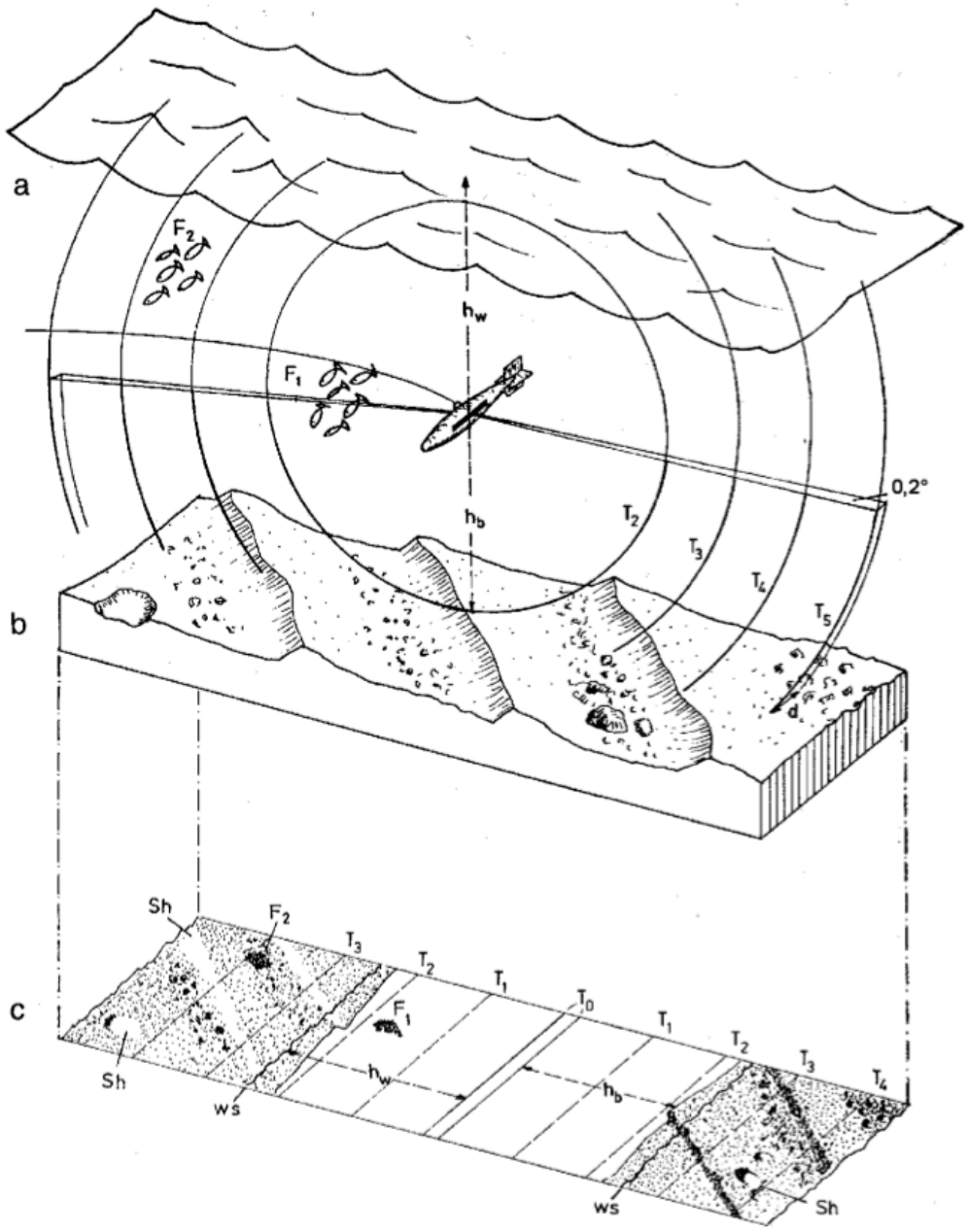

Fig. 1: Working principle of a side scan sonar system. Two transducers on a deep-towed towfish insonify a narrow stripe of the seafloor. The intensity of the backscattered signal depends on the characteristics of the sediments at the seafloor surface, as well as small-scale morphology. a: water surface. b: seafloor c: resulting side scan sonar image, strong backscatter is displayed in darker colours. T_0: Start time of the acoustic signal. T_1 to T_5: Position of the signal at different time slices (top) and the resulting image based on backscattered signals (bottom). S_h: Acoustic shadow due to stones, ripples, or depressions. F_1 and F_2: Fish swarm. h_w: Tow depth of the transducers. h_b: Height above ground. w_s: Reflection of the Water surface. Source: Newton et al. (1973).

Obviously, low grazing angles are avoided during side scan sonar operations, and form the main reason why these systems are towed closely above the seafloor. If the grazing angle is 0, i.e. the acoustic pulse is approaching the seafloor vertically, the resolution of a side scan sonar is equal to the horizontal resolution of sediment echo sounders (see section 1.3).

Given a typical 100 kHz system with a 0.1 ms pulse duration (therefore including 10 wavelengths) and an assumed sound velocity of 1500 m/s, the resolution at a grazing angle of $\pi/2$ would be in the order of 10 cm.

Along track resolution (R_y) depends on the spreading of the acoustic beam with increasing distance from the towfish. It is therefore approximated with the aperture of the horizontal directivity (β) of the side scan sonar transducers multiplied with the distance from the towfish (d); therefore: $R_y = \beta d$ (Jones 1999).

In contrast to across track-resolution, along track resolution decreases with increasing distance from the towfish. It should be further noted that these formulae is only valid for the resolution of a single ping. A further, major factor contributing to the along-track resolution of final side scans sonar mosaics is the distance between two pings, depending on the pings per second rate (pps), and the towing velocity.

The need for short pulse durations to achieve high spatial resolution is a major restriction, as the energy which can be released into the water in a given amount of time is limited, e.g. by design limitations of the transducers or by cavitation effects (Fish and Carr 2001). If a larger range is required, a longer pulse duration is needed, yielding a limited resolution. To resolve this problem, a comparably new technique was developed. Newer generations of side scan sonar systems emit a longer pulse with a constantly increasing frequency – hence, these system are called "chirp" sonars. The longer pulse duration leads to higher ranges, and more resistance against noise. A typical pulse duration for a 100 kHz sonar would be in the order of 10 ms (Fish and Carr 2001). Maximal across-track resolution is not affected by the longer pulse duration: upon receiving, the pulse is compressed according to frequency. For across track resolution, the effective pulse length equals the inverse of the used bandwidth. Most data shown in this study was collected with side scan sonar system using the chirp technology.

Side scan sonar data processing is a further, wide topic, which is for example summarized by Blondel (2009). The processing of data gathered for this work included:

1. Correction of changes in backscatter intensity (transmission loss) caused by geometric spreading of the acoustic signal and its continuous absorption in the water.
2. Correction of geometric distortions and inaccuracies. These especially include:
    a. Correction of the slant-range distortion. This distortion exists because side scan sonar systems measure the travel time of the acoustic signal to a given object. In uncorrected images, the length of an object equals the travel time difference between its start and end, not its actual distance on the seafloor. Therefore, targets close to the side scan sonar nadir appear compressed.
    b. Correction against changing towing velocity.
    c. Correction for the distance between the GPS antennae used to obtain navigation information, and the towfish behind the vessel (layback).
3. Corrections of the side scan sonar beam pattern, as the transducer directivity pattern is not necessarily identically at all angles.
4. Creation of mosaics by plotting several side scan sonar profiles on one map.

Systems used during this work included a Klein 595 side scan sonar with digital data acquisition (app. 400 kHz), a Benthos 1624 dual-frequency side scan sonar (chirp system, bandwidth around 100 and 400 kHz), and Teledyne-Benthos C3D system (chirp system, bandwidth around 200 kHz).

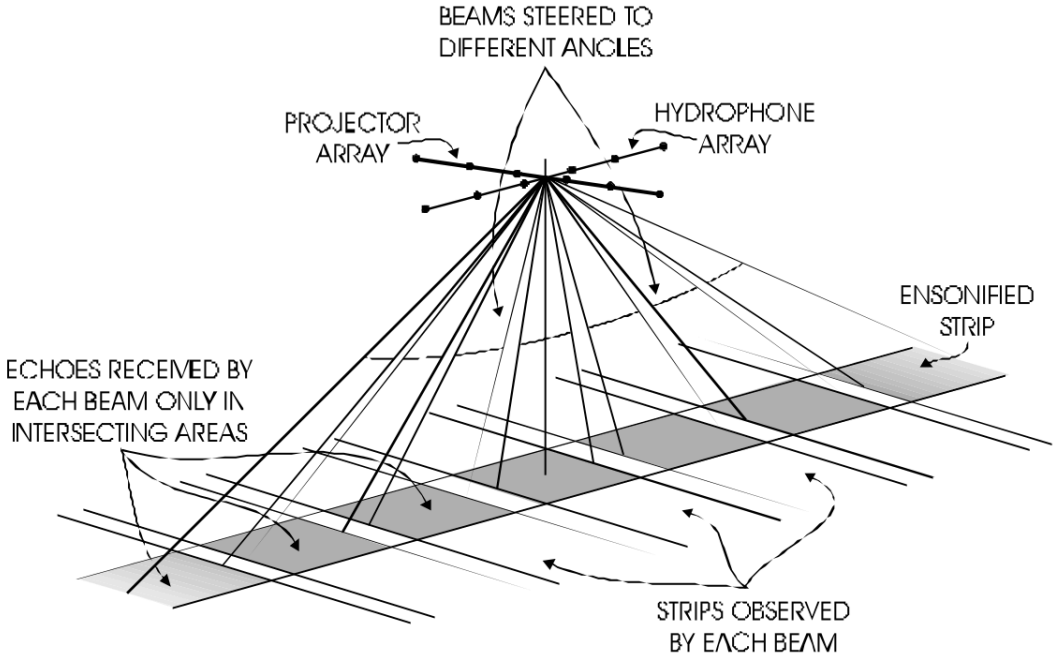

Fig. 2:. Principle of the Mills Cross. Perpendicular projection and hydrophone arrays, with perpendicular directivities, allow to receive return signals from a narrow intersecting area. See text. Source of image: Multibeam Sonar – Theory of Operation. © L-3 Communications SeaBeam Instruments. Used with permission.

1.2 Multibeam Echo sounder

A basic assumption of traditional side scan sonar systems is the flat earth assumption, i.e. the assumption that no morphology is present at the seafloor. Although some side scan sonar system offer the determination of bathymetry (Lurton 2002), the multibeam echo sounder remains the most widespread method to measure seafloor bathymetry. It is also used in this work.

Principally, multibeam echo sounders, under development since the early 1960's, are similar to side scan sonars. They emit an acoustic fan with a narrow horizontal directivity, and measure the arrival time and intensity of the backscattered signal. Therefore, multibeam echo sounders can also be used to determine the return signal intensity. However, multibeam transducers are fixed to the ship hull and their backscatter measurements are less effective compared to deep-towed side scan sonars due to the unfavourable grazing angle.

Because the transducers of a multibeam system are fixed to a ship hull, a motion sensor is used to correct for movements of the ship due to waves.

Multibeam echo sounders assign an arriving angle in addition to intensity and travel time to the return signal to determine the origin of the backscattered signal on the seafloor. Therefore, typically two perpendicular arrays for projection and reception of the acoustic signal are used ("Mills Cross", Fig. 2). The projection array emits a narrow acoustic signal with narrow directivity in the along-track direction. The receiver array is located perpendicular to the projection array. It records signals with a narrow directivity in the across-track direction; i.e. the "receiving" directivity is perpendicular to the "transmission" directivity. Thus, the receiver array is only sensitive to signals backscattered from a small area of the seafloor (Fig. 2), representing one beam. Many beams, directed at different angles, are necessary to obtain a wide coverage of the seafloor. In the case of the used SeaBeam 1185 (ELAC Nautik/L3 Communications), 126 beams cover a swath of 153.5° at maximum.

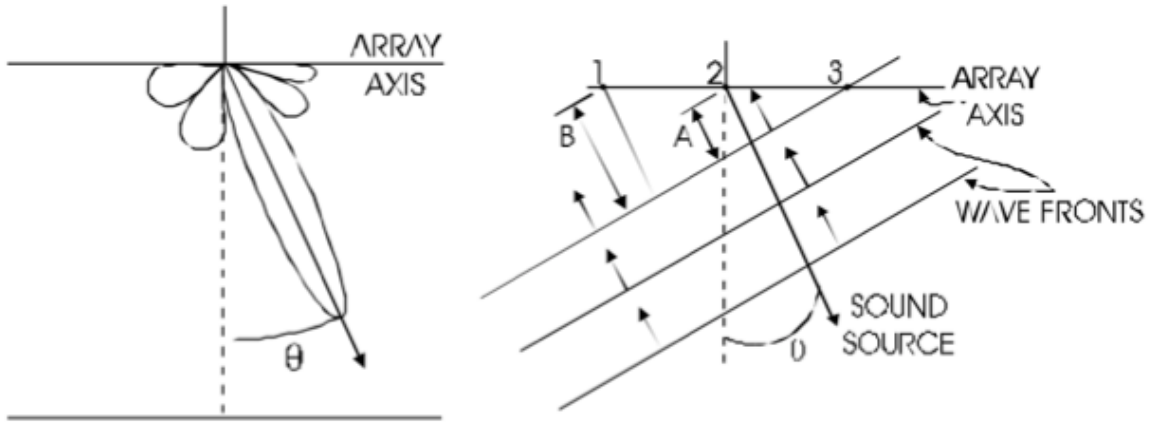

Fig. 3: Left: The principal directivity lobe of a receiver array can be shifted to θ by digitally adding an artificial time delay to the readings of the separate hydrophones to ensure constructive interference of acoustic waves approaching at that angle. Right: A wave front approaches the hydrophones 1, 2 and 3 with an inclination of θ. The required artificial time offset for constructive interference for hydrophone 2 is $T_2=A/c$, with c: local sound velocity. Likewise, the required time offset for hydrophone 1 is: $T_1=B/c$. Source of images: Multibeam Sonar – Theory of Operation. © L-3 Communications SeaBeam Instruments. Used with permission.

The principal directivity lobe of the receiver array, commonly composed of several dozens hydrophones, can be digitally adjusted to create different beams (Fig. 3): A wave front approaching the receiver array at an angle arrives at separate hydrophones at different times, i.e. with a phase difference depending on the local sound velocity and the distance between the hydrophones. The signals of the individual hydrophones interfere destructively due to the phase difference. However, the readings of the individual hydrophones can add constructively, if a certain artificial time offset is added. Effectively, this enables the receiver array to listen specifically at the angle for which the chosen time shift causes the signals to interfere constructively. Signals approaching from other directions are suppressed. Therefore, by adjusting the receiver array directivity, separate beams are digitally formed. Obviously, to determine the correct time offsets accurate information of the local sound velocity at the hydrophone location is crucial.

The maximal resolution of multibeam echo sounders in the across-track and along-track direction is described by the same formulae as for side scan sonar systems (Lurton 2002, see section 1.1)

The sound velocity (based on salinity, temperature, pressure) through the water column is normally not uniform. Therefore, arriving angle and travel time are not sufficient to locate the origin of a signal on the seafloor, because the acoustic wave is refracted according to Snell's Law ($\sin\theta_1/\sin\theta_2 = v_2/v_1$). To correct for this, a local sound velocity profile of the measurement area is needed. Then, the way of the acoustic signal can be traced from the receiver array back through the stratified water column, which is called raytracing (Fig. 4).

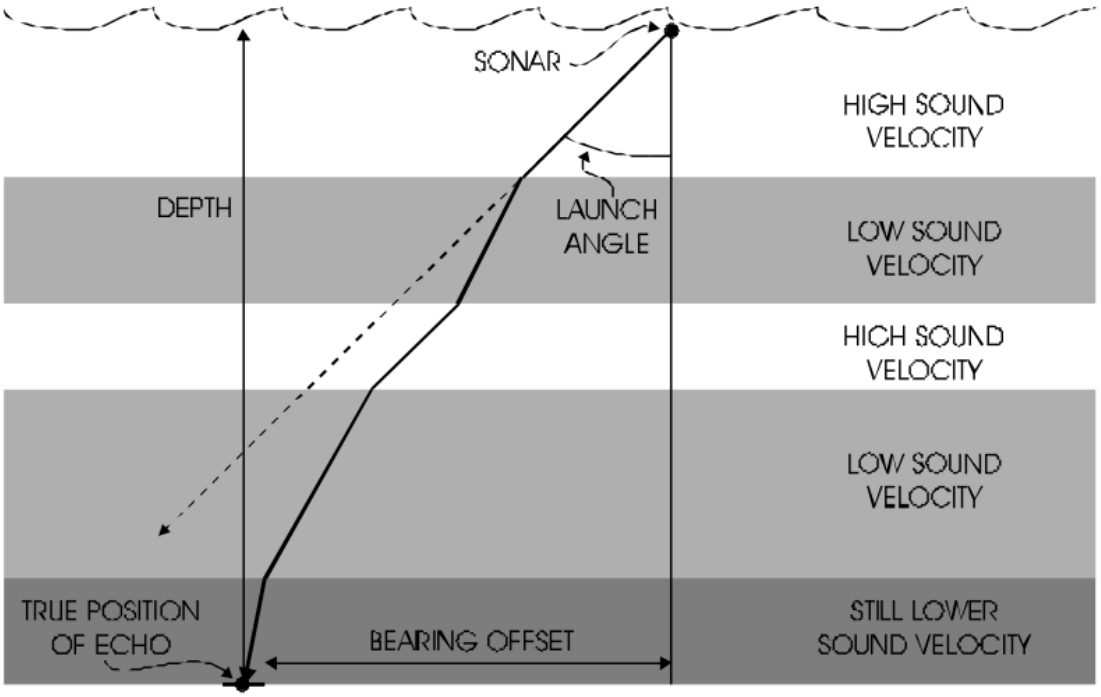

Fig. 4: An acoustic ray emitted by a multibeam echo sounder is refracted in a stratified water column. Information about the stratification is necessary to determine to true position of the echo. See text. Source of image: Multibeam Sonar – Theory of Operation. © L-3 Communications SeaBeam Instruments. Used with permission.

The processing of the acquired multibeam data included:

1. Correction against sound velocity profiles. Partly, this was not possible because of instrument failures, leading to lower quality data.
2. Automated and manual removal of erroneous depth and navigation data.
3. Correction for changing water levels due to tides and wind conditions.
4. Roll calibration of data: the horizontal reference planes of transducers and motion sensor are not necessarily identical, leading to a flat seafloor erroneously appearing inclined

During this work, a SeaBeam 1185 hull mounted on FK Littorina (180 kHz), and a mobile version of the same system have been used.

1.3 Single channel reflection seismic and subbottom profiler

In contrast to the methods described above, reflection seismic systems and subbottom profilers identify subsurface structures; therefore, the generated acoustic signal is directed approximately normal to the seafloor. Seismic systems, using separate devices for signal generation and recording, are typically not included in the term “hydroacoustic methods”. However, especially for reflection seismic the underlying principles are the same.

Principally, subbottom profilers use transducers, similar to classic single beam echo sounders, at lower frequencies (Lurton 2002). Newer generation models use different modulation techniques to improve the penetration depth of the acoustic signal. Devices used in this work use the chirp technique already described for the side scan sonar (C3D Subbottom profiler, Teledyne Benthos) or nonlinear acoustic effects (Parametric effect, Innomar system).

Fig. 5: A selection of hydroacoustic equipment used during this work. Left: Klein 595 digital sonar with buoyancy unit. Middle: Transducer of the C-Boom system Right: Transducers of the ELAC SeaBeam 1185 multibeam echo sounder system installed on RV Chakratong Tongyai.

Boomer systems generate a frequency band (typically between 400 to 15000 Hz) by rapidly moving two electrically charged plates apart, and allow for deeper penetration depths compared to subbottom profilers. In contrast to subbottom profilers, the signal generation and reception of seismic systems is separated, and towed arrays of hydrophones (streamer) record the reflected return signal. In this study only one array consisting of eight hydrophones was utilized (single channel seismic), which significantly simplifies the necessary post-processing.

All devices mentioned above rely on the reflection of acoustic P-waves at the interfaces between layers of different material (Lurton 2002); in this study layers of different sediment composition. The travel time of the returned signal is recorded, corresponding the depth of interfaces reflecting the acoustic energy.

A partial signal reflection occurs at interfaces between different layers due to changes in the acoustic impedance. The characteristic impedance Z is $Z = \rho c$, with ρ: density and c: sound velocity. If an acoustic wave is approaching an interface with normal incidence, the coefficient of reflection, i.e. the amplitude ratio of the reflected wave (Jones 1999) is:

$$R = \frac{Z_2 - Z_1}{Z_2 + Z_1}$$

where R: Reflection coefficient, Z_1: acoustic impedance of upper layer, Z_2: acoustic impedance of lower layer. Conversely, the ratio of the transmissed wave (transmission coefficient) is $T = 1 - R$. Differences in lithology, porosity, pore fluids and saturation as well diageneses can cause an impedance contrast (Bjørlykke 2010). Shear waves are generated in the case the incident angle is not normal; however these are of minor importance for reflection seismic.

Generally, higher frequencies are more quickly absorbed, resulting in lower penetration depths, but higher vertical resolution compared to lower frequencies. The decrease of the intensity I of the acoustic signal follows $I = I_0 e^{-\alpha x}$; with α being a (among else) frequency-dependent absorption coefficient, and x the distance.

Theoretically, two different interfaces can be differentiated if their distance is larger than one fourth of the wavelength (Jones 1999). For a boomer system with a peak frequency of 4000 Hz, and an assumed sound velocity of 1500 m/s, the theoretical vertical resolution is approximately 10 centimetres. However, the actually achieved maximal resolution is lower, and typically given with 30 to 100 cm. For systems emitting a frequency band, e.g. the boomer system, resolution decreases with increasing travel time, as higher frequencies are more quickly absorbed. Newer subbottom profilers use the chirp technology; hence, their resolution is dependent on the used bandwidth (Lurton 2002):

$$R_z = \frac{c}{2B}$$

where R_z: Vertical resolution, c: sound velocity, B: bandwidth.

A major factor for the resolution of final seismic profiles is the distance between two pings (or shots), depending on the number of shots per second and the tow velocity.

The horizontal resolution of a single shot is determined by the width of the first Fresnel zone: Signals reflected from a horizontal interface whose travel paths do not differ more than one-half wavelength interfere constructively. They form the main part of the recorded return signal. The zone width w_f for which this applies can be approximated with $w_f = \sqrt{2z\lambda}$ (Keary et al. 2002); with z: distance between reflector and signal source and λ: wavelength. Different reflectors within this zone cannot be differentiated. For a boomer system, with a peak energy at 4000 Hz and an assumed sound velocity of 1500 m/s, the first Fresnel width for a reflector at a depth of 45 m would therefore be around 5.8 meters. Similar to vertical resolution, horizontal resolution decreases with increasing depth, as higher frequencies are more quickly absorbed.

Processing of the subbottom data included high- and lowpass filter to remove acoustical noise, gain adjustments, stacking for noise cancelling and partly binning of shots to account for changing ship speeds. In the resulting graphs, the depth is given in Two-Way-Travel time (TWT). Depth values given in meters assume a constant sound velocity of 1500 m/s through water column and sediment, and are therefore approximations.

2. Sedimentological methods

2.1 Sediment sampling: grab sampler, gravity- and vibrocore

Different sampling devices were used in order to retrieve sediment for further analysis. In the Baltic Sea, a Van-Veen type grab sampler was used to obtain samples from the seafloor. Different models of grab samplers were employed in Thailand. Grain sizes distributions derived from the analysis of grab samples formed the base for ground-truthing of the side scan sonar data. Partially the first ten to fifteen cm of sediment could be retrieved, giving limited information about the structure of the subsurface over this depth interval.

Different kinds of gravity cores have been used to obtain a better insight into sedimentary subsurface structures, and to obtain material for age-control. In the Baltic Sea, a 3 m long vibrocorer, as well as a 6 m long gravity corer were used. Gravity corers comprise a metal tube with a plastic liner inside, and a heavy weight on top (typically around 1 ton). They are lowered with high speed (1 to 2 m/s) towards the seafloor. Soft sediment can be easily penetrated. A core catcher at the base of the core and a valve at the top, closing on contact with the ground, keep the sediment within the plastic liner during retrieval. On board, the plastic liner is removed from the metal tube and cut in meter-long pieces, which can then be further analysed in the laboratory. In contrast, a vibrocorer uses an electrical vibration head mounted on a metal frame to drive a metal tube into the seafloor. They are especially useful in sandy to slightly gravelly sediments, where a gravity corer cannot be used.

Onboard the smaller research vessels in Thailand the use of such heavy equipment were not possible. Here, a more lightweight Rumohr corer was used (Fig. 6), comprising a plastic liner, several weights rings composed of lead, and a mobile winch (electrical or manual operation). The working principle is identically to the gravity corer described above, despite being smaller in scale.

Fig. 6. Scientists and crew operating the Rumohr corer onboard MS Fahsai, offshore Khao Lak in March 2010.

2.2 Granulometric analysis: Mechanical and optical methods

Depending on the composition of sediment samples and the available sample size, grain size distributions were either determined by mechanical (sieving) or optical (laser diffraction) methods. Sandy material was sieved, while sediments with a dominant grain size fraction below 63µm were measured optically. All samples taken from sediment cores were measured optically, due to the limited amount of available material. Generally, grain sizes are presented in the Phi (Φ) scale, with $\Phi=-\log_2 d$, d=grain size in mm (Krumbein 1938). The mode of the grain size distribution was chosen as a central statistical parameter, because it is not affected by removing coarse (laser diffraction based method) or fine (sieving) parts from the grain size distribution. Modes can also be used for bimodal sediments. Sorting values, based on unimodal samples, are given using the geometric method of moments (calculation with the software Gradistat, Blott and Pye 2001).

Sieving of sediment samples mostly followed the ASTM (American Society of Technical Measurement) standard, although sediments <63µm instead of <40µm were removed prior to sieving. Between 20mm and <63µm, the sieving interval was 0.25Φ.

Laser diffraction measurements are based on the principle that particles diffract light at a certain angle, which is increasing with decreasing particle size (McCave and Syvitski 1991). Optical grain size analysis was done with a Mastersizer 2000. Carbonate and organic material were removed by HCl and H_2O_2 prior to analyses. Moreover $Na_4P_2O_7$ was added to avoid aggregation of fine particles during the measuring process. It is important to note that grains exceeding 1.7 mm could not be measured for technical reasons. Additionally, given the low amount of sample (2 to 3 grams), no representative grain size distribution can be measured for samples including grains in the medium and coarse sand fraction. This is an important restriction, as sediment cores contained layers of coarse material. Therefore, the obtained

grain size distributions for such layers do not fully represent the actual grain size distributions of the sediment, and must not be over-interpreted.

2.3 X-Ray Analysis

For selected sediment cores, thin slabs were retrieved for X-Ray analysis. The resulting radiographs give a high-resolution image of sedimentary structures and layers. The method allows the identification of layer boundaries and unconformities, as well as the identification of bioturbation traces.

2.4 ^{14}C dating

In this study, ^{14}C dating is used for age control of sediment layers in cores. ^{14}C dating is based on the radioactive decay of atomic nuclei. The rate of decay for a given radioactive isotope is constant, and is directly proportional to the present number of atomic nuclei N:

$$\frac{dN}{dt} = -\lambda N$$

with λ being an isotope-specific decay constant. Based on this relation, the remaining amount of radioactive isotopes *N* at a given time is: $N(t) = N_0 e^{-\lambda t}$, with a half time of:

$$t_{half} = \frac{ln2}{\lambda}$$

For ^{14}C, Willard Frank Libby originally gave the half time with 5,568 +- 30 years at the end of the 1940's. Later, the half time was corrected to 5,730 +- 40 years (Currie 2004).

If the relation *N* of a given radioactive isotope against a non-radioactive isotope is measured (in case of ^{14}C dating, ^{14}C is measured against ^{12}C), and the original relationship N_0 at a point in the past is known, the age of an object can be determined. However, for most applications of radiometric dating, N_0 is unknown. For ^{14}C dating, it is assumed that the ^{14}C/^{12}C ratio in living organism is representative for ^{14}C/^{12}C ratio in past times.

^{14}C is constantly generated in the upper atmosphere from collisions of free neutrons, generated by collisions of cosmic rays with atomic nuclei, with ^{14}N. Living organism are constantly exchanging material with the atmosphere, and therefore both have the same ^{14}C to ^{12}C relationship. This exchange of material ends with the death of an organism, and ^{14}C is slowly depleted by decay to ^{14}N. Therefore, the ^{14}C to ^{12}C ratio is continuously lowering, allowing determining the time *t* passed since the death of the organism:

$$t = -\frac{1}{\lambda_{14C}} ln \frac{N_t}{N_0}$$

The maximum age that can be determined with the available technology is around 40,000 years (Musset and Khan 2000), equalling approximately 7 half times.

Unfortunately, the natural relation between ^{12}C and ^{14}C is not constant, but varies over time; for example the intensity of cosmic rays changes due to changes of the earth magnetic field or changing solar activity (Currie 2004). Apart from these global changes, local reservoir effects have to be considered, for example due to dissolved old carbonates in ground water, which can be incorporated by living organisms. Partly, a correction against these influences is possible e.g. by creating calibration curves based on dendrochronology, which gives age control independent of ^{14}C/^{12}C ratios. Still, the correlation between measured ^{14}C-years and calendar years is not necessarily unambiguous (Musset and Khan 2000). In this work, uncorrected ^{14}C ages are used.

Chapter III
Geologic aspects of Fehmarn Belt (south-western Baltic Sea)

1. Introduction

The evolution of the Baltic Sea since the last glacial period was dominated by several transgression and regression events, which were mainly forced by melting glaciers and corresponding isostatic movements of the subsurface. In the Baltic proper, the individual phases of Baltic Ice Lake, Yoldia Sea, Ancylus Lake and Littorina Sea (which is further subdivided) can be clearly distinguished (Björck 1995, Niedermeyer et al. 2011). Prior to the first major marine transgression into the Baltic proper at 8,500 cal. yr BP (Berglund et al. 2005), today's Baltic Sea was frequently decoupled from the Atlantic Ocean, and the eustatic sea level rise. The majority of data available on the different Baltic Sea stages derive from the northern Baltic, especially Sweden (Björck 1995), where sediments deposited during the evolution of the Baltic Sea are available onshore due to the isostatic uplift. Details of the individual phases, however, are still under debate. This holds especially true for the southern Baltic, where all deposits of past coastline are situated offshore. One of the remaining questions is whether the regression of the Ancylus Lake (or a part thereof) was caused by an outburst through the Darss Sill area. A major problem in solving questions about potential outlets of the former lakes in the Baltic proper is the absence of local sea level curves (e.g. Lampe 2005). Given the separation from the world sea, the eventually varied pattern of isostatic subsidence and uplift (reported e.g. by Kolp 1979 and Dietrich and Liebsch 2000, rejected by Winn et al. 1986), local tectonic movements as well as the impact of compaction, regional sea level curves are needed – such need has been clearly demonstrated for the North Sea (Bungenstock and Weerts 2010). Meanwhile, it is commonly agreed that the Ancylus Lake (9,500 to 8,000 ^{14}C yr BP, Björck 1995) was originally dammed against the world sea level, and a major regression took place around 9,200 to 9,000 ^{14}C yr BP (Björck 1995). This regression was originally assumed to take place via the Darss Sill, the Fehmarn Belt and the Great Belt towards the Kattegat, lowering the water level in the main Baltic proper from a level around 20 m below sea level (b.s.l.) to around 30 m b.s.l. – the exact water levels vary between authors and places (e.g. Kessel and Raukas 1979, Kolp 1986, Björck 1995, Lemke 1998, Wohlfarth et al. 2008, see section 3.2 for details). However, recent reports of a threshold at the Darss Sill, preventing water level exchange below 24 m b.s.l. during the Holocene (Lemke et al. 2001), allow only for a partial outburst of the Ancylus Lake over the Darss Sill (Björck et al. 2008), if a maximal water level of 20 m b.s.l. is accepted as the AL highstand.

In this context, a large drowned river system was observed in the western part of Fehmarn Belt. It was the major aim of this study, based on several research cruises with FS Alkor, FS Poseidon and FK Littorina between 2007 and 2011, to verify whether the evolution of this river channel is in agreement with the model of a partial regression of the Ancylus Lake caused by an outburst through the Darss Sill area. While addressing this aim, knowledge on the landscape evolution of the Fehmarn Belt between the last glacial and the onset of the Littorina Transgression was acquired. This information is included in the study. Additionally, the final part of this study is concerned with a large subaqueous dune field in the central Fehmarn Belt, especially its formation and recent sediment dynamics. The latter is continued and enhanced work already presented by Feldens (2008). The main results of the research in Fehmarn Belt are presented in the form a research article currently under preparation (section 2) and a published article (section 3). Subsection and number of figures have not been changed and are therefore not continuous throughout the chapter.

2. A paleo river-channel in Fehmarn Belt (SW Baltic Sea)[1]

Abstract

The Baltic Ice Lake, Yoldia Sea, Ancylus Lake and Littorina Sea stages of regression and transgression controlled the history of the Baltic Sea since the last glacial. Many details regarding their development remain unknown, including the question of whether the 9,200 to 9,000 ^{14}C yr BP regression of the Ancylus Lake took place over the Darss Sill. In addition to describing the general geological evolution of the western Fehmarn Belt since the last glacial, this study addresses whether a drowned river system in the Fehmarn Belt (SW Baltic Sea) can be related to the drainage of the Ancylus Lake. The river channel is cut into the glacial till in the western Fehmarn Belt, reaching an incision depth of up to 12 m at a base level of 40 m b.s.l. (below sea level). Its continuation to the west appears in bathymetric data, and the channel is buried near Mecklenburg Bay. According to seismic surveys, it widens rapidly from several hundred meters to more than 1 kilometer and fades towards the east. Sediment thickness above the glacial till can exceed 30 m in the buried section of the channel. The channel was mainly shaped as part of a glacial meltwater system at a maximum water level of 30 m b.s.l., although it was eventually incised subglacially. During the lowstand of the Baltic Ice Lake, local, shallow water bodies covered the study area. A previously reported westward directed drainage of a lake in the eastern Fehmarn Belt could be restricted to a time interval following the highstand of the Ancylus Lake and prior to the Littorina Transgression. Timing, water level and potential water discharge of this event suggest its connection to the partial drainage of the Ancylus Lake over the Darss Sill. Subsequent to the regression, cliffs and lake deposits point to a local water level between 24 to 26 m b.s.l. However, finding a channel system filled with sediment deposited during the early Littorina transgression might indicate a short phase with a water level around 30 m b.s.l.

1. Introduction

The Baltic Sea evolved through the stages of Baltic Ice Lake (BIL), Yoldia Sea, Ancylus Lake (AL) and Littorina Sea (e.g., Björck 1995, Niedermeyer et al. 2011). However, many questions remain concerning the detailed development of its separate stages.

This study focuses geographically on the Fehmarn Belt and Mecklenburg Bay (SW Baltic, Fig. 1). The assumed pathway for a part of the Ancylus Lake regression (Björck et al. 2008) is situated in this area, roughly following the course of the "Dana River" postulated by von Post (1927). In addition, the first marine ingressions at the beginning of the Littorina Transgression took place through the Fehmarn Belt and Mecklenburg Bay (Rößler 2006). In fact, a drowned paleo-river can be recognized in bathymetric data offshore near Fehmarn (Fig. 2). This study is concerned with the evolution of this river system up to the onset of the Littorina Transgression and with its connection to the Ancylus Lake drainage.

The Baltic Ice Lake lasted from approximately 12,600 to 10,300 ^{14}C yr BP (Björck 1995) and is separated into an initial (BILi) and a final (BILf) phase. The maximum water level of the BIL in Mecklenburg Bay and the Arkona Basin was 20 m below sea level (b.s.l.) (Jensen et al. 1997) to 18 m b.s.l. in the Darss Sill area (Lemke et al., 1994). Local lakes in the Mecklenburg Bay area were connected to the main Baltic proper, flooding the Darss Sill (Jensen et al. 1997) during the BILf highstand (Lemke 1998). The BIL extended into the Great Belt (Bennike et al. 2004).

[1] To be submitted to Contintental Shelf Research

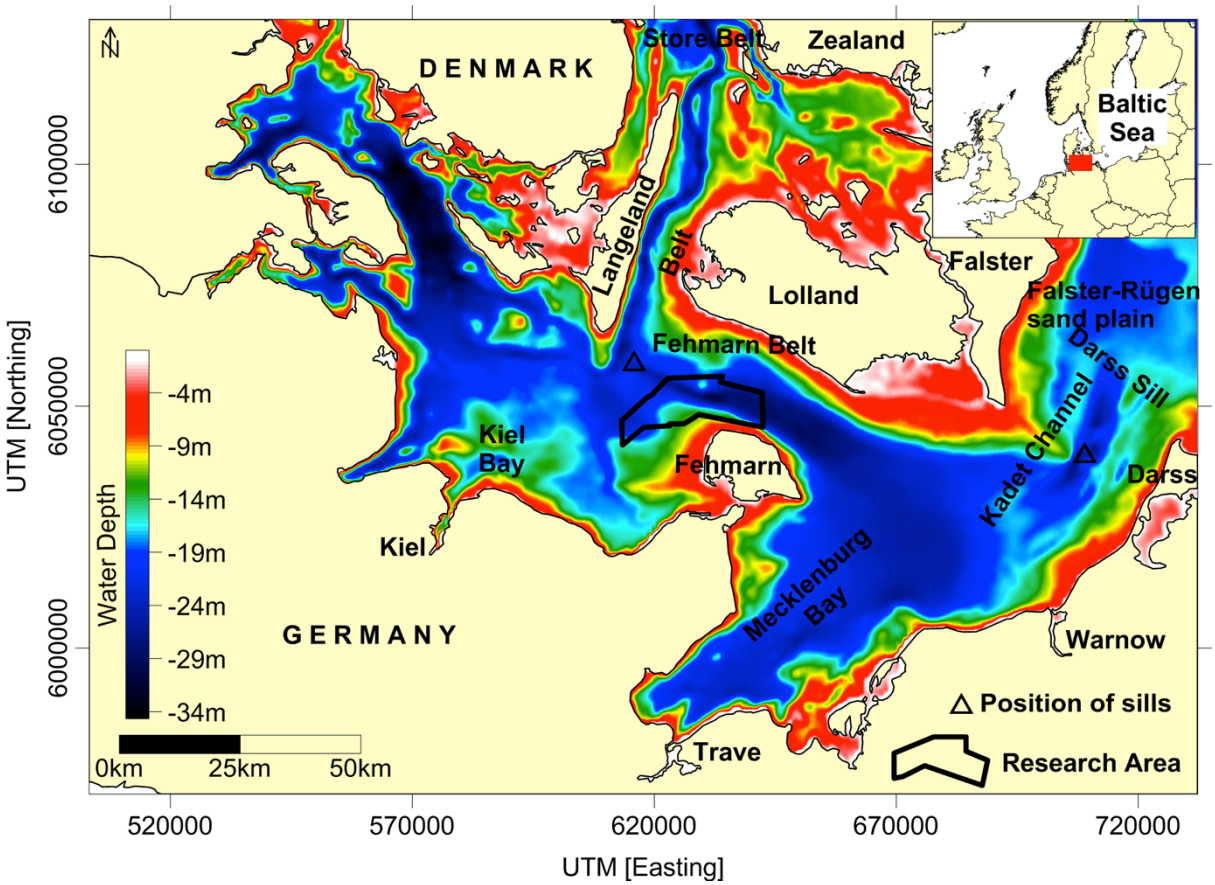

Fig. 1: The research area is situated between the Fehmarn and Lolland islands, in the SW Baltic Sea. Bathymetric data is based on Seifert et al. (2001). The positions of sills are indicated (based on Lemke et al. 2001), rising above 30 m b.s.l. in the south of Langeland Belt and to 24 m b.s.l. in the Darss Sill area.

The regression of the initial and final phases of the BIL took place through outlets at Örsesund and Mt. Billingen east of the Darss Sill, at 11,200 and 10,300 ^{14}C yr BP (Björck 1995, Jensen et al. 1997), although the details of the older regression event are still debated (Björck 1995). Following the regressions of the BIL, the water level in the southern Baltic east of the Darss Sill was situated at approx. 35 m b.s.l. (Lemke 1998) to 40 m b.s.l. (Jensen et al. 1997, Lampe 2005). No indications of erosion of the Darss Sill due to this regression were found, and Mecklenburg Bay and the Arkona Basin were separated when the water level fell below 24 m b.s.l. (Lemke et al. 2001). The shore level in the Fehmarn Belt west of the Darss Sill is indicated with approx. 35 to 38 m b.s.l. following both regressions of the Baltic Ice Lake (Jensen et al. 2005).

The Ancylus Lake stage, separated from the Baltic Ice Lake by the Yoldia phase (10,300 to 9,500 ^{14}C yr. BP), lasted from app. 9,500 to 8,000 ^{14}C yr. BP (Björck 1995). In the beginning, the AL was dammed above the world sea level (Kolp 1986; Björck 1995, Lemke 1998), with a maximum water level of 20 m b.s.l. (Wohlfarth et al. 2008), following a rapid transgression of 15 to 25 m (Björck 1995). Older literature indicates maximum water levels between 8 m b.s.l. (Kliewe and Janke 1982), 12 m b.s.l. (Kolp 1986) and 25 m b.s.l. (Kessel and Raukas 1979). A water level drop between 10 m (Björck 1995) and 20 m (Kolp 1986) occurred at approx. 9,200 to 9,000 ^{14}C yr. BP (Björck 1995). The resulting water level in the Arkona Basin east of the Darss Sill was 26 to 28 m b.s.l. (Lampe 2005) and 32 m b.s.l. in the Tromper Wiek area (Lemke 1998). In the Fehmarn Belt, the minimal shore level subsequent to the regression was approx. 26 to 28 m b.s.l. (Jensen et al. 2005)

The pathway of this regression is under discussion. Recently, Björck et al. (2008) suggested a sudden regression of 5 m, draining along the assumed pathway of the Dana River. It was followed by a period of 200-300 years during which the water level difference between the Ancylus Lake and the Atlantic Ocean quickly decreased due to the eustatic sea level rise (Björck et al. 2008).

Earlier theories suggest that the Darss Sill was the southwestern boundary of the Ancylus Lake prior to its regression (Kolp, 1986, Björck 1995). The previously filled Cadet Channel was rarely flooded during the BIL-time and was mainly eroded during the Ancylus Lake phase (Lemke et al. 1994, Lemke and Kuijpers 1995). Either a gradual downcutting (Björck 1995) or a catastrophic overflow (Kolp 1986) of a natural dam was suggested, leading to the formation of the Dana River at approx. 9,000 to 9,200 ^{14}C yr BP (Björck 1995, Lemke 1998). The further course of the river was assumed to be situated between Lolland and Fehmarn and along the eastern side of Langeland (Björck 1995). The above reasoning was subsequently rejected. Lemke et al. (2001) report that thresholds between the Cadet Channel, Store Belt and Langeland Belt prevented water exchange below 24 m b.s.l. during the Holocene and suggested the Cadet Channel was a succession of kettle holes. Thus, the formation of the hypothetical Dana River could not be responsible for the 10 m water level drop in the Ancylus Lake, if accepting a maximum water level of 20 m b.s.l. The absence of a prograding system west of the Darss Sill, expected to form during the draining of the AL, gave further reason to reject the Dana River theory (Jensen et al. 1999, Lemke et al. 2001).

2. Methods

Hydroacoustic data, sediment samples and gravity- and vibrocores were taken during several cruises with FK Littorina, FS Alkor and FS Poseidon between 2007 and 2011. A selection of these data is presented in this article.

Bathymetric data were collected using a multibeam echo sounder (SeaBeam 1185, L3 Communication/ELAC Nautik, 180 kHz). Shallow water reflection seismic data were obtained with an EG&G and a C-Boom (filtered between 0.5 and 5.5 kHz) boomer system onboard FK Littorina. Additional subsurface data was acquired using a parametric subbottom profiler (Innomar, between 7 and 9 kHz) and a subbottom profiler included in a towed C3D-system (Teledyne Benthos, 2 to 7 kHz), obtained during cruises onboard FK Littorina, FS Poseidon and FS Alkor. Seafloor depths of the seismic profiles were adjusted against bathymetric profiles based on multibeam echo sounder data. Depth values given in meters are approximations and assume a constant sound velocity of 1500 m/s through both water column and sediment. Side scan sonar data were gathered during previous cruises (Schwarzer and Diesing 2006) using a Klein 595 sonar with digital data acquisition. In this study, areas of higher backscatter intensity appear in darker colors.

Black and white values of side scan sonar and seismic images shown in this work were adjusted to display a better contrast of data. Effects of the isostatic rebound are not considered because the isostatic equilibrium-line strikes approximately through the Fehmarn Belt (Lampe 2005).

For calibration of the hydroacoustic data, surface sediment was retrieved with a Van-Veen type grab sampler. The grain size distribution of grab samples was determined by sieving. Gravity- and vibrocores were retrieved onboard FS Alkor and FK Littorina for age-control of the seismostratigraphic units. ^{14}C-datings of selected core material were provided by the Leibniz Labor für Altersbestimmung und Isotopenforschung, Christian-Albrechts-Universität Kiel, Germany. The dating results are given in radiocarbon years before present (BP). Additionally, the cores were subsampled every 1 to 5 cm (depending on sediment layers) for grain size analysis by laser diffraction using a Mastersizer 2000. Carbonate and organic

material were removed from the sediments prior to the analysis with HCl and H_2O_2. $Na_4P_2O_7$ was added to avoid aggregation of fine particles. Grains larger than 1.7 mm were separated prior to measuring.

3. Results

3.1 Seafloor surface

The Öjet is a prominent, elevated morphological feature in the investigation area (Fig. 2). South of the Öjet, there is a channel system known as "Winds Grave". The present base of the channel is situated in water depths between 30 and 40 m b.s.l., with the deepest point situated close to the Öjet. Further south, the seafloor rises towards the coastline of Fehmarn. A large subaqueous dune field forms a remarkable feature on this slope (Fig. 2) (e.g., Werner et al. 1974, Feldens et al. 2009).

The incision depth of the channel varies between 5 and 12 m. Directly south of the Öjet, the channel width is approx. 200 m. To the west, the shape of the main channel is clearly defined and is situated at the base of a wide U-shaped valley. Here, the top of the channel slope is situated at approx. 27 m b.s.l. Towards Kiel Bay, the course of the channel can be easily traced in both bathymetric and side scan sonar images (Figs. 2 and 3). The visibility of the channel in the bathymetric data quickly fades towards Mecklenburg Bay, although some remnants, 1 m deep at maximum, can still be recognized (Fig. 2E).

Several morphological features, typical for sub-aerial river systems, are observed in the drowned channel. They include terraces several hundred meters wide between 26 and 27 m b.s.l. To the west, escarpments situated between 24 and 26 m b.s.l cut these terraces. (Figs. 2A and B). Additionally, small-scale tributaries draining into the main channel are frequently visible in bathymetric and side scan sonar images (Figs. 2 and 3). The mounds of these tributaries can be traced down to 30 m b.s.l. At this water level, an elongated depression (up to 6 m deep, app. 2000 m wide and oriented E-W) connects to the main channel by small tributaries with an incision depth between 50 cm and 1 m (Fig. 2C). East of the Öjet, the channel meanders around two elevations, rising up to 28 to 32 m b.s.l.

To the east, the seafloor shows irregularly shaped morphological structures with elevations of less than 1 m (Fig. 2E), with the majority of seafloor distributed in the 27 to 30 m depth interval. A field of irregular but approx. N-S striking ridges exists between 22 and 26 m b.s.l. Additionally, subaqueous dunes are found at a depth of 27 to 28 m (Fig. 2D), with a wavelength of approx. 150 m and a relative crest height of approx. 1 m. They are not connected to the main dune field on the slope towards Fehmarn. A second local seafloor depression is observed nearby (Fig. 2D), also appearing in seismic data (Fig. 5). This depression is not connected to the main channel.

Surface sediment samples retrieved from the channel have a first mode between 1.3 and 2.2 Φ and are poorly to moderately well sorted. Although no samples could be retrieved from the small-scale tributaries, side scan sonar backscatter intensity indicates that surface sediments have similar grain size compositions as the sediment in the main channel. Stones and boulders are commonly observed at the slope of the main channel to the south and west of the Öjet (Fig. 3). A short vibrocore (vibrocore 1, Fig. 9), retrieved close to the top of the river slope (Fig. 3), included coarse gravel and stones at its base. On top, a normally graded sequence of sand is observed, and the uppermost 40 cm of the core are mainly composed of silt. Samples taken in close vicinity of the river channel are poorly to very poorly sorted, with first modes between 1.2 and 1.8 Φ. The samples are partly polymodal, with second modes of gravel size.

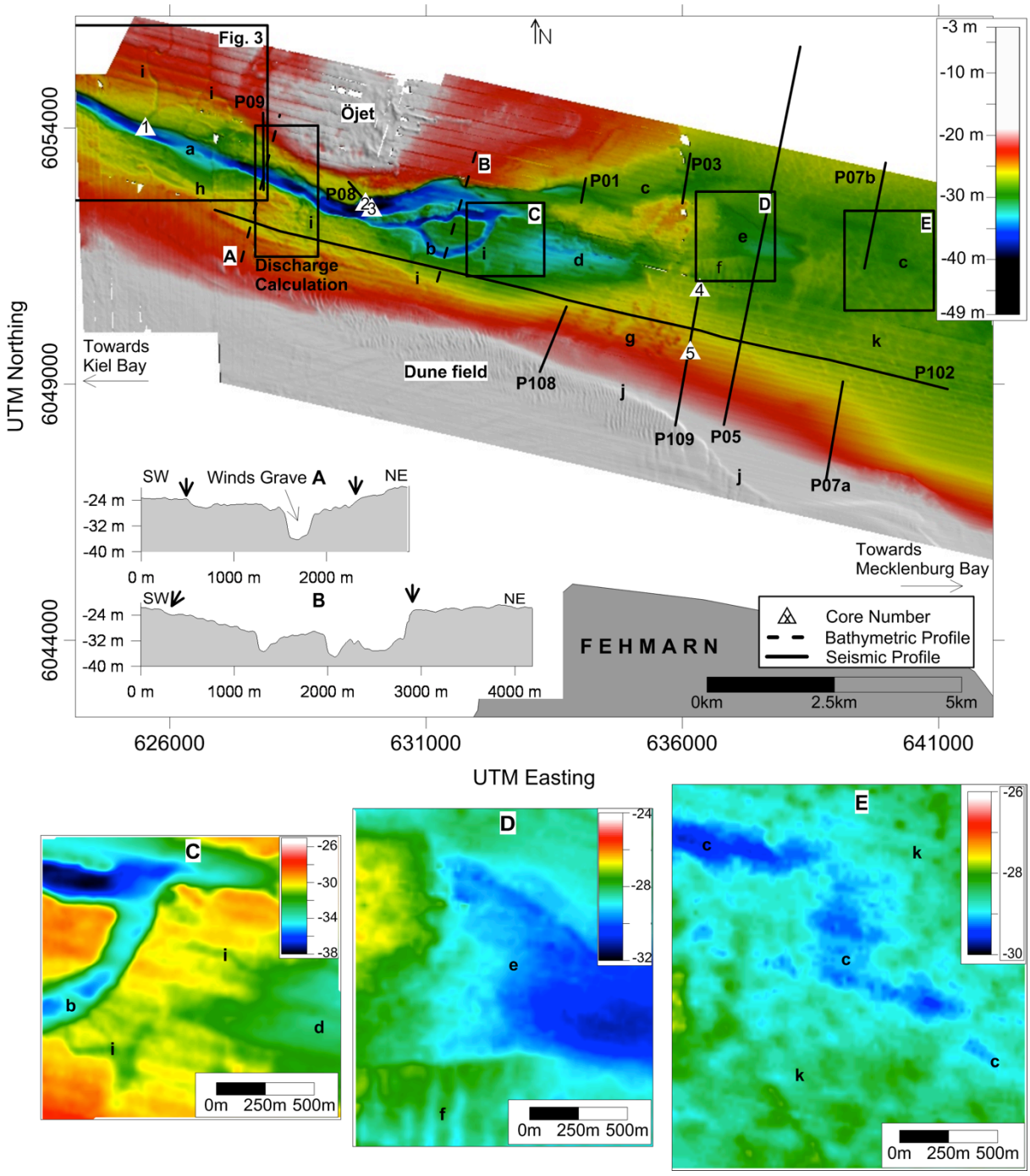

Fig. 2: Available bathymetric data in the Fehmarn Belt. Seismic and bathymetric profiles, sediment cores and the area used for discharge calculation are indicated. Insets A and B show morphological cross sections, and insets C, D and E give details of selected areas. Small characters indicate morphological features mentioned in the text: a) main river channel, b) channel meandering around elevations, c) the channel is fading in bathymetric data towards Mecklenburg Bay, d) local depression, connected to main channel by small tributaries (see inset C), e) second seafloor depression, f) subaqueous dunes not connected to main dune field, g) irregular, approx. N-S striking ridges, h) frequently visible escarpments between 24 and 26 m b.s.l. (see inset A and B, escarpments are marked by arrows), i) small tributaries flowing into the main channel, j) slope running through the main dune field and k) irregular morphological features in the eastern part of the research area.

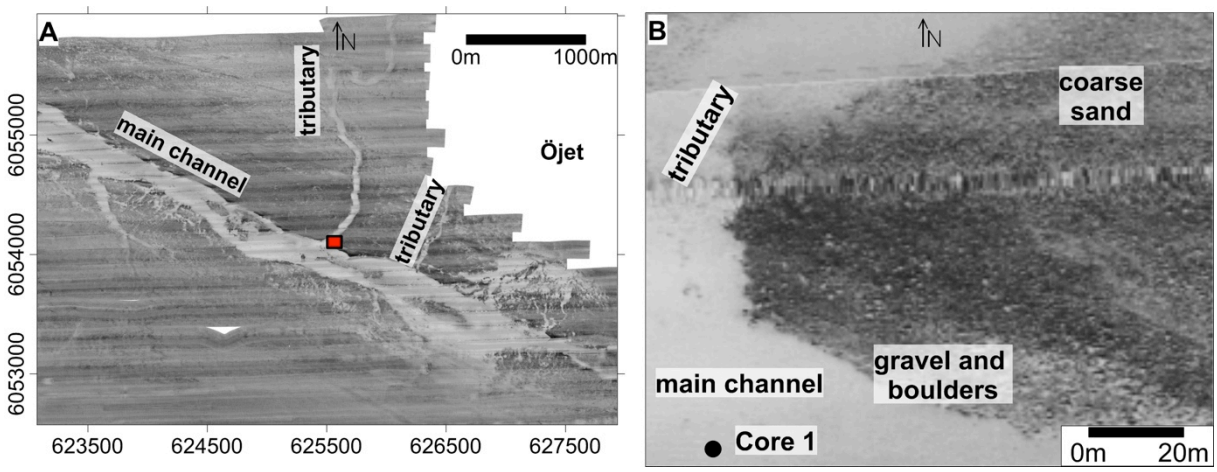

Fig. 3: The main river channel and small tributaries are visible in side scan sonar images in lighter colors due to the finer-grained sediment filling the sheltered environment of these incisions. Refer to Fig. 2 for the position relative to bathymetric data. The red rectangle marks the position of Fig. 5B. B: The river slope is frequently composed of gravel and boulders, which are less common away from the slope.

Coarser grained material (first mode 1.0 Φ), including gravel-sized components, was found at the base of grab samples (position marked with "e" in Fig. 2) within the eastwards seafloor depression. Towards the coastline of Fehmarn, the majority of sediment samples are composed of well-sorted to moderately well-sorted medium to coarse sand, with first modes between 1.2 and 1.8 Φ. No samples exist from the eastern part of the research area. According to sediment distribution maps (Kaufhold 1995) the surface of the seafloor in the eastern part of the research area is composed primarily of silty to fine sandy material with coarser material deposited towards the center of the Fehmarn Belt.

3.2 Subsurface structure

Six seismic units are differentiated. The general numbering of seismic units follows the scheme of Jensen et al. (1997), with seismic unit 1 representing glacial deposits. Seismic units 2 and 3 represent sediments of BIL time. Unit 4 represents deposits of the Ancylus Lake time, and units 5 and 6 represent material deposited since the beginning of the Littorina Transgression.

Seismic unit 1

Seismic unit 1A is present in all profiles at a highly variable depth. It is characterized by an abundance of diffraction hyperbolae, representing boulders (e.g., Fig. 4A, Fig. 7) and diffuse internal layers. However, the internal structure of unit 1A is not further differentiated in this study.

An approximately 2 m thick layer, comprising seismic unit 1B, is commonly observed on top of unit 1A (Fig. 2B), often filling the irregular surface of unit 1A. Its acoustic appearance is more homogenous than unit 1A but not entirely transparent. In large parts of the research area, seismic unit 1 crops out at the seafloor, especially towards the northwest. The observed channel system is incised into the sediments of seismic unit 1. To the east, sediment completely fills the channel (Figs. 2 and 6). The width of the buried channel increases to the east, reaching 1000 m in the easternmost profile (Fig. 6). Incision depths of up to 60 m are observed in the buried section of the channel (Fig. 6). South of the Öjet and to the west, the channel is either not filled or only partially filled, and its acoustic base is observed in a depth of 40 m (Fig. 7). Generally, the channel fades to the east because the incision depth decreases, and the width increases in that direction (Fig. 6).

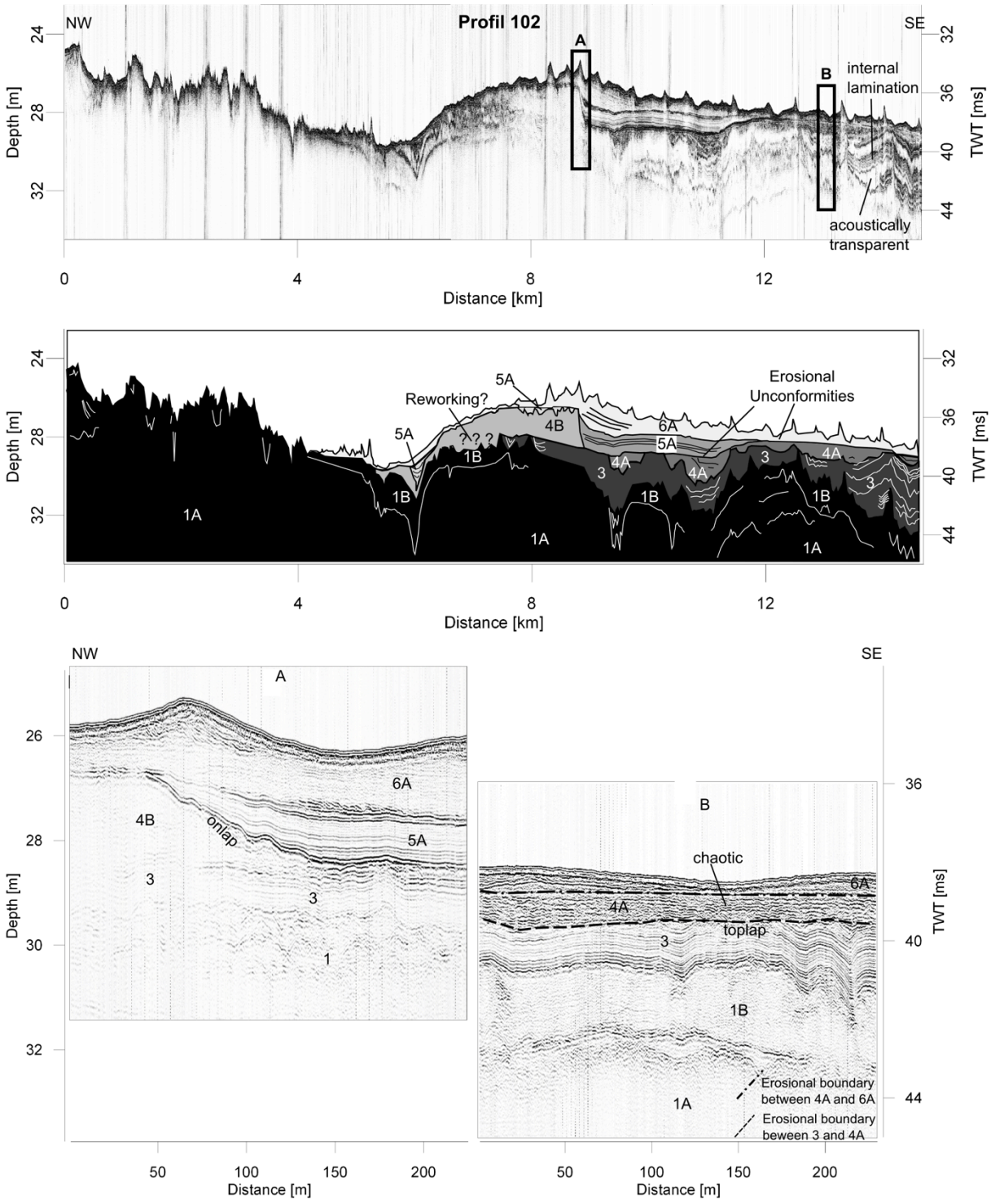

Fig. 4: Profile 102 (subbottom profiler) is crossing the western part of the Fehmarn Belt from East to West. Vertical exaggeration (v_{ex}) approx. 400x. Two different environments are clearly observed: in the east, internally layered sediments are visible, although such sediments are absent towards west. Detailed insets (A and B, v_{ex} 30x) show the appearance of seismic units as discussed in the text.

Seismic unit 2 and 3

Seismic unit 2, deposited above unit 1, can be traced down to app. 60 m b.s.l. in the buried sections of the river channel and reaches a maximal thickness of more than 20 m (Fig. 6). Toward its base, layers dipping to the north (Fig. 5) or south (Fig. 6) are recognized. In the center of the Fehmarn Belt, the unit is situated closely to the surface, correlating with generally coarser surface sediments found in a local seafloor depression (Fig. 5). Meanwhile,

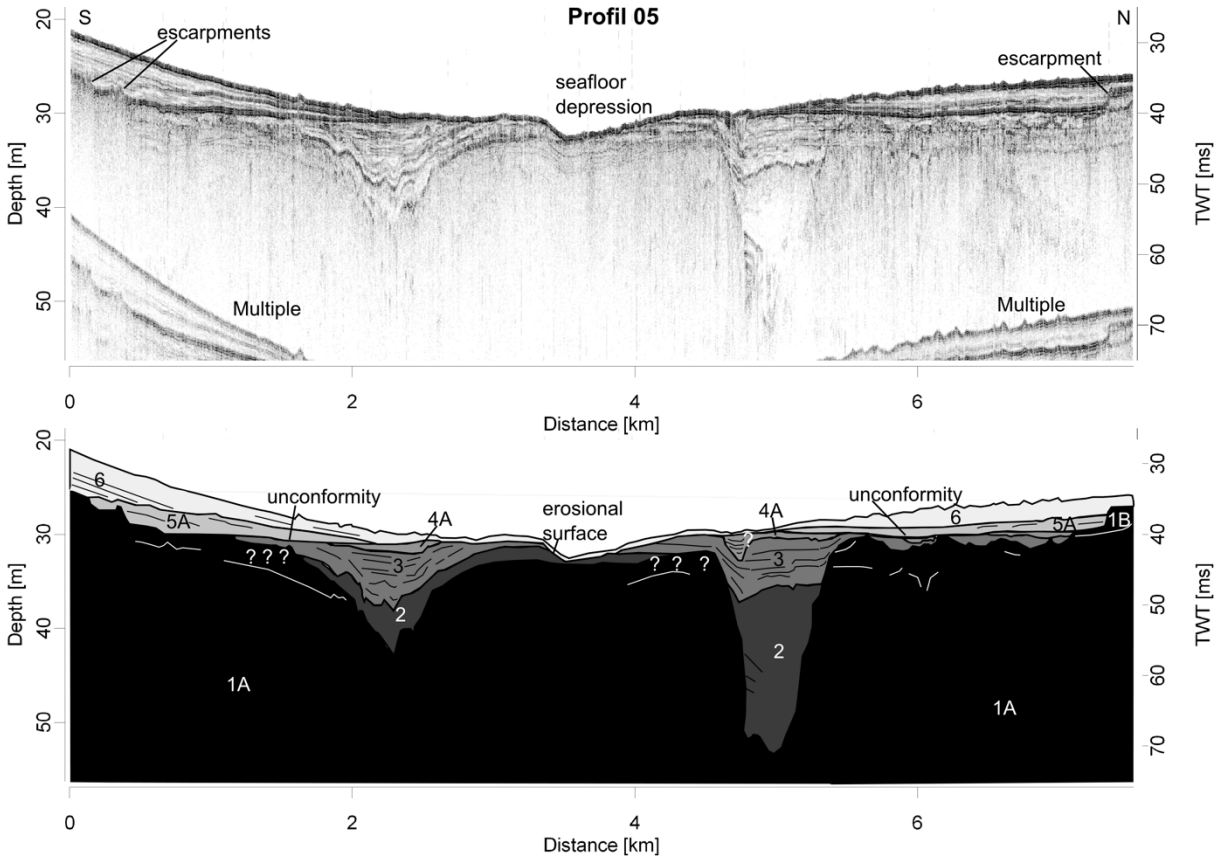

Fig. 5: Profile 05 (boomer, vex approx. 66x) is crossing the Fehmarn Belt from South to North. The buried channel system is clearly visible. Younger sedimentary units disappear towards the center of the Fehmarn Belt.

the bulk of the unit appears acoustically homogenous and is separated from the overlying unit 3 by a high-amplitude reflector with an irregular morphology from 35 to 37 m b.s.l. (Fig. 6).

For surveys recorded with sediment echo sounders, this boundary frequently forms the base of acoustic penetration (Fig. 6).

Seismic unit 3 appears internally heterogeneous (e.g., Figs. 6A and B) and is recognized both inside and outside the channel. Outside of the river channel, the depth and maximal thickness of unit 3 increases towards Mecklenburg Bay, reaching a maximal thickness of 6 m outside the channel (Fig. 4) and 4 m inside the channel (Fig. 6). Parallel but deformed and folded internal laminations are frequently recognized (Fig. 4B), although a chaotic internal appearance prevails in part (e.g., profile 108, Fig. 8). Beneath 30 m water depth, meter-thick, acoustically transparent layers are separated from the laminated material by medium-amplitude reflectors (e.g., Fig. 6). The top of unit 3 is recognized as an erosional unconformity (erosional overlap) against either unit 4 or 5 (e.g., Figs. 4B and 5). The depth of these boundaries is situated between approx. 29 and 31 m b.s.l. Sediment core 04 (Fig. 9) contains material comprising the chaotic internal layers of seismic unit 3, including sand clasts and interbedded sand and silt layers. For the purpose of this study, the internal stratigraphy of unit 3 is not further differentiated.

Seismic unit 4

Unit 4A is commonly filling truncations at the top of unit 3 and is frequently observed over depressions of the underlying units (e.g., Fig. 2). It is mostly characterized by a chaotic high-amplitude internal appearance, but infrequently parallel internal laminations are observed. Unit 4A is observed down to 32 m b.s.l., with a maximal thickness of less than 2 m. It is separated by a sharp, erosional unconformity against seismic unit 5 (e.g., Fig. 8). Based on

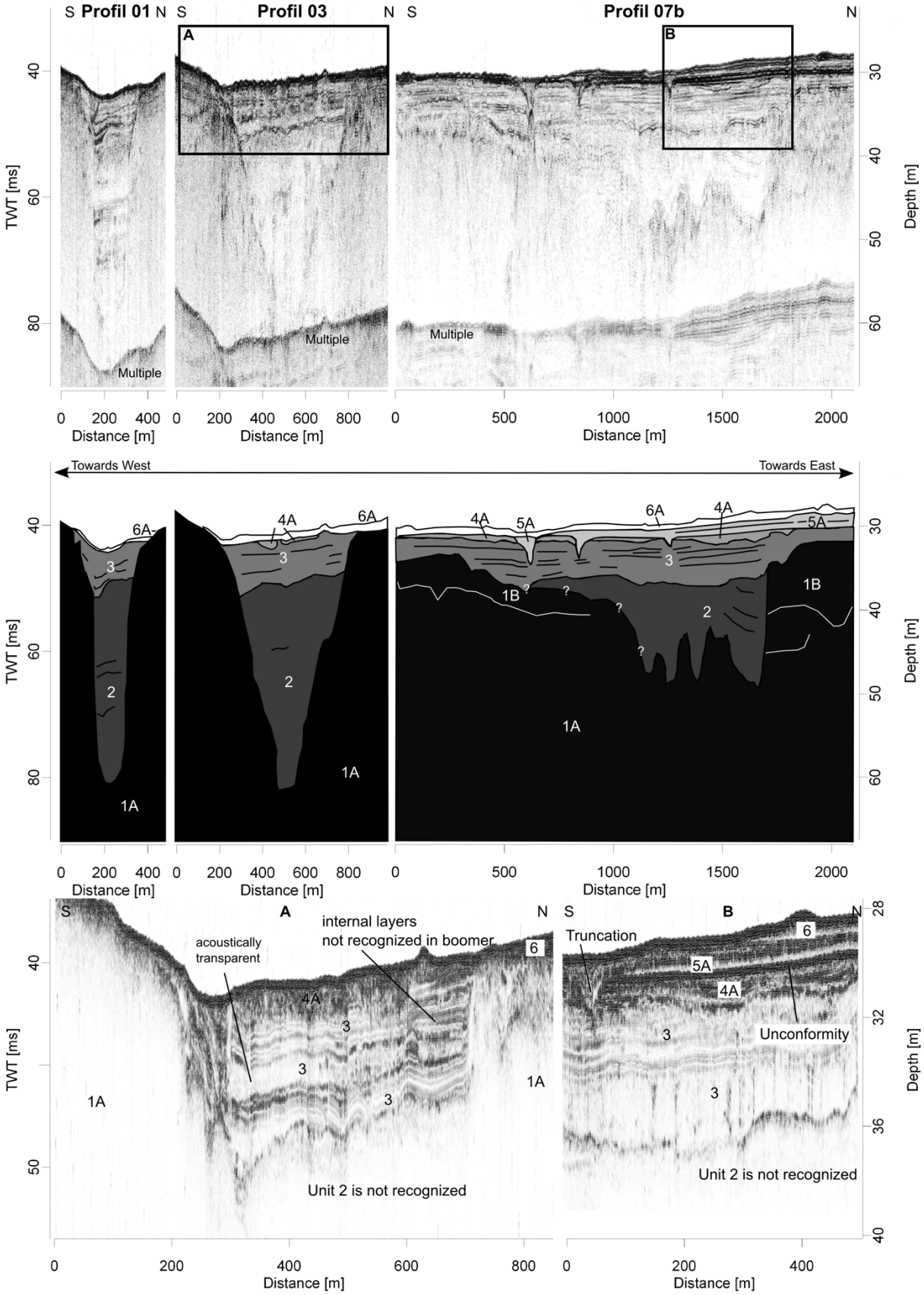

Fig. 6: Details of several seismic profiles showing the widening of the buried channel to the east. The maximal incision depth of the channel exceeds 60 m. Top: Data recorded with the boomer system, v_{ex} approx. 38x Bottom: Details based on subbottom profiler data, v_{ex} app. 47x. The interpretation is based on the boomer records. See text for details.

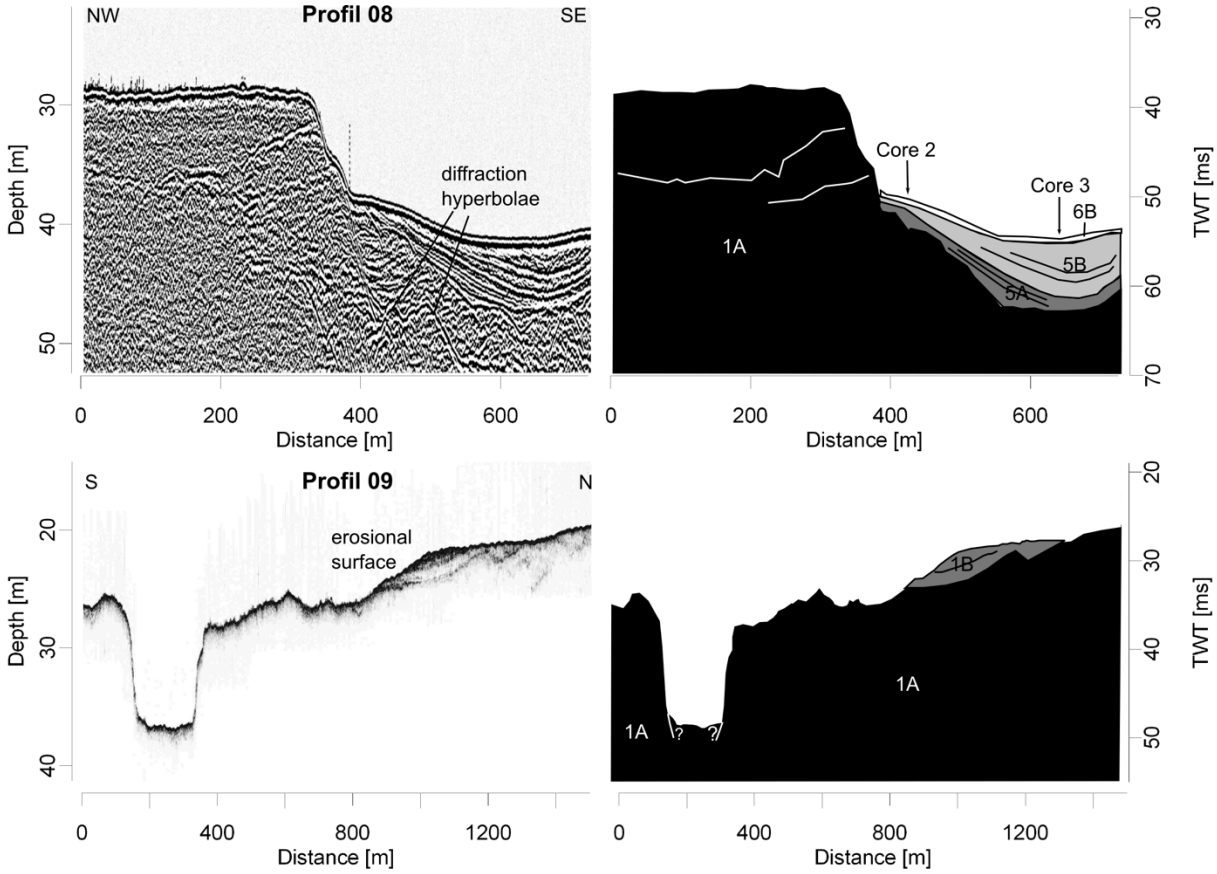

Fig. 7: Top: Detail of a seismic profile (C-Boom) crossing the deepest part of the channel as observed in bathymetric data. v_{ex} approx. 17x. Bottom: An erosional surface, forming a small escarpment, is observed between 21 and 25 m. Recorded with a sediment echo sounder, v_{ex} approx. 34x.

vibrocore 05 (Fig. 9), unit 4A is partly composed of peat deposits that are deposited below an erosional boundary. The peat was retrieved at a core depth of 266 cm (app. 27.5 m b.s.l.) and was dated to 9,450 +- 40 ^{14}C yr. BP. This age corresponds to the time interval between the second regression of the Baltic Ice Lake and prior to the Ancylus Lake highstand. The age and depth of the peat (unit 4A) are situated slightly below the eustatic sea level curve for the Arkona Basin (Jensen 1995, Bennike and Jensen 1998, compiled by Lampe 2005).

Unit 4B is only recognized locally (Fig. 2, profile 108 in Fig. 8), in the same area where N-S striking ridges appear in the bathymetric data. Appearing acoustically transparent, it is deposited between units 3 and 5A, with a maximal thickness of approx. 2 meters. Reflections of unit 5A overlap on the upper surface of 4B (Fig. 2A). The lower boundary to unit 3 is only faintly visible, and its type cannot be recognized based on the available data. The unit is fading to the east and north. To the west, an increasingly chaotic internal appearance prevails (marked in Fig. 2). Potentially, the source area of this unit is a small escarpment at 21 to 23 m b.s.l. (profile 108 in Fig. 8), from which material is transported downwards.

Seismic units 5 and 6

Unit 5A, recognized inside and outside the river channel (e.g., Figs. 5 and 7), is characterized by parallel internal laminations. Generally, its lower boundary is unconformable, although the upper boundary to sediments of unit 6 is conformable. Outside of the channel, its onset is observed at a small escarpment at approx. 25 m b.s.l. in the north and south of the Fehmarn Belt (Figs. 5 and 8).

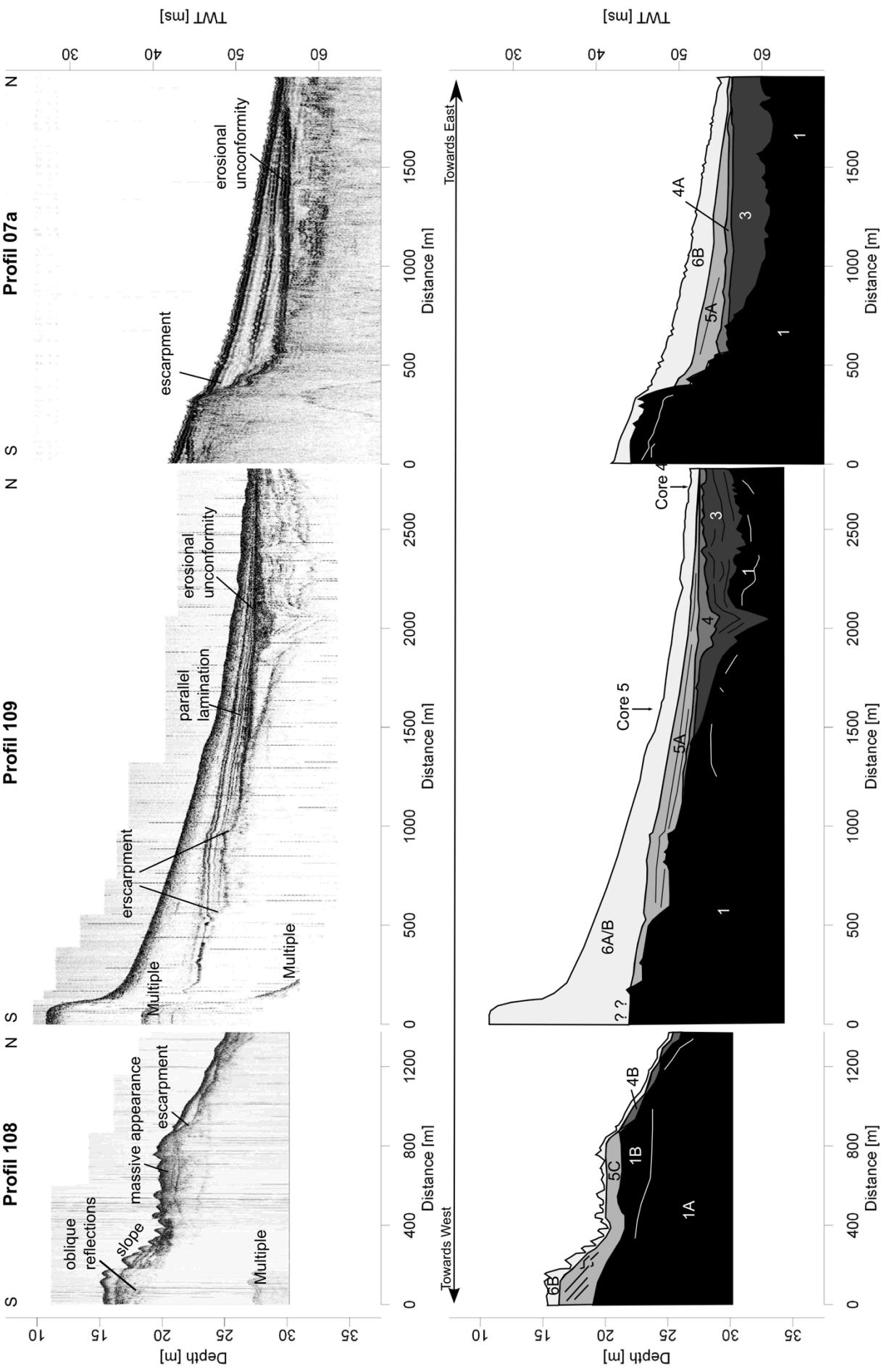
Profil 108
Profil 109
Profil 07a
S
N
oblique reflections
slope
massive appearance
escarpment
Multiple
erscarpment
parallel lamination
erosional unconformity
escarpment
Depth [m]
TWT [ms]
Distance [m]
Towards West
Towards East
Core 5
Core 4
6A/B
5A
4B
5C
1B
1A
6B
4A
6B
5A
3
4
1

Fig. 8. Previous page: details of seismic profiles crossing escarpments visible of approximately 25 m b.s.l. Profile 108 and 109 were recorded with a subbottom profiler, profile 109 was recorded with a boomer. v_{ex} approx. 63x.

The thickness of unit 5A, 1.5 to 2 m at maximum but more in incisions of underlying units, continuously decreases towards the center of the Fehmarn Belt, where the unit disappears completely (Fig. 8). Material of seismic unit 5A partially fills small truncations incised in underlying units. Typically recognized in water depths approx. 30 m b.s.l., these incisions reach a depth of up to 3 m and a width of up to 100 m (Fig. 6). It is uncertain whether the incisions are part of a continuous channel system or local depressions. Seismic unit 5A is represented by predominantly silty material showing cm-thick laminations without notable change in material (vibrocore 05, Fig. 9). A wood fragment retrieved close to the top of this unit has an age of 7,610 +- 40 ^{14}C yr. BP, representing the early phase of the Littorina Sea.

In the river channel, interbedded sand and silt layers (vibrocore 2, Fig. 9) represent the internal lamination visible in the seismic data. Wood fragments in the silty material indicate an age of 7,860 +- 40 ^{14}C yr BP at 99 cm core depth to 7,450 +- 35 ^{14}C yr BP at 232 cm core depth. Here, older material deposited on younger sediments points to reworking. Meanwhile, all material was deposited after the onset of the Littorina Sea transgression.

Seismic unit 5B is only recognized in the river channel (Fig. 7), where it is conformably deposited above sediments of unit 5A. In the seismic images, the unit shows a chaotic internal appearance represented by an approx. 1 m thick sequence of silt and sand, containing an abundance of shell fragments (vibrocore 3, Fig. 9). ^{14}C dating shows that carbonate fragments have an age of 4,975 +- 40 ^{14}C yr BP at 13 cm core depth, 6,645 +- 40 ^{14}C yr BP at 112 cm core depth and 7,220 +- 45 ^{14}C yr BP at 200 cm core depth.

Unit 5C is only recognized locally between 13 and 20 m b.s.l. (profile 108 in Fig. 8) Internally, oblique reflections, sharply terminated by the boundary to unit 6B, dip towards the center of the Fehmarn Belt. At approx. 20 m b.s.l., the internal appearance is dominantly massive, but faintly visible and almost horizontal laminations are partly recognized. The slope at the transition between the massive and oblique appearance appears in bathymetric data throughout the subaqueous dune field (marked with "j" in Fig. 2). However, the transition between unit 5C and other seismic units is uncertain, and its stratigraphic position is therefore speculative.

Sediment unit 6A is conformably deposited above unit 5A and composed of acoustically mainly transparent material, with faintly visible internal lamination (e.g., Fig. 5). Its maximal thickness is 3 m, and the unit disappears towards the center of the Fehmarn Belt. The appearance of continuously coarser surface sediments towards the center of the Fehmarn Belt (Kaufhold 1995) is related to the fading of unit 6A. Separated by an unconformity from units beneath it, seismic unit 6B forms the subaqueous dune field observed on the slope towards Fehmarn (profile 108 in Fig. 8).

4. Discussion

4.1 Depositional environment

Four different sediment facies appear in the research area. They are related to glacial environments (seismic unit 1), sediments deposited following the last glacial and through the Baltic Ice Lake time (seismic units 2 and 3), those deposited prior to the regression of the Ancylus Lake (seismic unit 4) and those deposited subsequent to the Ancylus Lake regression to the present day (seismic units 5 and 6).

The appearance and poor sorting of sediment comprising seismic unit 1A is typical for glacial till, which is widespread in the Baltic Sea (e.g. Niedermeyer et al. 2011). Due to the

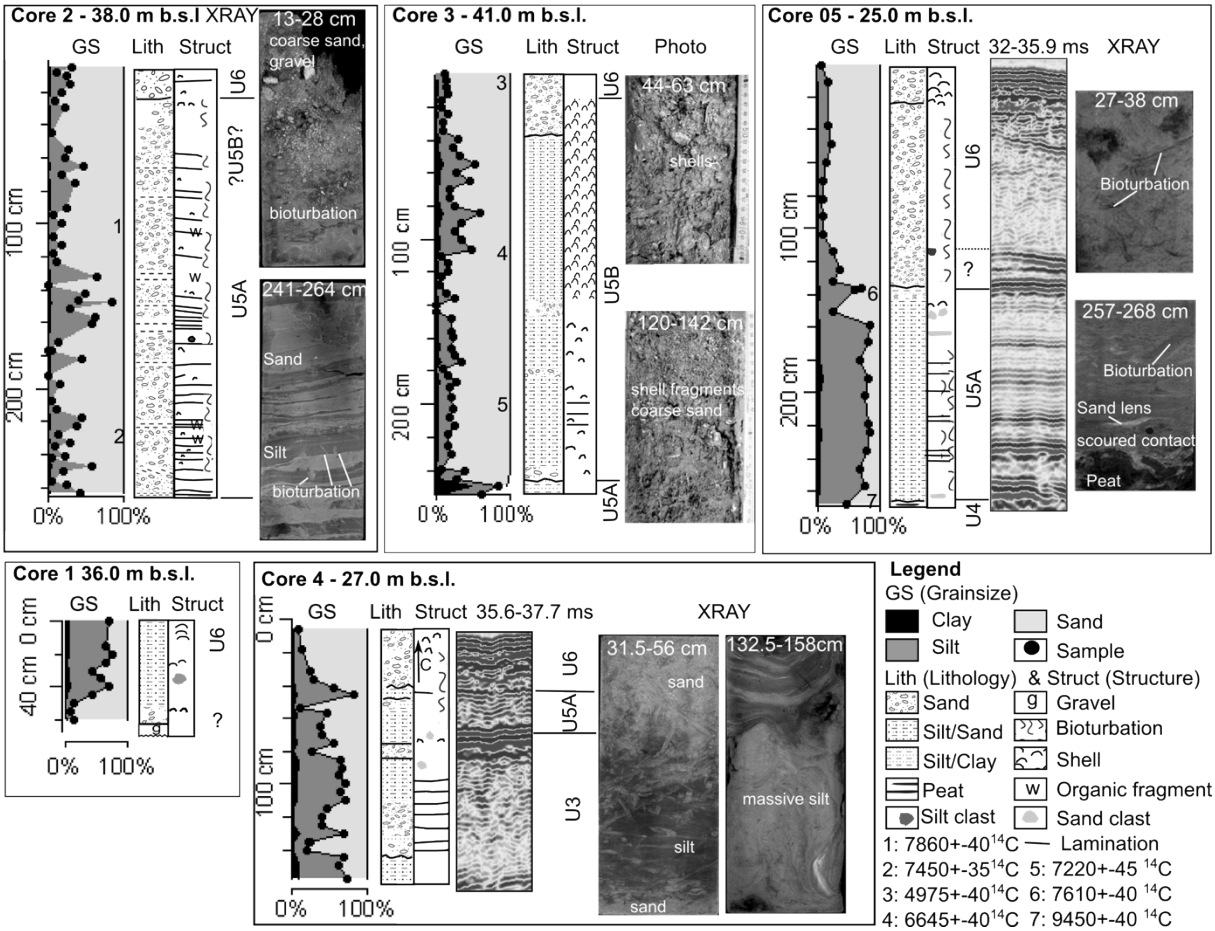

Fig. 9: Sediment cores 01 to 05. The corresponding seismic units are mentioned. For positions, refer to Fig. 2. Subbottom profiler data (Innomar) is available over the positions of cores 4 and 5. Here, a direct correlation between sediment layers and seismic reflectors is possible.

recognized internal structure, unit 1A is interpreted as a succession of various glacial till deposited during the Elsterian and/or Weichselian glacial. Where seismic unit 1A crops out at the seafloor surface, it is covered by a thin layer of lag deposits due to winnowing processes.

The homogenous but not entirely transparent internal appearance of seismic unit 1B is typical for sandy sediments (e.g., similar to unit 5D), where little variation of the acoustic impedance is observed. Given that the ice margins during the last two ice advances of the Young Baltic Ice advance were situated at the Flensburg Fjord and the Darss Sill (Stephan 2001), seismic unit 1B might be either interpreted as glacial till deposited during the last ice advance, although in this case a less homogenous seismic appearance would be expected, or as a deposit in the ice marginal environment. In the latter case, it is to be interpreted as flow till (Menzies 2003).

The buried channel was infilled with sediment comprising seismic unit 2. Similarly to unit 1B, its internal acoustic appearance points towards a mainly sandy composition, probably similar to a sediment filling a buried channel in the Darss Sill area (Lemke et al. 1994, Lemke and Kuijpers 1995) or late-glacial sand deposits forming the Falster-Rügen sand plain (Lemke et al. 2001). Partly visible internal layers in the deepest part of the units point to changing energy conditions, allowing for the deposition of different material. Given the markedly different appearance in the seismic images, indicating different lithology, and the irregular shape of the boundary between seismic unit 2 and 3, a hiatus, different environmental conditions and potentially some erosion between the deposition of these two units can be expected.

The internal configuration of seismic unit 3 corresponds to seismic unit W3 of Jensen et al. (1999), which was dated to the Baltic Ice Lake time. It is commonly recognized in the eastern Fehmarn Belt and Mecklenburg Bay area (e.g. Kolp 1986, Jensen et al. 1999). No dateable material was found within this unit, but its deposition below unit 4, dated to the early Anclyus Lake time, further supports a BIL-time of unit 3. The appearance of originally parallel internal layers within unit 3 supports deposition in a lake environment. The deformation of these internal layers, easily observed in most of the seismic profiles, may be related to post-depositional processes, e.g., compaction. Partly, the internal layering appears chaotic, as represented by core 4. During the BIL phase, none of the research area was more than a few kilometers from the coastline of the lake and was therefore subject to events (e.g., storms) that were able to disturb sedimentary layers or deposit event layers.

Peat, part of seismic unit 4A, was deposited subsequently to the final Baltic Ice Lake regression and prior to the Ancylus Lake highstand. Organic material of a similar age is reported to the east in the Mecklenburg Bay area at approx. 30 m b.s.l. (Jensen et al. 1997). Although separated from the main Baltic Ice Lake, and therefore not directly affected by its regression, the Fehmarn Belt and Mecklenburg Bay area water level lowered below the Darss Sill threshold (Jensen et al. 2005). This may relate to missing water inflow from the main Baltic proper over the Darss Sill, while outflow from Mecklenburg Bay was not hindered. Minimal water level values reported in Mecklenburg Bay and the Arkona Basin are similar, following the BIL regression (as shown in Lampe 2005, Jensen et al. 2005). This suggests a connection despite the morphological separation; this is also supported by the age and depth values of peat retrieved in the Fehmarn Belt, agreeing with a water level curve for the Arkona Basin. A groundwater connection may have existed between Mecklenburg Bay/Fehmarn Belt and the Arkona Basin. Similar water exchange, albeit on a smaller scale, is observed between isolated wetlands and nearby river streams (Winter and LeBaugh 2003). Whether a water exchange through groundwater is feasible heavily depends on the sediment composition within buried meltwater channels (Lemke et al. 1994), which would form a continuous aquifer. With an assumed distance of 20 km between the lakes east and west of the Darss Sill, a hydraulic gradient of 5 m, a connection through buried channels with a combined surface area of 25.000 m^2 and a hydraulic conductivity of 10^{-4} m/s (representing a sandy infill, Lemke et al. 1994), groundwater discharge would be app. $2*10^{-5}$ km^3/a according to Darcy's law. At this level, it would require 30.000 years to lower the water level in Mecklenburg Bay and the Fehmarn Belt from 25 to 30 m given that the volume between these two depths is approx. 0.6 km^3, based on the bathymetric data of Seifert et al. (2001), for the area between the Darss Sill and the western entrance of Fehmarn Belt. However, if parts of the meltwater channel are mainly composed of gravel, with a hydraulic conductivity of 10^{-2} m/s, water levels could align across several hundred years. Although these are only rough estimates, it shows that a groundwater connection has to be kept in mind when explaining corresponding minimal water levels east and west of the Darss Sill.

With the water level below 30 m following the BIL regression, large parts of the research area were exposed to subaerial erosion, explaining the partially observed erosional unconformity between unit 3 and unit 4A. Unit 4A comprises deposits of shallow water bodies and bogs (notably peat and gyttja), either remaining after the regression of the BIL or created with the rising water level at the beginning of the Ancylus Lake phase (Jensen et al. 2005).

The presumably sandy, homogenous material of unit 4B may originate from a small cliff observed between 20 to 22 m water depth, eroded during a highstand of a lake. Ridges observed in the bathymetric data in this area are potentially composed of the same material. The stratigraphic position of unit 4B above unit 3 and below unit 5A (Fig. 4A) suggests that the cliff was active during the highstand of the AL lake in the Fehmarn Belt, which was

around 20 m b.s.l. (Jensen et al. 2005, Lampe 2005). To the west, the chaotic appearance of this unit in seismic images, combined with a lack of clear unit boundaries, might correspond to a later reworking of sediment following deposition. This is supported by the existence of an incised tributary at 30 m b.s.l. in close vicinity.

Sediment comprising units 3 and 4 were eroded during a later event, as indicated by the marked erosional unconformity beneath unit 5A (e.g. Figs. 4, 5 and 8) and the general scarcity of preserved early AL-time deposits in our study area. This is in contrast to the eastern Mecklenburg Bay and Fehmarn Belt, where deposits of Ancylus Lake time are more frequently observed (e.g. Kolp 1986, Novak and Björck 2002, 2004).

The sediments of unit 5A were deposited in a lake environment at the end of the Ancylus Lake phase and the beginning of Littorina Transgression. During this time, freshwater conditions were still prevalent in the SW Baltic, despite the established connection to the Atlantic Ocean (Winn et al. 1986). This is supported by the age and depth of a wood fragment deposited close to the shoreline of a water body (seismic unit 5A, vibrocore 5) that agrees with the eustatic sea level curve by Mörner (1976), as presented by Lampe (2005). Similar sediments were dated by Jensen et al. (1999) to the time of the AL-Lake, following its regression. Following the regression of the AL and during the beginning of Littorina Transgression (initial Littorina Transgression according to Andrén et al. 2000), freshwater conditions were not changing significantly (Winn et al. 1986), except for a continuously rising water level. Therefore, the deposition of a continuous sedimentary sequence can be expected. Again, interbedded sand and silt layers correspond to the regular occurrence of events (Palinkas et al. 2006), such as storms. The reworking of material during events may explain the deposition of older material on top of younger sediments in the channel. With increasing marine and higher energy conditions, shells were washed together in the local depression of the river channel close to the Öjet, forming seismic unit 5B.

The oblique reflections of unit 5C and its unconformable boundary against unit 6 are typical indications for progradation and continuous erosion, and they likely relate to a local water level – lacustrine, or more likely, marine – highstand. However, the timing cannot be decided based on the available data, as the stratigraphic position of unit 5C to units 2, 3, 4 and 5 is unknown. Seismic units 6A and 6B represent the most recently deposited sediments in the research area and were deposited during the Littorina Transgression, which is not the focus of this study.

4.2 Formation of the river channel

According to the general morphological appearance, the minimal depth of the onset of the river slope and the depth of the tributaries, the maximum water level in the river was approx. 30 to 32 m b.s.l. Water level curves recently published for the Arkona Basin (Lampe 2005) and shore levels for the Fehmarn Belt (Jensen et al. 2005) indicate that such water levels were present before the BIL time and following the initial and final regression of the Baltic Ice Lake. Kolp (1986) also reports water level of 32 m b.s.l. in Mecklenburg Bay following the Ancylus Lake regression.

The possible water discharge through the channel in the Fehmarn Belt was calculated along a 991 m long section of the river channel close to the Öjet (indicated in Fig. 2), where its narrow shape can be clearly defined, and glacial till was observed at the base of the channel. The volume beneath an upper surface of 31 m b.s.l. is app. 1.23 x 10^6 m³ in the area considered for the flow volume calculation. The average cross section equals 1250 m², accounting for small irregularities in the channel shape along the observed length. With an assumed flow velocity of 1 m/s, the discharge of the river is two orders of magnitude larger compared to today's discharge of the local Trave and Warnow rivers flowing into

Mecklenburg Bay (8 m^3/s and 19 m^3/s, source: "Küstenatlas Ostsee", www.ikzm-d.de, queried 19.01.2011). The potential discharge seems rather large for the drainage of a local lake in Mecklenburg Bay that had no direct connection to the main Baltic proper at a water level of 30 m b.s.l. Because seismic units 2 and 3 were deposited during or before the BIL period, the river channel must have been shaped during an earlier period. Therefore, the river channel was originally formed as a glacial meltwater system that seismic unit 2 deposits would represent. In the southern Baltic, NE-directed glacial drainage is reported in the Darss Sill area (Lemke and Kuijpers 1995), and previous glaciofluvial channels were filled with sandy material (Lemke et al. 1994) during the initial transgression of the Baltic Ice Lake (Lemke and Kuijpers 1995).

A threshold in the southern Langeland Belt is reported to rise above 30 m b.s.l. (indicated in Fig. 1) when stripped of its postglacial infilling (Lemke et al. 2001, Jensen et al. 2005). The nature and potential relative movements of this threshold should be investigated in more detail because a natural dam of glacial till above 30 m b.s.l. in close vicinity would prevent the existence of the observed river channel with a water level at or slightly below 30 m b.s.l.

Due to its changing depth and its quick widening and fading towards Mecklenburg Bay, the channel system may have originally been incised subglacially (Lutz et al. 2009). Such subglacial channels were incised up to several hundred meters during the Elsterian glacial and were frequently reactivated as subaerial meltwater channels during the Weichselian glaciation (Stuckebrandt 2009). These channels are widespread in northern Germany (Stuckebrandt 2009), Denmark (Jørgensen and Sandersen 2009) and the North Sea (Lutz et al. 2009).

The deposition of seismic unit 3 was not confined to the river channel (Fig. 5) and displays no obvious signs of fluvial deposition, indicating that the channel was not active during the majority of the BIL phase. Following the regressions of the BIL, at a water level of around 35 m b.s.l., the Fehmarn Belt was likely dominated by small, local water bodies, with subaerial erosion responsible for the observed unconformities. This is in agreement with the findings of Lemke et al. (1994) that state that buried channels at the Darss Sill were not reactivated during the BIL stage and that calm conditions prevailed.

4.3 The AL regression in the Fehmarn Belt

The most marked erosional unconformity in the study area is situated beneath unit 5A (e.g., Fig. 4), frequently observed at approx. 28 to 30 m b.s.l. Because this unconformity separates seismic unit 3 and 4 from unit 5A, it was formed subsequent to the final regression of the Ancylus Lake and before the onset of the Littorina transgression. Its origin may be related to the westward drainage of a previously dammed lake with a maximum water level of 19 to 20 m b.s.l. (Novak and Björck 2002). This drainage took place either after the final BIL or the AL regression, leading to the development of a fluvial system with a water level of approximately 25 m b.s.l. and continuously decreasing energy levels (Novak and Björck 2002, Novak and Björck 2004). Based on our data, this event occurred following the AL highstand.

This highstand might be preserved by a cliff between 20 to 22 m b.s.l. Geomorphological indications of the water level subsequent to the lake regression from 20 m to 25 m b.s.l. (Novak and Björck 2002, Novak and Björck 2004) are still visible in the form of cliffs north and south of the river channel between 24 and 26 m b.s.l. Similar cliffs, dated to the AL time, were observed at a slightly higher level of 23 m b.s.l. in Mecklenburg Bay (Kolp 1986). Isostatic effects may explain the depth difference. The base of unit 5A was interpreted to have been deposited following the AL regression and is found up to this water level as well.

The volume beneath an upper surface of 24 m b.s.l. is approx. 6.44 x 10^6 m³ in the area considered for the flow volume calculations, yielding an average cross section of 6500 m². The freshwater discharge of the entire Baltic Sea is given with app. 4.8 x 10^{11} m³/a, with discharge during the Boreal not significantly different from today (Lemke et al. 2001). A realistic flow velocity of approx. 2.3 m/s would be required to drain the Baltic freshwater discharge at this water level. The huge potential discharge combined with strong indicators of erosion support the model of Björck et al. (2008), suggesting a 5 m water level drop by an outburst of the AL across the Darss Sill along the pathway previously suggested for the Dana River. The event was also responsible for erosion of material deposited prior to the AL highstand from the channel south of the Öjet. Due to the decreasing cross-section south of the Öjet, flow velocity and erosive power were increasing. Further along the suggested course to the Kattegat, fluvial deposits dated to the maximum level of the Ancylus Lake were described in the Great Belt (Bennike et al. 2004, Jensen et al. 2005).

Originally, the erosion of the Cadet Channel from 20 to 32 m b.s.l. was attributed to this drainage (Lemke et al. 1994). However, no prograding system could be found east of the Darss Sill (Lemke et al. 2001), and the Cadet channel was interpreted as a succession of kettle holes. No major erosive action could take place at the Darss Sill. Most recent publications agree that the AL highstand transgressed the Darss Sill (e.g., Jensen et al. 2005), although older publications saw the Darss Sill as the southwestern boundary of the AL (e.g. Björck 1995). In this context, when no signs of strong erosion are present in the Darss Sill area, but signs of strong erosion and a westward directed drainage of a lake are found in the Fehmarn Belt (Novak and Björck 2002), the dam separating the Ancylus Lake from the Kattegat should be located west of the Fehmarn Belt.

Additionally, we cannot rule out a further water level decrease below 25 m b.s.l. following the AL regression in the Fehmarn Belt area based on our data. Small incisions filled by sediments of seismic unit 5A, frequently observed down to 30 m water depth, might be part of a local drainage system. Fluvial conditions in the northeastern Fehmarn Belt with a water level less than 25 m b.s.l. were also suggested by Novak and Björck (2002) and Kolp (1986). As water levels east of the Darss Sill fell below 25 m b.s.l., with a water level of 32 m b.s.l. reported for the Ancylus Lake NE of the island Rügen (Lemke 1998) and a water level of approx. 28 m b.s.l. in the Arkona Basin (Lampe 2005), a corresponding water level should be expected west of the Darss Sill. This indirectly lowering water level, however, would still only allow for a partial drainage of the AL over the Darss Sill.

The lack of any lake deposits in the eastern part of the study area remains interesting. Although it is reasonable to expect that material deposited before the Littorina Transgression was eroded by the erosional event during the Ancylus Lake regression, only in the deepest section of the channel little sediment that was deposited during the Littorina Transgression was preserved. This marked difference is clearly observed in seismic E-W profiles (Fig. 2). At water levels around 20 m b.s.l., comparably large water bodies to the east and west are connected through the narrow cross-section south of the Öjet (Fig. 1). During storms directed from east and west, large water masses that were potentially able to erode sediment deposited during calmer periods had to move through this area. This effect might still be active today given that little sedimentation is observed in the channel south of the Öjet.

5. Conclusion

Hydroacoustic and sedimentological data gathered in the western part of the Fehmarn Belt suggests the following:

1. A paleo-river channel incised into the seafloor off Fehmarn was part of a glacial meltwater system, at a maximal water level of approx. 30 m b.s.l.

2. During the time of the Baltic Ice Lake, calm conditions prevailed in the river channel.

3. A previously reported drainage of a lake in the eastern Fehmarn Belt (Novak & Björck 2002) took place at the time of the Ancylus Lake regression, leading to an app. 5 m water level drop down to 24-26 m b.s.l. and to widespread erosion of older sediments in the western Fehmarn Belt.

4. The timing, water level and potential water discharge of this drainage event suggests a connection to the main Baltic proper, supporting a partial drainage of the Ancylus Lake over the Darss Sill through the pathway of the Dana River (Björck et al. 2008).

3. Genesis and sediment dynamics of a subaqueous dune field in Fehmarn Belt (south-western Baltic Sea)[2]

P. Feldens[1], K. Schwarzer[1], C. Hübscher[2], M. Diesing[3]

[1] Institute of Geosciences, Department of Sedimentology, Coastal and Continental Shelf Research, Christian-Albrechts-University, Olshausenstr. 40-60, D-24118 Kiel, Germany

[2] Institute for Geophysics, Center for Marine and Climate Research, University of Hamburg, Bundesstrasse 55, D-20146 Hamburg, Germany

[3] Centre for Environment, Fisheries and Aquaculture Science, Remembrance Avenue, Burnham-on-Crouch, Essex, CM0 8HA, United Kingdom

Abstract

A subaqueous dune-field, consisting of large bedforms, is located in Fehmarn Belt, south-western Baltic Sea. These bedforms have been investigated several times but their genesis and recent dynamics is not completely understood. Application of high-resolution hydroacoustic methods allows further insight into the development and dynamics of these structures. An area of approximately 75 km² has been mapped in full coverage with a multibeam echo sounder. Additionally, 40 nm (nautical miles) of high-resolution shallow water seismic profiles (parametric echo sounder and boomer-system) have been recorded. The subaqueous dune-field is situated in water depths of about 11 to 25 m, with an extension of about 8.1 km E – W and 1.8 km N - S. It consists of asymmetric dunes with crest heights of up to 2.5 m. The sediment of the subaqueous dune-field is composed of allochthonous, well sorted medium to coarse sand, forming a sediment layer of up to 4.5 m thickness. Sand ribbons, connected to the subaqueous dune-field and protruding from the field towards the south-west, are supposed to be sediment-conduits. Based on repeated bathymetrical mappings during a 1.5 years period, no movements of the dune crests have been observed in the central part of the subaqueous dune field. However, compared to older maps an increase in the spatial extension of the subaqueous dune field towards west and southwest has been observed due to newly formed bedforms. It is assumed that sediment movements in the subaqueous dune field occur mainly during west-storm conditions, when salt water intrudes from the North Sea into the Baltic Sea.

1. Introduction

Fehmarn Belt is located in the south-western Baltic Sea (fig. 1) between the islands Lolland (Denmark) and Fehmarn (Germany). Fehmarn Belt is of special importance for the hydrographical setting of the Baltic Sea, as about 70% of the water exchange between North Sea and Baltic Sea is passing through it (Lemke 1998). According to Werner (1974), the cross section surface of Fehmarn belt close to the research area is about 0.4 km², with a distance of about 20 km between Fehmarn and Lolland. In the future, the importance of Fehmarn Belt will increase, due to a planned connection between the islands. Previous studies (Werner et al.

[2] This article was published in „Marburger Geographische Schriften, 2009, Vol. 145, p. 80-97. Reprinted with permission of the „Marburger Geographische Gesellschaft“.

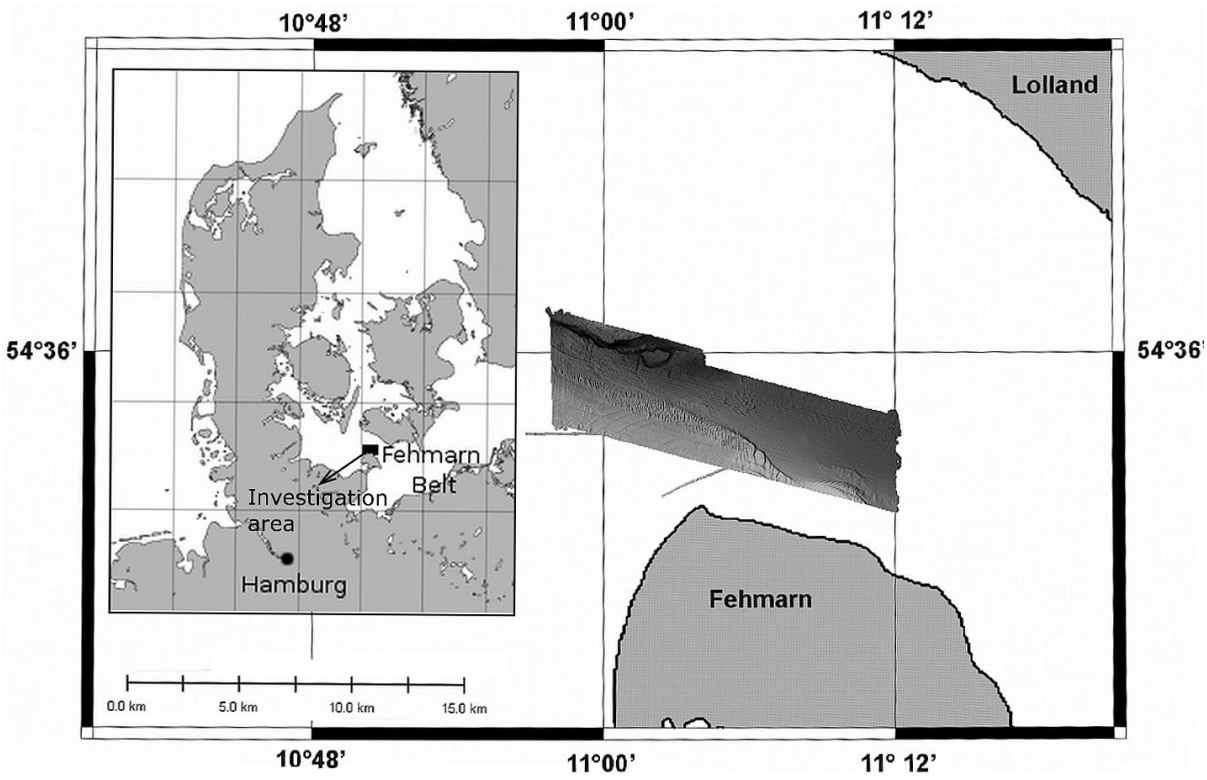

Fig. 1: Overview of the investigation area at Fehmarn Belt, including the obtained bathymetric data.

1974; Kaufhold 1988) describe an area consisting of large to very large subaqueous dunes situated at the south-western entrance of Fehmarn Belt. However, up to the present it could not be clarified conclusively, how these bedforms have been formed and if they are dynamic or stationary. In this study we focus mainly on the dynamics of the large-scale bedforms. To obtain information about the sediment dynamics in the subaqueous dune-field, new bathymetric- and shallow water seismic data were combined with results taken from older studies. Bedform classification is done based on the classification by Ashley (1990), who considers all flow-transverse bedforms with a length exceeding 0.6 m as subaqueous dunes (small dunes: 0.6 - 5 m; medium dunes: 5 - 10 m; large dunes: 10 – 100 m; very large dunes: > 100 m). Large subaqueous dune fields are formed in areas with high current velocities. They are commonly known from areas strongly influenced by tides, for example tidal inlets, where the dunes are highly dynamic, due to the changing current direction over a tidal cycle (e.g. Bartholdy et al. 2002). However, in the Baltic Sea no tidal influence is present, and comparatively stable subaqueous dune fields are mainly reported in the narrow straits between Kattegat and Baltic Sea (Kuijpers 1980).

In our study we will use the following abbreviations:

SDF = Subaqueous Dune Field
H = height of a subaqueous dune
L = distance between two subaqueous dune crests (wavelength)
d = water depth

2. Previous investigations

The SDF at Fehmarn Belt has been investigated several times. Werner et al. (1974) describe its spatial dimensions with 7 km in E-W direction and 2 km in N-S direction. Different values are given by Kaufhold (1988) and Werner (2000); both authors report extensions of 9 km in E-W direction and 1.5 km in N-S direction, whereas Milkert & Fielder (2002) found values

of only 6 km E-W and 3 km N-S. For the boundaries of the SDF given by Werner et al. (1974) and Kaufhold (1988) see figure 12. According to the investigations by Werner et al. (1974), the SDF is mainly built up of medium sand. A steep slope, striking NW – SE in water depths from 17 to 20 m, is separating the SDF into two different terraces. The south-eastern part of the SDF ends abruptly at a slope (Werner et al. (1974). To the north, the mean grain size of the sediment changes to silty sand (Werner et al. 1974; Kaufhold 1995), while the sea floor south of the SDF, towards the northern coast of Fehmarn, is composed of lag deposits (Werner et al. 1974; Bux 1982). Observations regarding the SDF-dynamics, based on investigations of benthos organisms, have been made by Werner et al. (1974). They conclude that the SDF has been stable for at least several years. Kaufhold (1988) performed detailed observations of small-scale dynamics in-between the SDF. He found an extension of the SDF towards the west of about 1.5 -2 km, while dunes in the northern part have vanished. Compared to the results of Werner et al. (1974), he observed an enlargement of the area with dune heights of more than 1.8 meters. Based on a comparison with previous investigations, Milkert & Fielder (2002) describe an extension of the SDF towards the west. Comet marks, which are found frequently in the SDF (Jensen & Lemke 1996), indicate a dominant current direction from west to east. Shallow seismic investigations of the SDF with a boomer system have been done by Wittmaack (1988). He concludes that the dunes are deposited on top of a sandy layer, up to eleven meters in thickness, while the base is built up of glacial till.

3. Methods

To obtain a detailed bathymetry of the investigation area, approximately 75 km² have been mapped in full coverage using a multibeam echo sounder (Sea Beam 1185, 180 kHz) which is hull mounted on the research vessel FK LITTORINA. The cruises were carried out in May, June and August 2007. To get information about short term bedform dynamics, parts of the SDF have been mapped twice, in May and in June 2007. Additionally, bathymetric data recorded with the same multibeam echo sounder system in January 2006 were used to get a better insight into the bedform dynamics. Fig. 2 gives an overview of the data. Unfortunately, the depth data taken in 2006 cannot be compared with the data of 2007, due to undocumented changes of the draught of FK LITTORINA. However, the position of the features observed in 2006 and 2007 can be compared. Based on several surveys Ernstsen et al. (2006) estimate the accuracy of a mobile multibeam echo sounder setup with +/- 30 cm in the horizontal and +/- 8 cm in the vertical direction. Dismounting the multibeam echo sounder system between several surveys and rough weather conditions during the surveys were the main factors contributing to the error. In our case the multibeam echo sounder is mounted permanently onboard FK LITTORINA, with a relative error between our surveys in the range of +/- 6 cm in the vertical direction; the horizontal error is negligible. During a cruise with FS POSEIDON in August 2007 approximately 40 nm of seismic profiles were recorded with a parametric echo sounder system (Innomar system, 12 kHz). Additionally, reflection seismic was carried out with a boomer system during a FK LITTORINA cruise in August 2007. For ground truthing 63 sediment samples were taken with a Van Veen grab sampler during the cruises (see Figure 3).

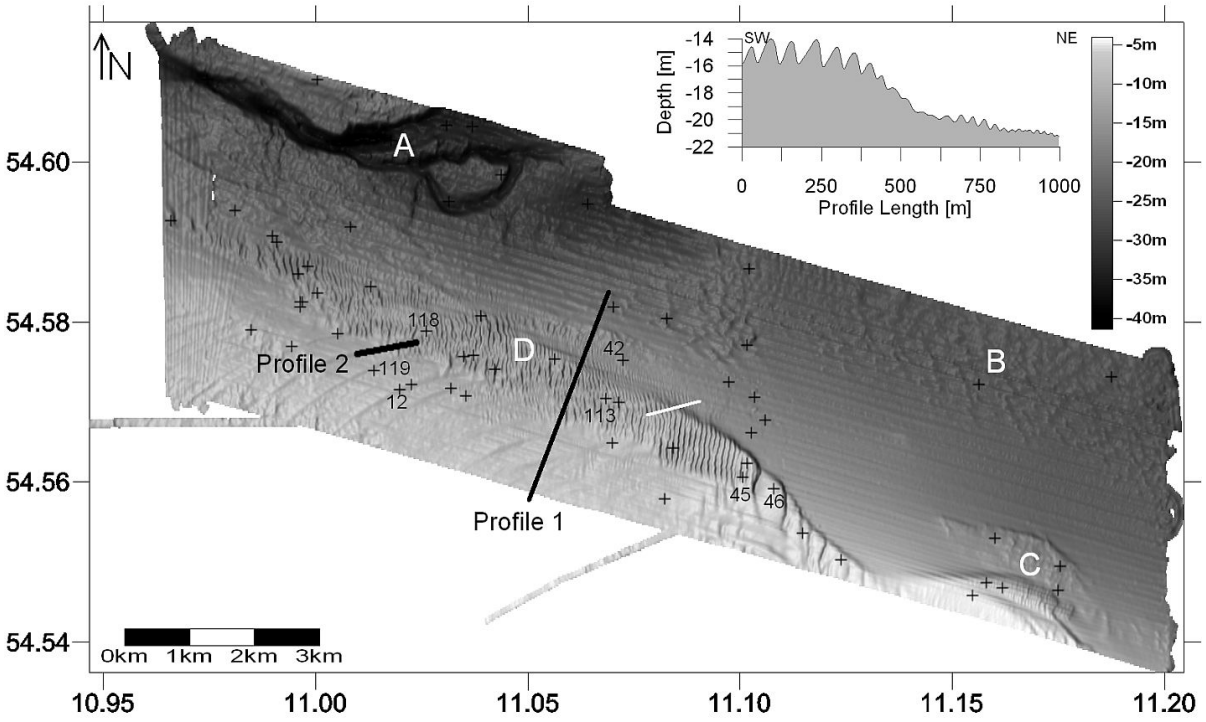

Fig. 2: Overview of the multibeam echo sounder data. A: Ancient river bed. B: Small scale geomorphological elevations. C: Dune-field II. D: Dune-field I. The white line represents the position of the bathymetric profile (upper right) showing the location of the dune-fields in different bathymetric levels. Profile 1 and 2 are the seismic profiles shown in this work. Small crosses represent the available sediment samples. Samples mentioned in this article are numbered.

4. Results

4.1 Geomorphology of the dune field

The bathymetric map is shown in figure 2. Remarkable structures are an ancient river system in the north-west, a series of small elevations in the north and north-east, a smaller dune-field in the south-east and an area with large and very large subaqueous dunes in the south and south-west of the investigation area. Only the area with the large subaqueous dunes (dune field I in fig. 2) will be discussed here.

The SDF, displayed in detail in fig. 3, extends approximately 8.1 km in E-W direction and 1.8 km in N-S direction. It is situated on two terraces in water depths ranging from 11 m to 25 m (see bathymetric profile in fig. 2). All dunes are asymmetric, with their lee side facing towards the east. The height of the bedforms reaches up to 2.5 m in the south-western and from 1 m to 1.5 m in the central part of the field. Crest heights of about 2 m also appear in an elongated extension of the SDF protruding from the main field towards the north-west (see fig. 3). The relation between the distance of the dune crests (L) and the height of the dunes (H) is shown in figure 4. Most of the dunes are situated below the H/L relationship found by Flemming (1988), based on the investigation of 1491 dunes.

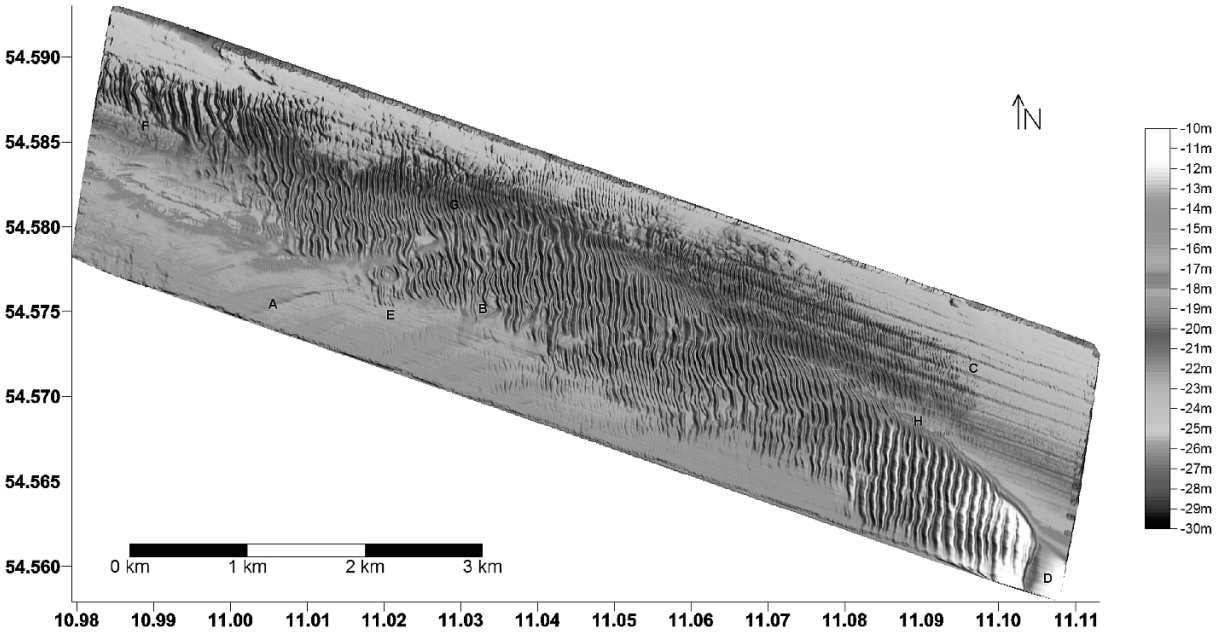

Fig. 3: Detailed view of the area containing the large subaqueous dunes (SDF). A: Sand ribbons. B: Flat surface between dune crests. C: Fading of the SDF in the north-east. D: Abrupt ending of the SDF at an incision in the south-east. E: Sharp onset of the SDF in the south. F: Elongated extension of the SDF in the west. G: Bifurcation of dune crests. H: Steep slope striking through the SDF.

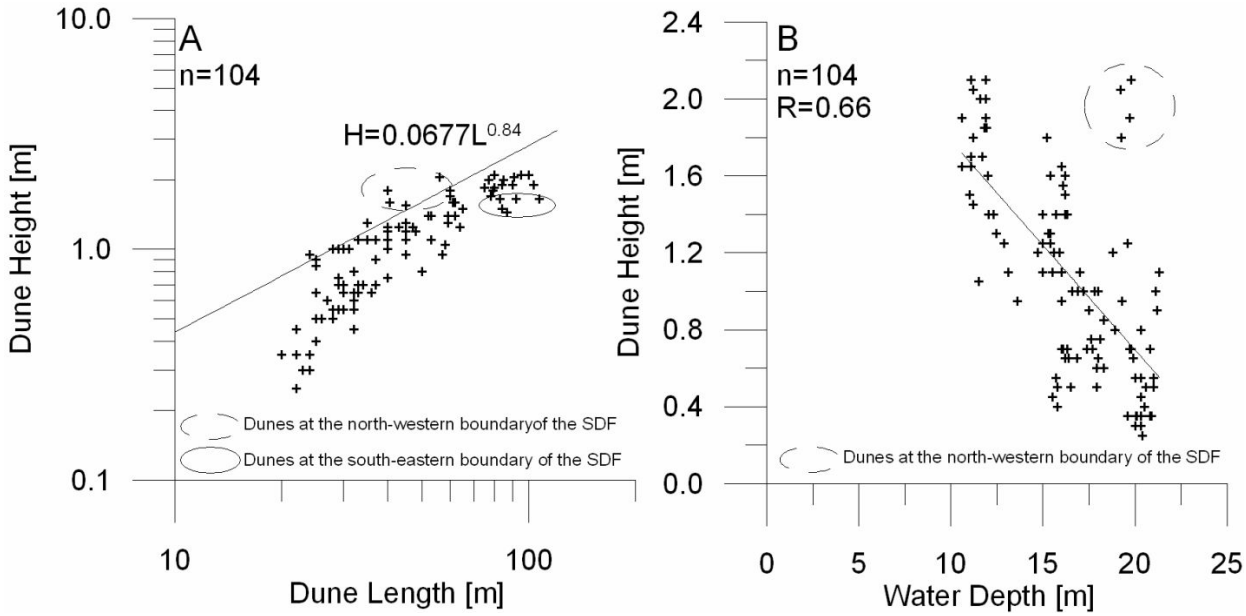

Fig. 4: A: Dune length (L) plotted against dune height (H). The H/L relationship found by FLEMMING (1988) is included. B: Relation between water depth and height of the subaqueous dunes.

Exceptions are dunes located in the elongated extension of the field in the north-west, which plot above the line. The H/L relation of the subaqueous dunes close to the south-eastern boundary of the SDF is lower; compared to the dunes of similar wavelength further east. This decrease in height is also visible in the bathymetric profile displayed in fig. 11C. The correlation between H and the water depth (d) is not very strong (Fig. 4B). Four dunes in the north-western extension of the SDF deviate strongly from all other subaqueous dunes, as H exceeds 2 m in water depths of more than 20 m. Many dune crests are not parallel to each other. In the central part of the SDF flat surfaces between the dunes are visible. The single

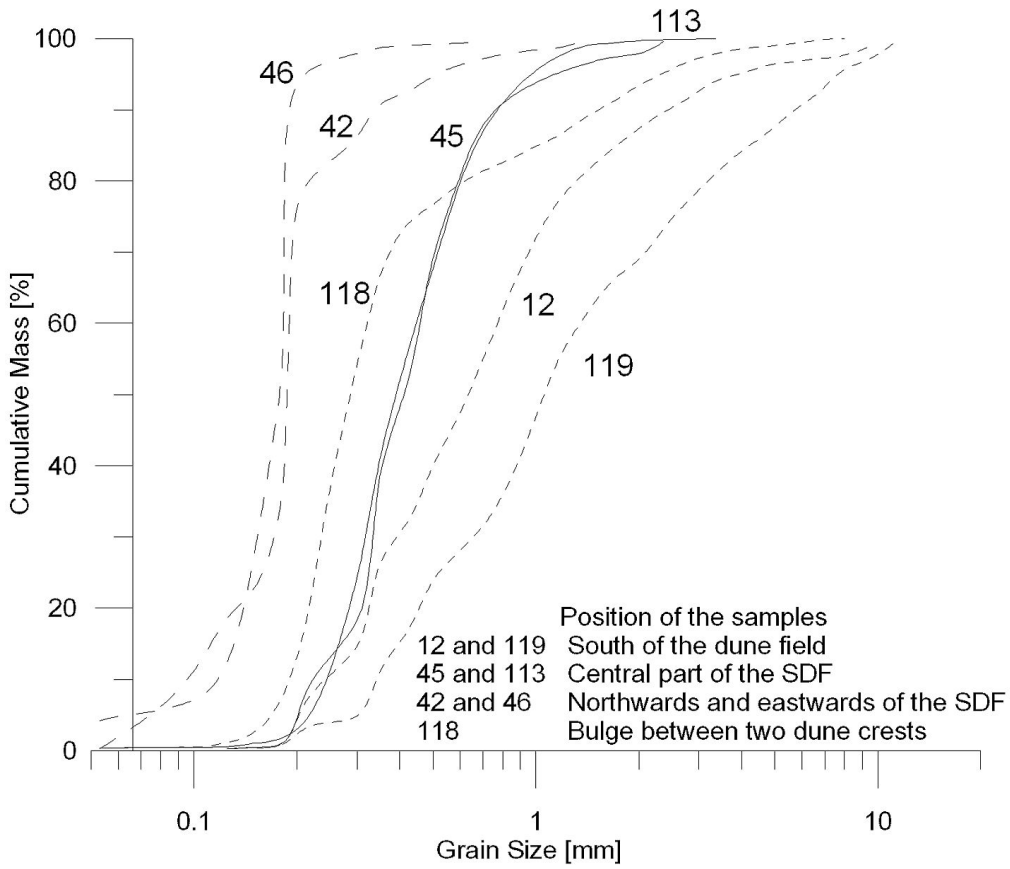

Fig. 5: Grain size distributions of some typical sediment samples from the subaqueous dune field at the south-western entrance of Fehmarn Belt (see figure 2 for exact positions).

subaqueous dunes are generally striking N - S, with some slight variations to NNW-SSE in the north-western part of the SDF and on the slope between the two terraces (visible in fig. 3). The transition from the dunes to the surrounding seafloor is very distinct in the southern part of the SDF; here, sharp contacts can be observed. Towards the south, sand ribbons are found in prolongation of the subaqueous dunes (fig. 3 and fig. 13). The heights of these ribbons vary between 0.5 m and 1 m. The sea floor between the ribbons appears rough in the bathymetric data, especially further to the south-west, indicating lag deposits or exposed till. The SDF fades out smoothly towards the north and north-east. Westwards, the SDF converges and forms an elongated extension. In the south-east, the SDF ends abruptly at an incision about 2.5 m deep (see fig. 11, profile C), as already observed by Werner (1974).

Results of the grain size analysis of some representative sediment samples taken during the cruises are shown in figure 5. Samples representing the central part of the SDF have a very homogeneous grain size distribution, composed of medium to coarse sand. Remarkable is sample 118, obtained from one of the flats between the dunes in the central part of the field. Compared to the samples taken from the dunes, this sample contains a larger fraction of coarse material (coarse sand and gravel). Its coarse part resembles some samples located south of the dune field. At the northern and north-eastern boundary of the SDF, a sudden decrease in grain sizes is apparent, for example between samples 45 and 46 or between samples 113 and 42. Sediment obtained in areas with smaller bedforms (in the order of decimeters) is mainly composed of fine sand. South of the SDF, towards the northern coast of Fehmarn island, the grain size distribution is getting coarser, with an amount of gravel of up to 30%.

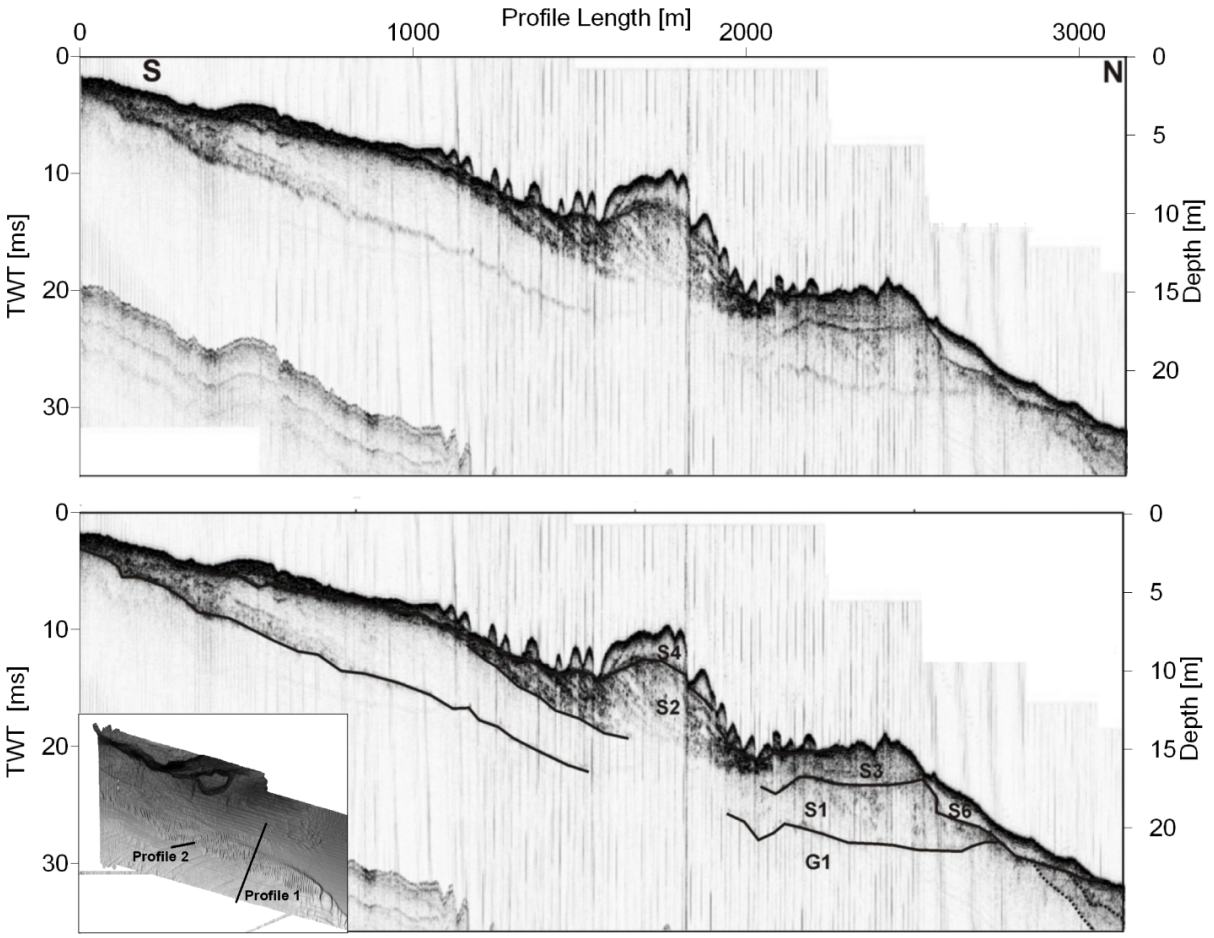

Fig. 6: Sediment echo sounder profile 1 (P1).

4.2 Seismic Profiles

Two profiles, representative for the SDF, are described in detail. Profile 1, extending from North to South through the central part of the SDF (see figure 6) was recorded with a parametric echo sounder. In the southern part of this profile a northward dipping reflector (above G1) forms the base of the acoustic penetration. This reflector terminates against the lower boundary of unit S6 in the north. Layer S1, deposited above G1, is also truncated in the north. S1 rises towards the south and seems to crop out at the seabottom. In the central part of the profile, layer S2 is deposited above S1. Unit S2 shows distinct, northward-dipping internal reflectors and crops out at the sea floor in the southern part of the profile. Northwards, S2 forms a steep slope. Further to the north, unit S3, containing faintly visible, horizontal internal reflectors is deposited above S1. The dunes (S4) are visible at the very top of the sequences S2 and S3. They do not form a continuous layer, as S2 crops out between the dune crests. The maximum thickness of the sediment forming the dunes is about 2 m in this profile; however, the maximum thickness observed in other seismic profiles is close to 4.5 meters.

The boomer profile P2, (fig. 7) was recorded about parallel to one of the ribbons protruding from the south of the dune field. The same ribbon was crossed several times during this profile. The base of the acoustic penetration is formed by the horizontal reflector “C” (fig. 7) in about 33 ms TWT depth, about 7 m below the seabottom. A second reflector (B), which runs parallel to the sea floor, is visible in a depth of about 25 ms TWT, approx. 3 m below the seabottom. The ribbon (A), crossed multiple times during this profile, is separated from the unit beneath.

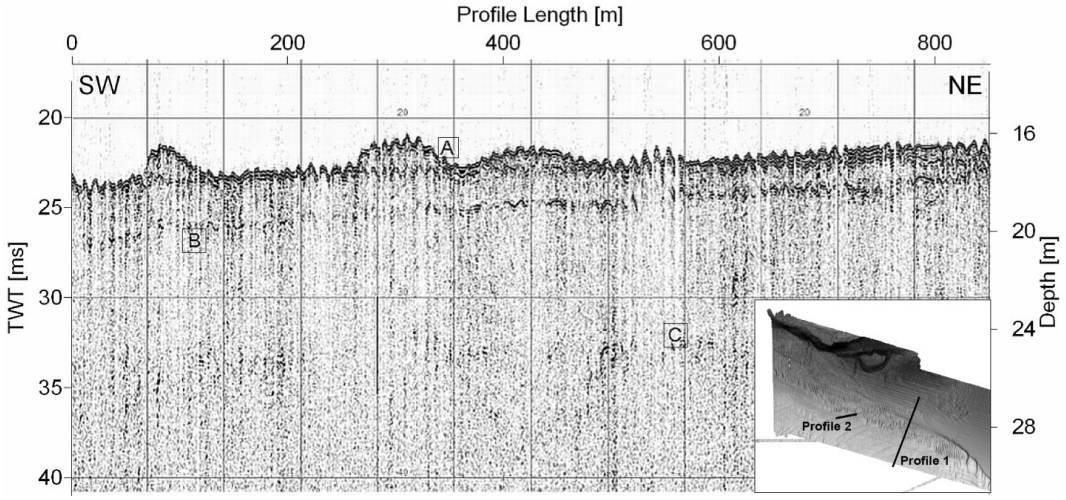

Fig. 7: Boomer profile 2 (P2).

4.3 Comparison of the Bathymetry

Comparison between May and June 2007

To estimate short term variations in the volume of the bedforms, small areas of the SDF have been mapped twice, in May and June 2007. Based on the multibeam data bathymetric profiles were constructed (fig. 9, for location of the profiles see fig. 8). The comparison of these profiles allows to directly asses short-term changes in the bathymetry of the dune field. Two profiles shown in fig. 9A are located close to the northern boundary of the dune field, an area with crest heights of only a few decimeters. Based on the comparison of the profiles movement of the dunes in the range of 10 meters towards west is obvious. The profiles shown in fig. 9B are located further to the south, in an area with heights of about 1 m. In these profiles, no movement of the dune crests can be observed.

Figure 10 shows the depth difference, calculated from the bathymetric data of a small area located in the north-western part of the SDF where bathymetric surveys were carried out in May and June 2007 (fig. 8). The result is displayed over a 3D surface of the bathymetry as recorded in June, 2007. It can be seen that during one month, sediment was eroded at the western slopes and deposited at the eastern slopes of the subaqueous dunes. This equals a movement of the dunes towards the east. The amount of the movement can only be quantified correctly, if it is assumed that a given dune crest is not migrating further than one wavelength (L). A balance between erosion and deposition results in neither loss nor gain of material, in the range of the accuracy of the multibeam echo sounder.

Comparison between 2006 and 2007

Further bathymetric profiles have been calculated based on multibeam data taken in January 2006 and May 2007 (fig. 11, for location of the profiles see fig. 8). However, only the positional data can be compared between these profiles (see section 3). The profiles shown in fig. 11C are located in the eastern part of the field, where the highest dunes are situated. A comparison of the dune positions of 2006 and 2007 reveals little differences in the western part of the profile, where the crests did not move. In the eastern part of the profile, some dunes moved eastwards in the order of approximately 20 m. The profiles shown in fig. 11D are running through the central part of the SDF up to its northern boundary. In the western part of the profiles, which corresponds to the central part of the SDF, no changes in position or height of the dune crests are observed. However, in the eastern part, corresponding to the area of the northern boundary of the SDF, some dune crests appear to have moved towards west.

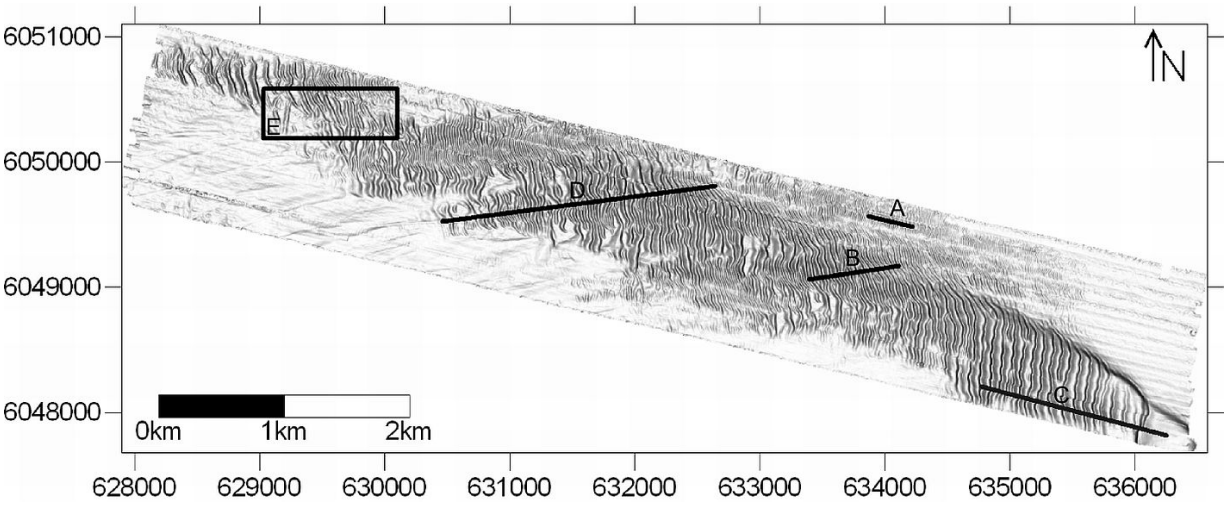

Fig. 8: Position of the compared bathymetric profiles (A-D) and the compared area (E).

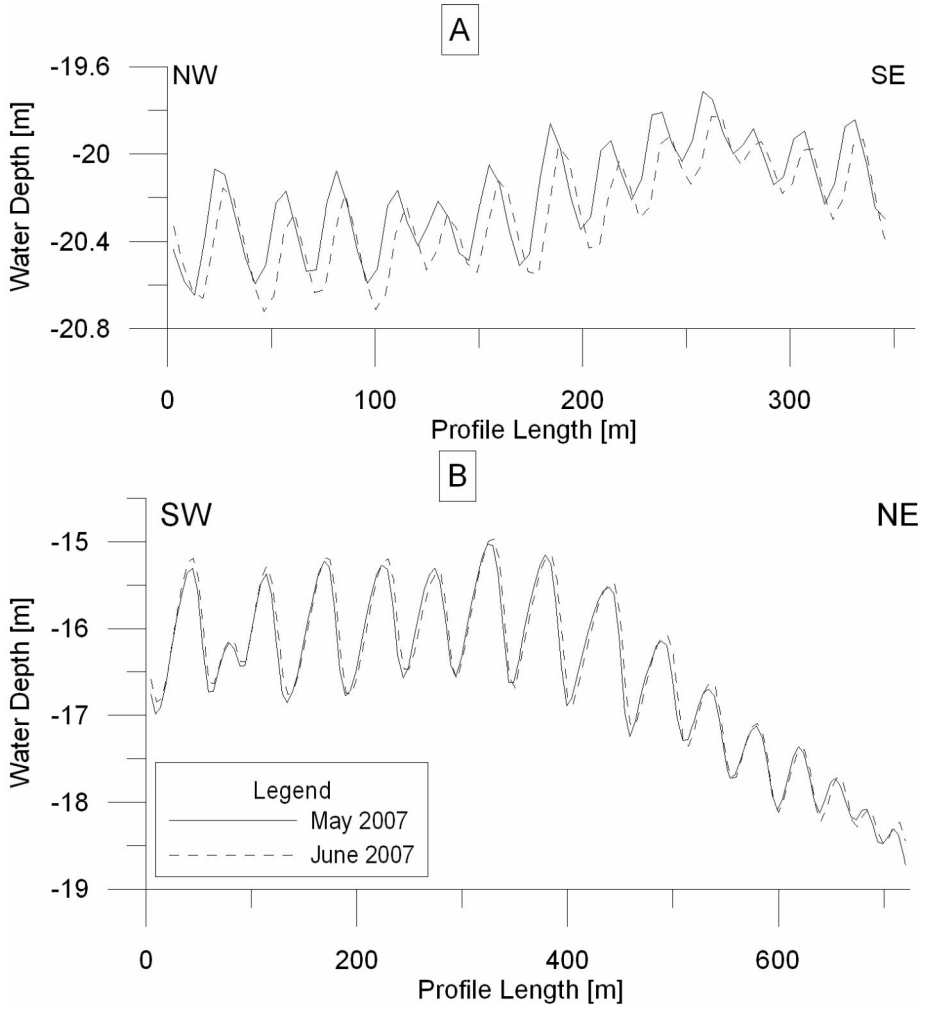

Fig. 9: A: Comparison of two bathymetric profiles close to the northern boundary of the SDF. B: Comparison of two bathymetric profiles in the central SDF. For detailed position of the profiles, see fig. 3. The legend is valid for A and B.

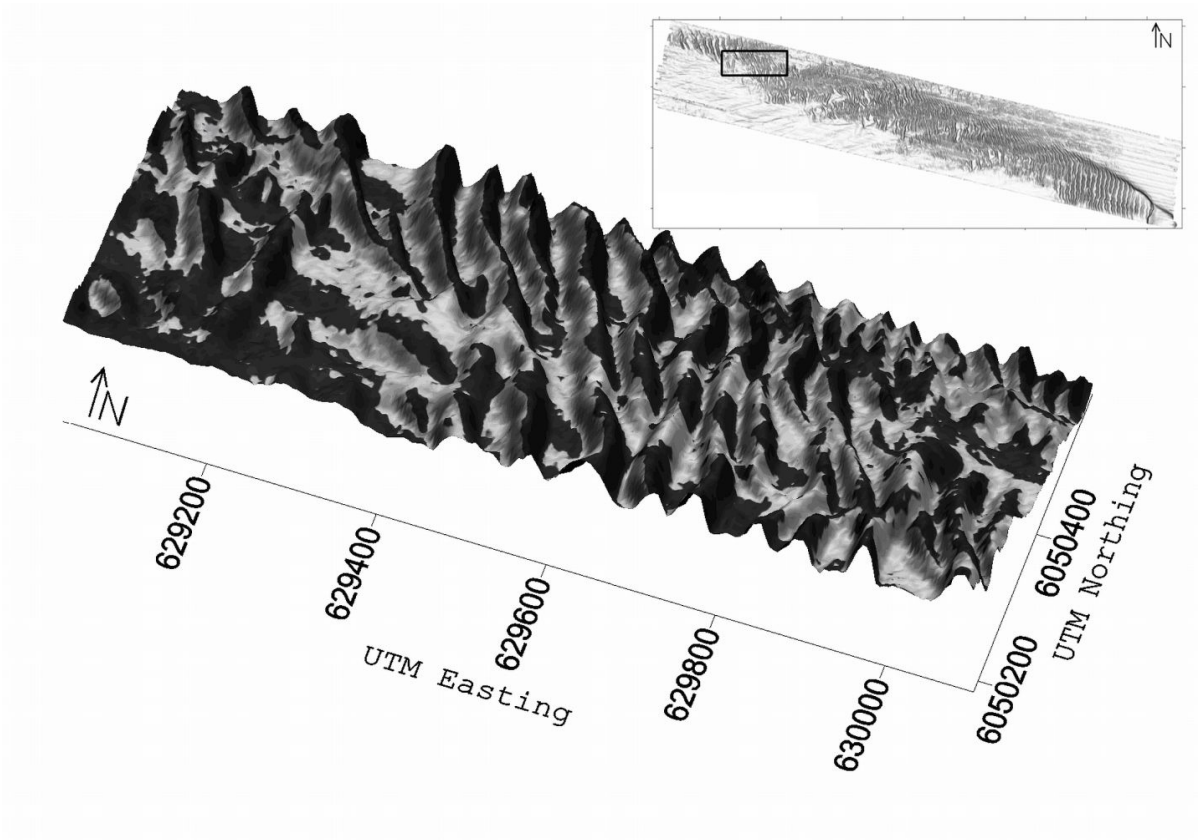

Fig. 10: The depth difference of the surveys done in May and June 2007. Black colours mark areas where sediment is deposited, grey colors mark areas where sediment is eroded.

Long term dynamics

The boundaries of the dune field as given by Werner et al. (1974) and Kaufhold (1988) are incorporated in figure 12. Positioning in former times was done using a DECCA navigational system, of which the accuracy for the research area is given with values of up to +/-50 m (Kaufhold 1995). In the first mapping, Werner et al. (1974) observed a large gap in the central dune field, as well as two smaller satellite fields towards the west. Additionally, the N-S extension of the field is larger when compared to later investigations. Maps from Kaufhold (1988) show two separate arms protruding from the central dune field towards the west, the area where Werner et al. (1974) mapped satellite dune fields. Also, the gap in the central field, as observed by Werner et al. (1974), closed between 1974 and 1988. Our multibeam data shows an accretion of the two extensions on the western side of the SDF, as well as several new dunes westwards of the older boundaries. Additionally, the SDF expanded towards south-west, while the N-S extension seems to have become smaller. The south-eastern boundary of the SDF did not change significantly.

5. Discussion

The seismic data shows clearly that the subaqueous dunes can be differentiated from the underlying units, and form a thin sediment layer (S4). This result differs from observations made by Wittmaack (1988), who stated that the subaqueous dunes form the top of a sediment layer, up to 11 m in thickness. It is unlikely that the large dunes are made up out of reworked material of seismic unit S2. Samples taken directly from seismic unit S2, outcropping south of the SDF and probably in the flats between the dunes (sample 118) are composed of coarser material than samples taken in the dune field. Usually, reworking of sediment composed of sand and gravel results in coarsening of the remaining material. Here this is not the case.

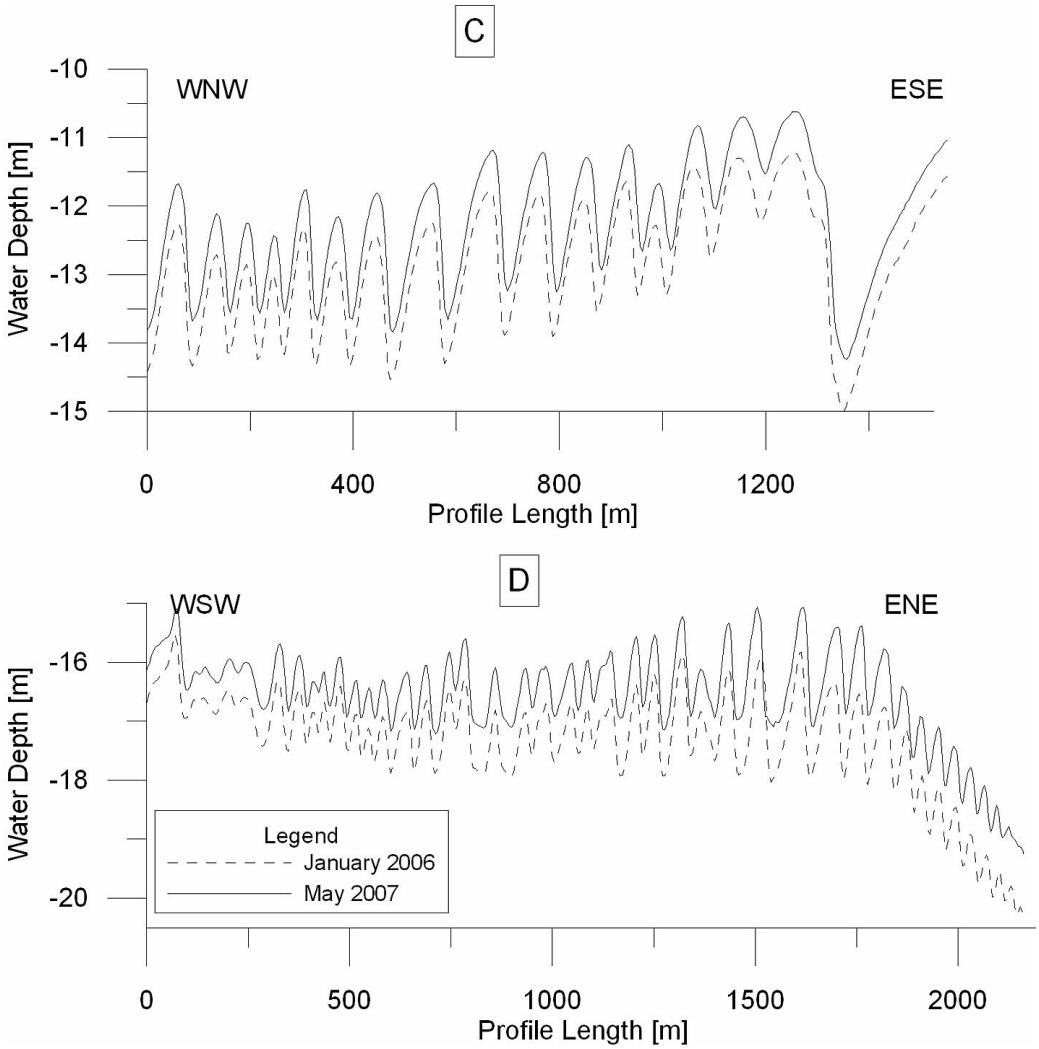

Fig. 11: C: Comparison of two bathymetric profiles in the eastern part of the SDF. D: Comparison of two bathymetric profiles running through the central part of the SDF. For detailed position of the profiles, see figure 3. The legend is valid for C and D.

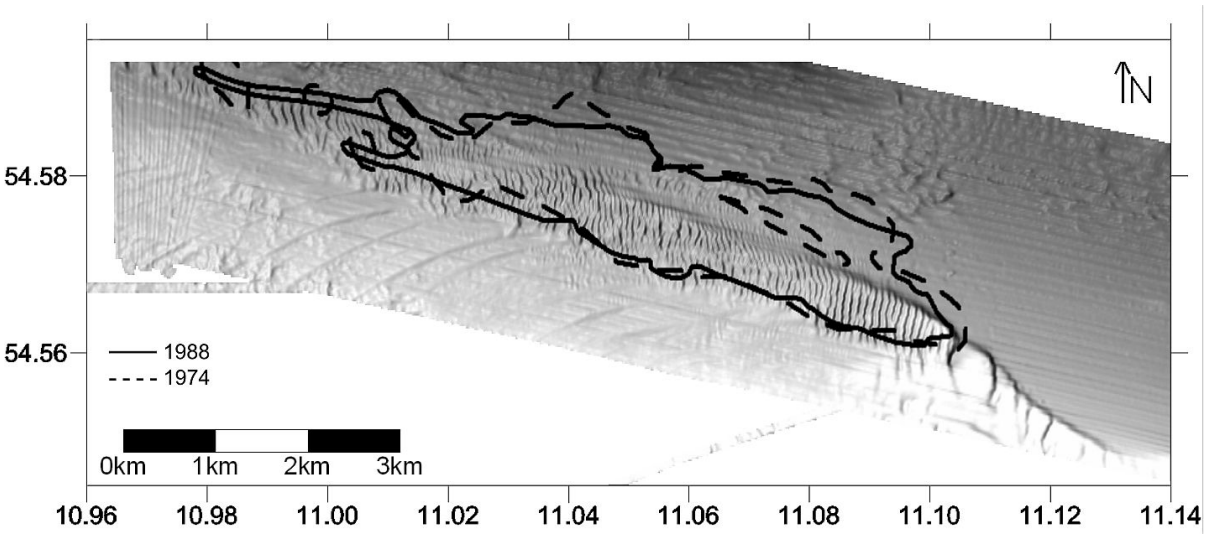

Fig. 12: Boundaries of the dune field as reported by Werner et al. (1974), dotted line, and Kaufhold (1988), solid line.

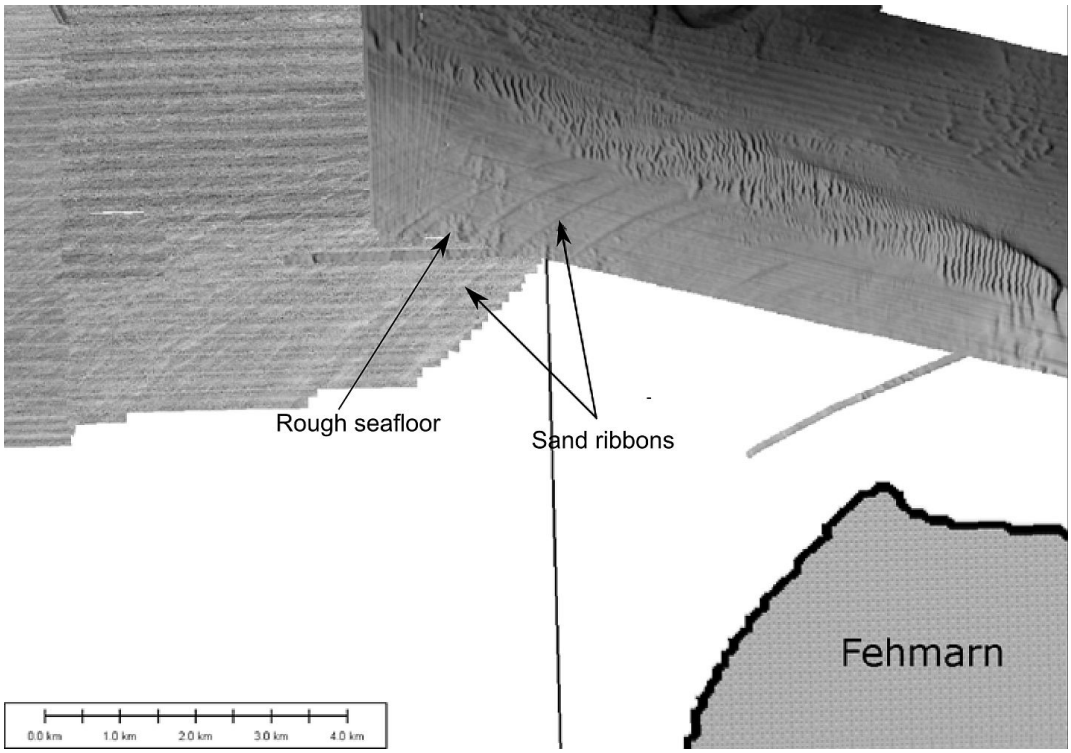

Fig. 13: The available side scan sonar data shows that the sand ribbons, visible as thin white lines, take course about parallel to the western side of Fehmarn (Side scan sonar data are taken from Schwarzer & Diesing (2006) and Schwarzer et al. (2007)

The good sorting (coefficient of unconformity around 2) of the medium to coarse sand forming the dunes is an indicator of a transport process. Additionally, distinctly different sediment samples can be found at the south-eastern boundary of the SDF (samples 45 and 46), although the steep slope visible in the bathymetric data further to the east (fig. 2) indicates that unit S2 is continuing into this area. Therefore it can be assumed that the sediment, forming the large subaqueous dunes has been transported to this area.

It can be assumed that the sand ribbons protruding from the SDF towards south-west (fig. 13) are conduits for sediment, as the dunes form directly in extension of these ribbons. The ribbons are, according to the boomer data, separated from the sedimentological unit below. The roughness of the sea floor between the ribbons, as apparent in the bathymetric data, might be related to glacial till exposed at the seabottom. Sand ribbons, albeit of a smaller scale, as shallow water features aligned with the sediment transport direction have been described and modelled by McLean (1981). He states that these ribbons commonly overlay coarser sediment, which is exposed between them. Those ribbons occur in regions with low sediment supply.

Long term observations reveal that the spatial extension of the SDF increased especially towards west and south-west. According to the comparison of the boundaries of SDF since 1974, the dunes in the elongated western part of the field have been formed recently.

This is supported by the higher H/L relation of the dunes in this area of the field, compared to supposedly older dunes, especially at the south-eastern boundary of the field. The south-eastern boundary of the field did not move significantly within the last 30 years. Looking at the H/L relation, the troughs between the dunes at the south-eastern boundary of the field seem to have been filled up. Observations of the shrinking N - S extension are more ambiguous, as the dune field is slowly fading in the north and the different mapping techniques used over the last decades have different spatial resolutions. However, it can be stated that infrequent movements of the field exist, and that the central dune field is almost

unaffected by weather conditions encountered during one annual cycle, as shown by the bathymetric comparisons. This supports the assumption that movements of the SDF are caused by salt water intrusion from the North Sea to the Baltic Sea (e.g. Werner 2000), which occur only infrequently. According to the bathymetric data, it is unambiguous that the dunes have been formed as a result of E-W currents, also supported by observations of comet marks (e.g. Jensen and Lemke 1996). This flow direction is in accordance with the path salt water intrusions follow from the North Sea to the Baltic Sea (Werner et al. 1974). It is during these events with their associated high current velocities, especially in the narrow strait between Fehmarn and Lolland, that sediment is nourishing the dune field. Our data suggests that the field has not yet reached an equilibrium state, and further change is to be expected.

6. Conclusion

Investigations with a multibeam echo sounder, sidescan sonar and shallow water seismic systems, as well as the analysis of sediment samples and comparisons with data from previous investigations (Werner, 1974; Kaufhold, 1988) have been conducted in SDF in the Fehmarn Belt. It was found that the sediment of the subaqueous dunes forms only a thin layer covering the sediment unit beneath. The material of the dune field is allochthonous. Sand ribbons protruding from the dune field in the south-west are the supposed conduits for the sediment. The central part of the SDF is unaffected by storms regarding one annual cycle, while over a time span of thirty years, an increase of the spatial extension of the field towards the west is observed due to the formation of new dunes. The north-south extension of the field is probably decreasing. The movements of the SDF are assumed to happen during salt water inflows from the North Sea to the Baltic Sea during west-storm conditions. Further change of the dune field is to be expected.

Acknowledgement

We are grateful to the “Federal Agency of Nature Conservation (BfN)” who supported parts of this study financially. We thank masters and crews of FK LITTORINA and FS POSEIDON for their support during our cruises.

4. Conclusion and Outlook

It was the main aim of this study to embed results of extensive hydroacoustic mapping in Fehmarn Belt into the existing knowledge on the Baltic Sea evolution. Some aspects of the geologic development of Fehmarn Belt since the last glacial could be resolved, and especially a distinct erosional event, which effects are visible in Fehmarn Belt, could be linked to a partial regression of the Ancylus Lake behind the Darss Sill. The data agrees to an Ancylus Lake regression model recently suggested (Björck et al. 2008). The river channel itself, however, was formed as a glacial meltwater system and has no direct connection to the Ancylus Lake drainage. Additionally, the formation and sediment dynamics over the last decades of a subaqueous dune field could be worked out.

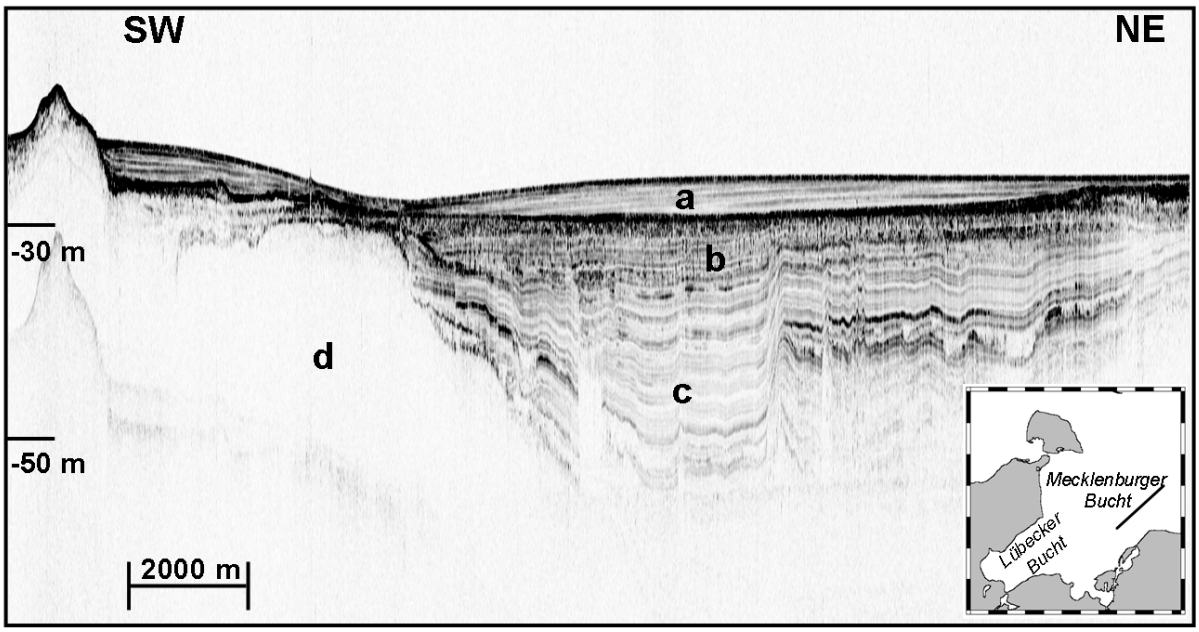

Fig. 1: Extensive high-resolution seismic surveys were done in Mecklenburg Bay, to extend the work done on geologic evolution in Fehmarn Belt. This seismic line, prepared for Niedermeyer et al. (2011), shows similar units as found in Fehmarn Belt. a) young marine deposits, b) Ancylus Lake deposits c) deposits of the Baltic Ice Lake d) glacial till.

However, many questions remain. Being situated west of the Darss Sill, it was suggested that Mecklenburg Bay and Fehmarn Belt shared the same evolution since the last glacial. Extensive seismic surveys in Mecklenburg Bay were already carried out to check whether the proposed evolution of Fehmarn Belt agrees to the evolution of Mecklenburg Bay. Preliminary results looks promising, as a principally identical sedimentary sequence is observed in seismic images (Fig. 1). The combined dataset of Mecklenburg and Fehmarn Belt will allow to obtain a more detailed insight into landscape evolution west of the Darss Sill.

Ultimately, as discussed in the introduction to this section (page 23), a local sea level curve for the Mecklenburg Bay and Fehmarn Belt area since the last glacial will be needed, to compare these areas with the Arkona Basin. Especially a clarification of the heavily debated water level at the time of the highstand of the Ancylus Lake east and west of the Darss Sill would be helpful to further determine details of its regression, and to determine whether a second outlet is actually needed to explain its regression. For this purpose, the available seismic dataset allows the retrieval of sediment deposited close to the shoreline during different phases of the Baltic Sea. In specific places, sediments from all phases of the Baltic Sea evolution are both deposited close beneath the surface, allowing for a relatively easy sampling, and deposited closely above glacial till, minimizing effects of compaction.

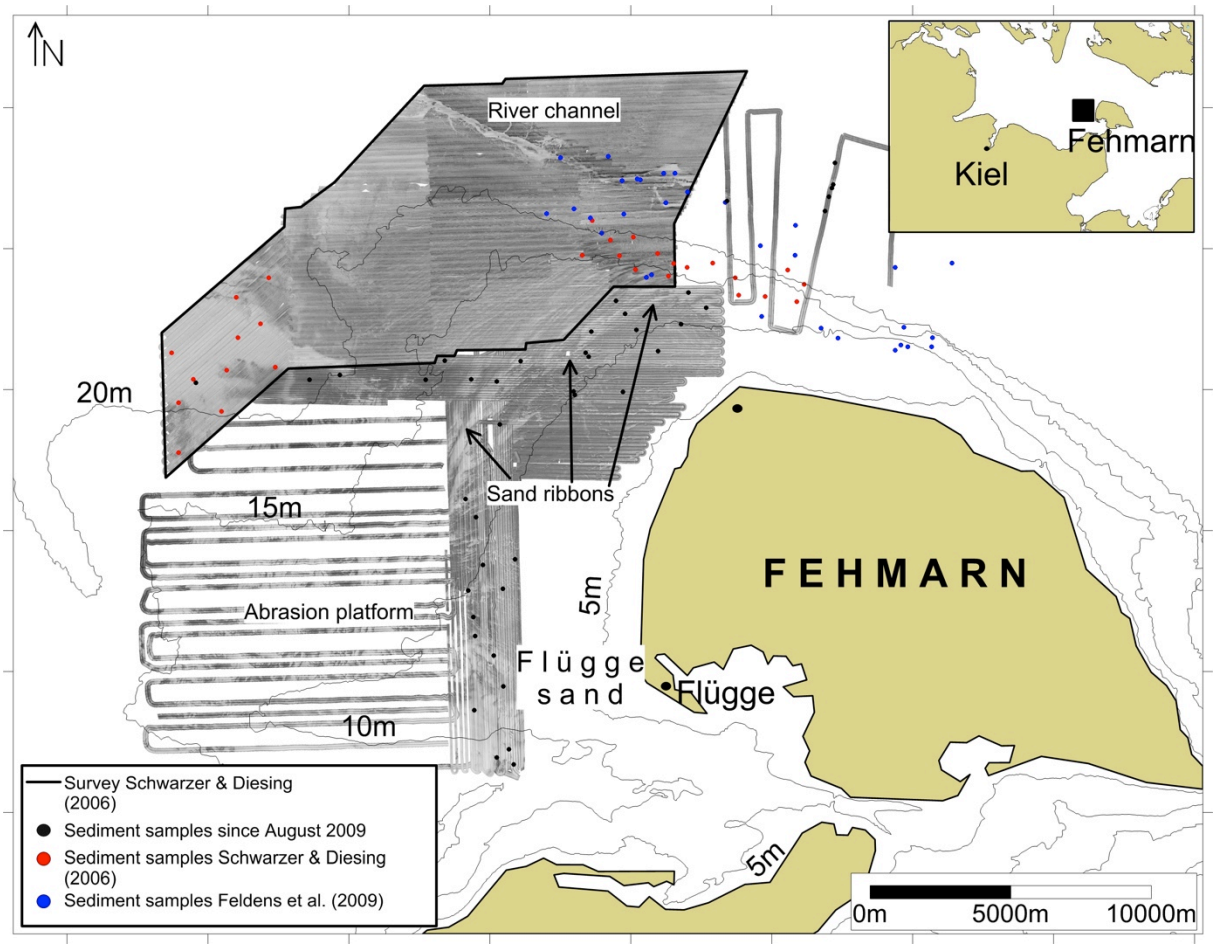

Fig. 2: Extensive side scan sonar surveys show elongated ribbons composed of sand, extending from the subaqueous dune field in the central Fehmarn Belt towards an abrasion platform west of Fehmarn. The continuation of river channel incised in Fehmarn Belt is visible in side scan sonar data gathered by Schwarzer and Diesing (2006). Data gathered in cooperation with the LLUR (Landesamt für Landwirtschaft, Umwelt und ländliche Räume des Landes Schleswig-Holstein).

Further research, including extensive side scan sonar surveys, was started – in cooperation with the LLUR (Landesamt für Landwirtschaft, Umwelt und ländliche Räume des Landes Schleswig Holstein), project "Identifizierung mariner Lebensraumtypen in der Kieler Bucht westlich von Fehmarn" – to determine the sediment distribution on an abrasion platform west of Fehmarn. In the course of this project, further information about the sediment dynamic west of Fehmarn was acquired. It was proposed that material transported northwards from this platform might nourish the subaqueous dune field in the central Fehmarn Belt (section 3.3). In fact, elongated SW-NE striking sand ribbons could be traced onto the platform (Fig. 2), giving further indications for a SW-NE directed sediment transport. Future monitoring and resampling of these sand ribbons will allow more detailed assessment and quantification of local sediment dynamic.

Chapter IV
Effects of the 2004 Indian Ocean Tsunami offshore Thailand

1. Introduction

Despite the immense losses of live and property, the 2004 Indian Ocean Tsunami allowed scientists and engineers of different disciplines to study its effects in detail, providing a better understanding of tsunami phenomena. A general overview of the current knowledge on tsunami generation, propagation and effects is e.g. given by Shiki et al. (2008) or Bryant (2009). The focus of this work is to enhance knowledge about offshore effects of the 2004 Indian Ocean Tsunami.

Generally, offshore tsunami effects and deposits resulting due to tsunami action - including run-up and backwash - are poorly understood, especially compared to onshore influences. Theoretically, offshore effects might be significant even in deep waters (Weiss and Bahlburg, 2006) and are speculated to be widespread in the geological record (Dawson and Stewart, 2007). Satellite images show large plumes of sediment transported offshore, hinting towards potential effects of the backwash. In contrast, other authors propose offshore effects to be minor (e.g. Bourgeois, 2009).

Before this study, only few authors described offshore deposition (Szczucinski et al. 2006; Geronimo et al., 2009), or offshore erosion (Razzhigaeva et al. 2006; Hawkes et al., 2007; Dahanayake and Kulasena 2008) due to tsunami. However, the available studies are mainly based on samples taken at arbitrarily chosen points, and no large-scale, full-coverage hydroacoustic mappings were done. The interpretation of such samples is inherently problematic, as offshore tsunami effects are reported to be channelled, and focused to some areas (Le Roux and Vargas 2005).

Recently, it was pointed out (Shanmugam 2011), that tsunami do not represent a single depositional process and detailed analysis of worldwide, modern tsunami deposits is necessary to develop proxies for the identification of paleo-tsunami. A combination of different proxies will be needed especially to differentiate tsunami deposits from storm deposits (Phantuwongraj and Choowong 2011). This differentiation was found to be difficult even for modern tsunami deposits, where historical data is available. Obviously, a modern tsunami deposit of unquestioned origin would highly useful for defining a paleo-record. In this regard, the December 2004 tsunami offered the opportunity to catalogue geomarine effects from a very well recorded series of events.

The approach of this study was to identify tsunami-impacted areas, morphological features related to the tsunami and tsunami deposits on the inner continental shelf. Subsequently, the lasting offshore impact of the tsunami, and the preservation potential of tsunami deposits were to be identified. Towards this aim, extensive hydroacoustic surveys were carried out to obtain full-coverage information of the seafloor. Subsequently, sediment sampling for ground truthing and identification of possible tsunami deposits was possible even from small-scale seafloor features (refer to chapter II for more information on methods).

The coastline off Khao Lak (Andaman Sea, Thailand) was chosen as the study site (Fig. 1). The continental shelf of the Andaman Sea adjacent to the Malay Peninsula is narrow and slightly inclined. Rocky cliffs altering with sandy lowlands and pocket beaches dominate the coastal area. It is monsoon dominated with the NE-Monsoon active during winter (Oct. – March) and the SW-monsoon during summer (May-Oct.). Strong storms are rare at this part

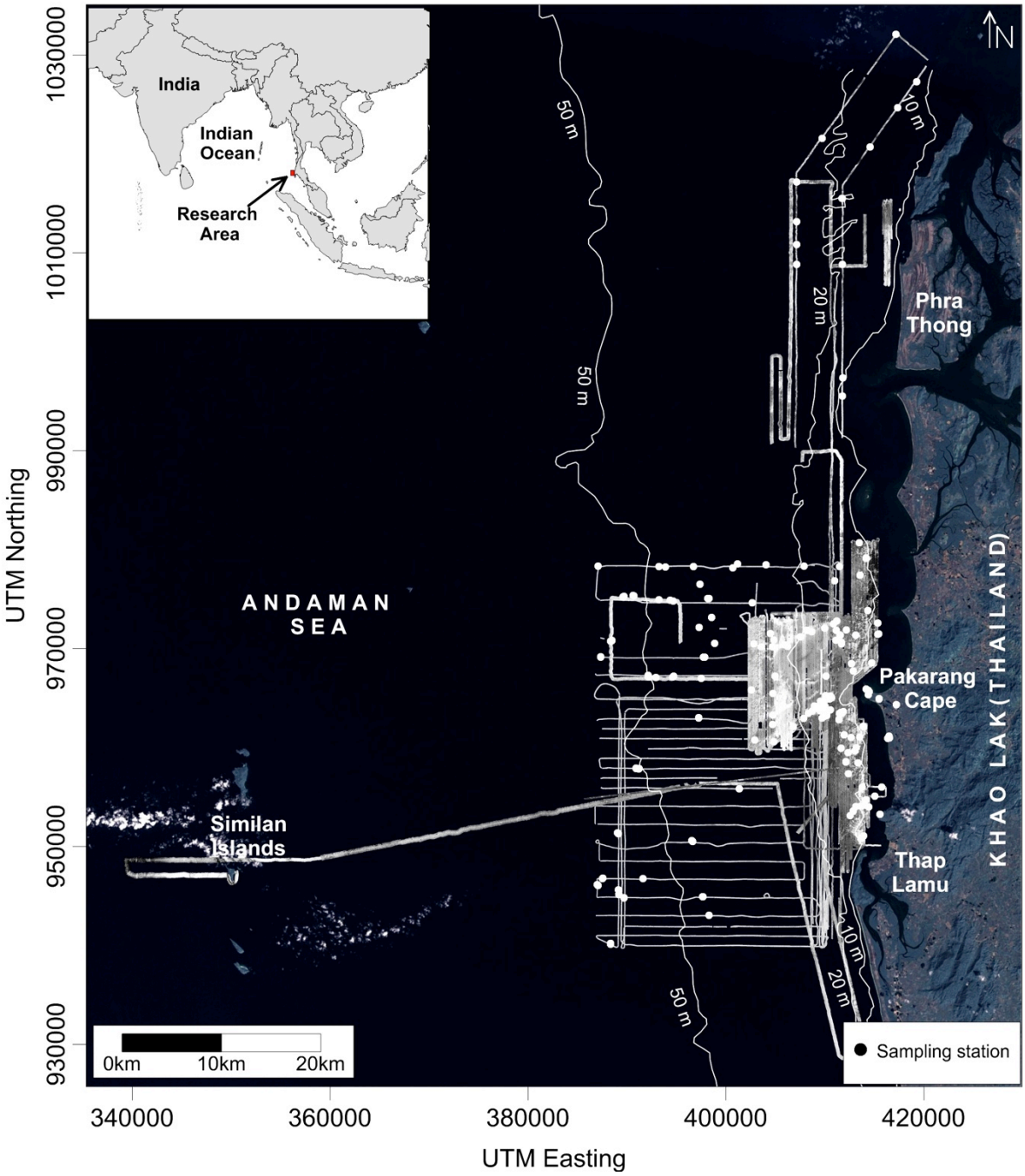

Fig. 1: The research area off Khao Lak, Thailand. The area was severely affected by the 2004 Indian Ocean Tsunami. Available side scan sonar data and sediment sampling station (including grab samples and coring station) are indicated.

of Thailand's coastal areas (e.g. Jankaew et al. 2008). The tide is mixed semidiurnal, ranging between 1.1 m and 3.6 m (Thampanya et al. 2006).

The research area offshore Khao Lak, between Thap Lamu and Phra Thong Island comprises approximately 1.000 km² (Fig. 1). It was selected for the investigations as it was severely hit by the 2004 tsunami (Bell et al. 2005, Tsuji et al. 2006, Thanawood et al. 2006). The wave run-up spiked at 15 m above the normal water level at Pakarang Cape (Siripong 2006) and up to 20 m at Phra Thong Island (Jankaew et al. 2008). At Pakarang Cape an area of about 12.500m² was eroded by the tsunami waves (Synolakis and Kong, 2006). Hundreds of reef

boulders and rocks were left and could be observed on the flat intertidal area after the coast was hit by the tsunami (Goto et al. 2007).

In the past, extensive tin mining activities took place in the coastal area of Phang Nga province on- and offshore up to – 50 m water depth, but ceased in the 1980s long before the tsunami hit the coastal area. Some sediment dispersion was created by the tin mining (Suwanwerakamtorn et al. 1990). Fluvial discharge is negligible in this area. This was thought to ease the identification of tsunamigenic features on the seafloor as they would not be covered by land-derived sediment during the rainy season.

Approximately 2000 nautical miles of hydroacoustic profiles, 156 sediment samples and 60 short gravity cores were acquired during three research cruises in 2007, 2008 and 2010. In section 2, an overview of the aims, focus and most important results of the separate cruises are given. The results and conclusions are then presented in form of three research articles in sections 3, 4, and 5. Subsection and figure numbers have not been changed from original articles, and are therefore not continuous throughout the chapter.

2. The research cruises

2.1. Research Cruise November to December 2007

In order to identify, and subsequently characterize and quantify tsunami influence, an overview mapping between 10 and 90 m water depth was done in November and December 2007, using RV Chakratong Tongyai (belonging to Phuket Marine Biological Center). The aim was to localize seafloor features that might indicate event influence, and to identify environments able to preserve sediment deposited during events. Additionally, the cruise served to gain a broad overview about the previously unknown shelf geology off Khao Lak.

The findings included a channel system partly filled with fine-grained sediment as potential sediment depocenters in water depths between 14 to 18 m. Land-based material incorporated in stiff muddy material suggested transport in high density hyperpycnal flows during the tsunami backwash. In contrast, the preservation of submarine relief in former underwater mining areas pointed to limited impact of the tsunami, while a second channel system beneath 18 m water depth in combination with complex bedforms structures, about parallel to the observed tsunami backwash, indicated a possible higher impact. Therefore, the tsunami impact seemed to be focused on some areas. It was speculated that the channel structures could be connected to tsunami return channels incised at the coastline (Fagherazzi and Du, 2007). However, this could not be proofed during later cruises. Several boulders, which might have been deposited during the tsunami backwash flow, were found in the channels in front of Pakarang Cape. The results of this cruise are presented in section 3 (Feldens et al., 2009).

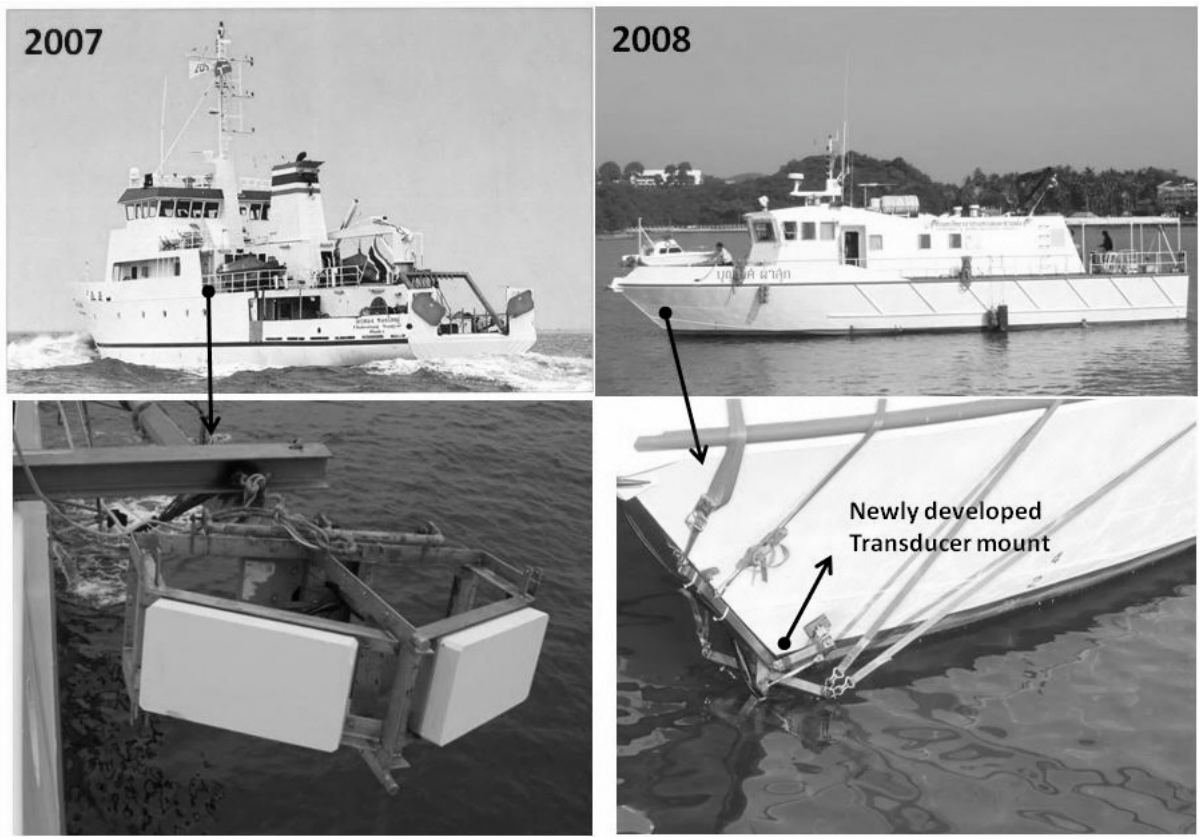

Fig. 2. Research vessels RV CHAKRATONG TONGYAI (left) and RV BOONLERT PASOOK (right) both belonging to Phuket Marine Biological Centre (PMBC). On RV CHAKRATONG TONGYAI multibeam transducers were welded to the port side of the ship, while on RV BOONLERT PASOOK the transducers were fixed at the bow of the ship using a special mount created by technicians of IfG.

2.2. Research cruise November to December 2008

Most traces suggesting tsunami influence during the 2007 cruise were found close to the coastline. Therefore, the 2008 cruise was carried out in the smaller vessel Boonlert Pasook (belonging to Phuket Marine Biological Center), allowing to record hydroacoustic data and to take sediment samples between 5 m and 10 m water depth.

An important objective of the 2008 cruise was to clarify the origin of the two channel systems identified in 2007. It was found that no direct connection between the channel systems exists. Channels found between 14 and 18 m water depth in 2007 continue into more shallow waters, and are connected to large patches of mainly silty composition. Such fine-grained sediments are unusual for this water depths offshore open, wave dominated coastlines. However, not enough data were available to determine their origin and potential connection to the 2004 Indian Ocean Tsunami subsequently to the 2008 cruise.

The channels in water depths beneath 18 m were identified as incisions at northwestern slopes of an extended sand ridge system, existing prior to the 2004 Indian Ocean Tsunami. Delicate, "flame-shaped" bedforms found on the slopes of the sand ridges indicated an SW-NE directed current. Fading of these bedforms between 2007 and 2008, combined with indicators for backwash influence reported in this area (Sugawara et al. 2009), may suggest that they are related to a large event like the 2004 Indian Ocean Tsunami, and not to annual monsoon-related circulation. This is further supported by mud deposits interbedded in coarse sand at the base of the sand ridges, eventually representing events transporting fine material observe

further onshore towards offshore. These deposits were found in similar water depths as stiff muds including plant material during the 2007 cruise.

Boulders, not connected to subsurface structures, were identified. These boulders had to be transported to their current positions. However, although the backwash was theoretically strong enough to transport boulders towards offshore, no final proof that the boulders were moved during the tsunami event can be given. These findings were published (Feldens et al. 2010), and are presented in section 4.

2.3. Research cruise February to March 2010

It was decided to focus the last cruise in 2010 again on the shallow water area between 5 and 10 m water depth, using the chartered diving boats Aree and MS Fahsai. It was found that the channel system above 18 m water depth is incised into an old paleo-reef platform. The silty material forming the surface sediments within the channels and the larger fine-grained sediment patches were found to derive from onshore. This onshore-offshore transport is not related to the tsunami event, but was likely the effect of changed land-use during the last decades.

In sediment cores and several grab samples an event layer was identified, partly sandwiched by dominantly silty sediments deposited offshore due to the anthropogenic impact (Sakuna et al. 2010). This event layer, only covered by approximately 5 centimetres of sediment, could be traced down to 18 m water depth with further sediment cores and grab samples. It consists mainly of sand and contains compounds of terrigenous origin (e.g. laterites). It is interpreted as a 2004 Indian Ocean tsunami deposit, which was the last major event in the area. While these event deposits might be preserved in some areas, they will commonly be subject to reworking, given the observed sediment dynamics in the area.

In the majority of the studied area no lasting impact of the tsunami is identified in the seafloor morphology, sediment distribution or specific offshore tsunami deposits five years after the tsunami event. These results will be published in Earth Planets Space (Feldens et al., accepted with minor revision as of March 2011), see section 5.

3. Impact of 2004 Tsunami on Seafloor Morphology and Offshore Sediments, Pakarang Cape, Thailand[3]

P. Feldens[1]*, K. Schwarzer[1], W. Szczuciński[2], K. Stattegger[1], D. Sakuna[1], P. Somgpongchaiykul[3]

[1]Institute of Geosciences, Coastal and Shelf Research, Kiel University, Olshausenstrasse 40, 24118 Kiel, Germany

[2]Institute of Geology, Adam Mickiewicz University in Poznań, Maków Polnych 16, 61-606 Poznań, Poland

[3]Biogeochemical and Environmental Change Research Unit, Prince of Songkla University,P.O. Box 50, Kho Hong, hat Yai, Songkhla 90112, Thailand

Received: 8 October, 2008

Accepted: 25 November, 2008

Abstract

This study documents seafloor morphology and sediments based on multibeam, side-scan sonar and boomer surveys, as well as sediment samples taken on the inner to mid shelf of the Andaman Sea after the 2004 Indian Ocean tsunami. Preservation of submarine relief in former underwater mining areas points to limited impact of the tsunami, while channel structures parallel to the observed tsunami backwash indicate a possible higher impact. Therefore, the tsunami impact seems to be focused on some areas. The impact was probably most effective during the backwash, when stiff mud deposits containing grass, wood fragments and shells were transported by high density backwash flows. Moreover, several boulders, which might have been deposited during the tsunami backwash flow, were found in the channels in front of Pakarang Cape.

Keywords: 2004 Indian Ocean tsunami, seafloor mapping, tsunami backwash, inner continental shelf, Andaman Sea

1. Introduction

Most of the research published about erosion and deposition of recent tsunamis focus on the onshore areas. The offshore effects, although theoretically significant (Weiss 2006) and more common in older geological records compared to onshore deposits (Dawson and Stewart 2007), have only been documented in a few studies (van den Bergh et al. 2007, Noda et al. 2007, Abrantes et al. 2008). Surprisingly, offshore impacts of the well studied 2004 Indian Ocean tsunami are also almost unknown. Few authors reported offshore deposition of muddy sediments (Chavanich et al. 2005, Szczuciński et al. 2006, Di Geronimo et al. 2008). Offshore erosion was postulated through analyses of microfossils in onshore tsunami deposits (Razzhigaeva et al. 2006, Hawkes et al. 2007, Dahanayake et al. 2008, Kokociński et al. 2009).

This article presents results of a four-week research cruise, undertaken in November and December 2007, focussing on the inner continental shelf next to Pakarang Cape (Phang Nga province, Thailand). During this cruise, hydroacoustic data (side-scan sonar, multibeam echo sounder, shallow water reflection seismic) as well as sediment samples were collected to obtain further insight about the impact of the 2004 tsunami on the shallow seafloor.

[3] Reprinted with permission of "HARD" Publishing Company. The article was originally published in the Polish Journal of Environmental Studies, Volume 18(1), pages 63-68 in 2009.

2. The Research Area

The Andaman Sea continental shelf adjacent to the Malay Peninsula is narrow and slightly inclined. The area is dominated by two monsoonal winds: the northeast monsoon from mid October to March and the southwest monsoon from May to September. The southwest monsoon generates the highest waves along the coast. The tide is mixed semidiurnal with a tidal range between 1.1 and 3.6 m, taking into account spring and neap tide (Thampanya et al. 2006). The research area, about 1,000 km2, is situated off Khao Lak (Phang Nga province), in water depths between 10 and 70 meters. For decades, tin mining activities took place in parts of the studied area (Usiriprisan et al. 1987), but ceased about 20 years ago. This study focuses on a part of the shelf next to Phang Nga province, especially around Cape Pakarang (Fig. 1). The research area was chosen because tsunami-induced change of the seafloor can be expected in this area, as the coastline was highly damaged during the tsunami (Bell et al. 2005, Tsuji et al. 2006). Furthermore, the absence of large river mouths in this area increases the visibility of tsunami-induced structures on the seafloor in hydroacoustic data. The run-up at Pakarang Cape reached a height of more than 15 m (Siripong 2006) due to shoaling processes and the interaction of the tsunami wave with the seabottom. During the tsunami event a layer of a few cm to about 0.5 m thickness, composed of sand and silty sand, was deposited over almost the whole inundation zone (Szczuciński et al. 2005, Szczuciński et al. 2006, Hori et al. 2007, Choowong et al. 2007). According to eyewitnesses reports, the tsunami wave arrived from three different directions at Pakarang Cape (Siripong et al. 2006). The backwash pattern was documented by satellite images taken after the tsunami (indicated in Fig. 2). Obviously, the waves were forming a complex run-up and backwash pattern, heavily influenced by the nearshore bathymetry (Szczuciński et al. 2006). At the tip of Pakarang Cape, an area of about 12,500 m2 was completely eroded during the tsunami (Synolakis and Kong 2006). Hundreds of reef rocks more than 1 m in diameter were transported landwards by the tsunami and deposited in shallow waters around Pakarang Cape (Goto et al. 2007, Goto et al. 2008). Tsunamigenic incisions, with a spacing between 50 and 200 m at the coastline of Khao Lak, were created during the run-up, and enlarged during the backwash of the tsunami (Fagherazzi and Du 2004). Furthermore, it was observed that the channels are fan-shaped, and are wider at the coastline and narrower further inshore. This indicates a control of spacing and dimension of these return channels by the wave height of the tsunami (Fagherazzi and Du 2004). Westward of the research area, about 2 m sand from the seafloor have been eroded around a coral reef boulder in 30 m water depth, probably due to the tsunami (Chavanich et al. 2006).

3. Methods

Material for the study was collected during a research cruise on RV CHAKRATONG TONGYAI in November and December 2007. Acoustic properties of the seafloor sediment were measured using a side scan sonar (500 kHz) with digital data acquisition. A shallow water multibeam echo sounder with a working frequency of 180 kHz was welded to the portside of the research vessel to record bathymetric data. Shallow water reflection seismic data were obtained using a high resolution EG&G boomer system (about 500-15000 Hz). The covered area is shown in Fig. 1. For ground-truthing of the hydroacoustic data and for further sediment analysis, 77 grab samples were taken using a Van-Veen-type grab sampler. 40 short sediment cores of up to 125 cm in length were obtained using a gravity corer. However, for the present study only grab sample material was analyzed. To determine the grain-size parameters, sediment samples were dried and sieved. The grainsize statistics were calculated using Gradistat software (Plott and Bye 2001).

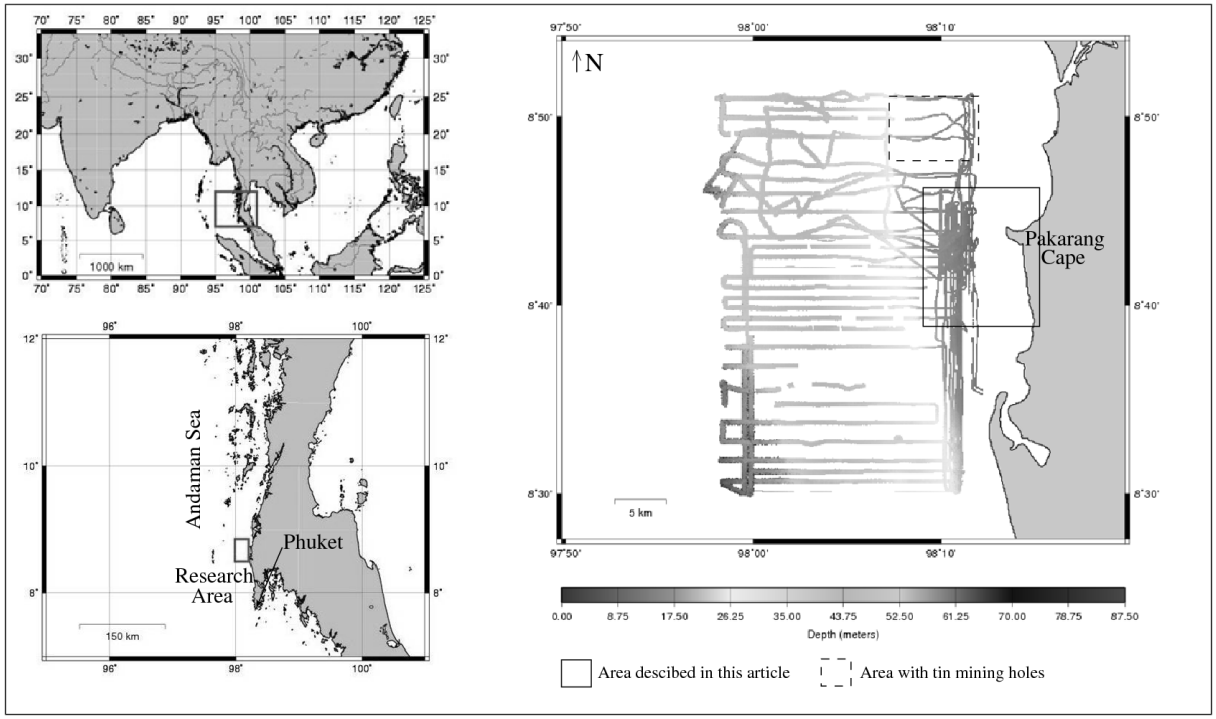

Fig. 1. The research area offshore Phang Nga province.

4. Results

4.1 Bathymetry

The obtained bathymetric map of the area in front of Pakarang Cape is shown in Fig. 2. Down to 18 m, the slope is inclined with an angle of about 0.8°. Below this depth, the overall slope angle decreases (to about 0.1°), and the seafloor shows a "step like" morphology (Figs. 2 and 3). At the base of the southern slope of these steps, SW-NE

striking channels, with a width of several hundred meters and a depth between 0.5 to 2 m are cut in the seafloor. Bathymetric cross sections (Fig. 3) reveal that the channels are asymmetrical, with the deepest incisions situated close to their southern slope. The dipping angles of the channels are low, reaching 1 to 1.2° at the southern slopes and about 0.2° at the northern slope. Towards the coastline, corresponding with the onset of the steeper slope angle in water depths between 14 and 18 m, the number of channels increases. The continuation of these channels both in deeper and shallower water is unknown, although first data from shallow water reflection seismics suggests a continuing propagation of the channels further offshore. The seismic data does not show any connection between the channels and subsurface structures. Remnants of these tin mining activities in this area (indicated in Fig. 1) are visible in the form of steep holes up to 7 m deep.

4.2 Seafloor Sediments

Large elongated sediment patches, appearing nearly white in the side-scan sonar images, with the same strike direction as the aforementioned channels, were documented in front of Pakarang Cape. There is a distinct transition between these areas and the surrounding seafloor (appearing darker in the side-scan sonar image shown in Fig. 4). Light-coloured areas in the side scan sonar data correspond to finer or non-consolidated sediment, while darker areas correspond to coarser or more consolidated sediment. The southern boundary of the elongated patches is very irregular and appears "flame-shaped" (Fig. 5).

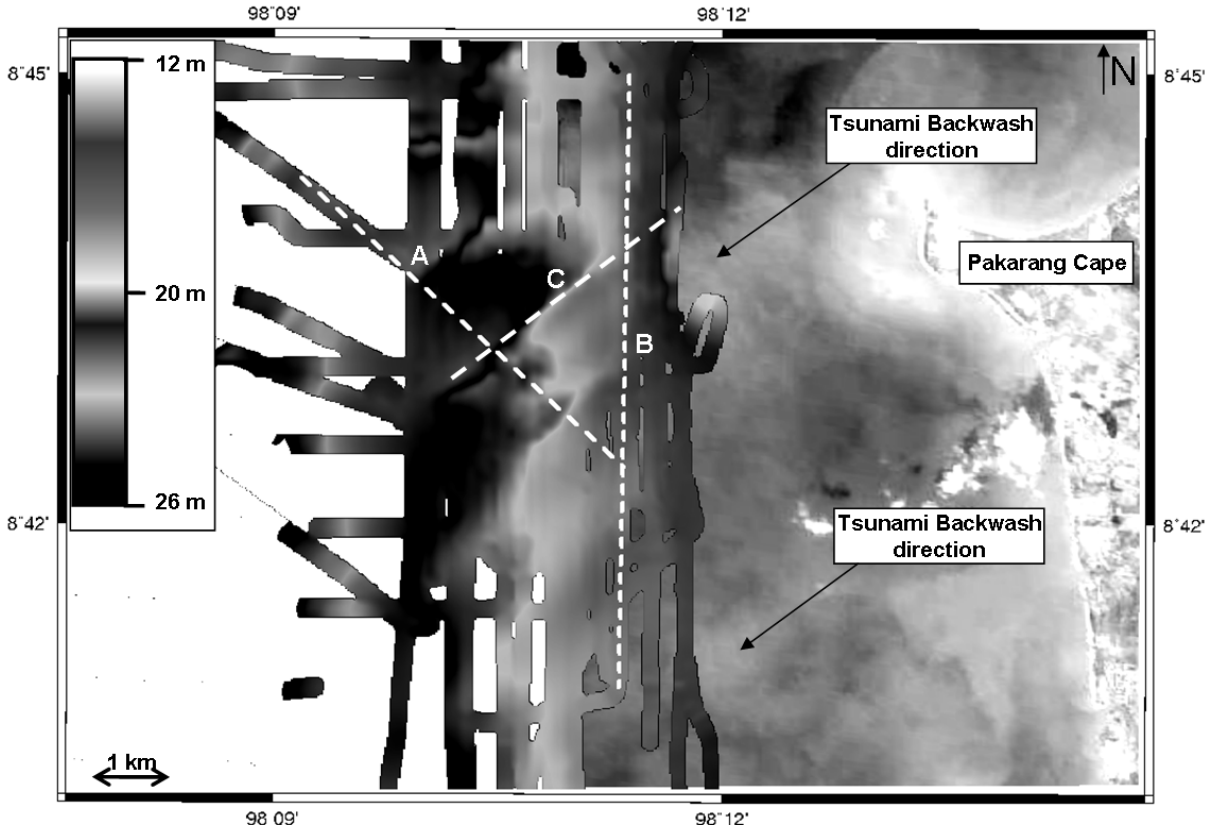

Fig. 2. Bathymetry around Pakarang Cape merged with a satellite image taken shortly after the 2004 tsunami. The dashed lines indicate the profiles shown in Fig. 3. (satellite image: Images acquired and processed by CRISP, National University of Singapore. IKONOS image © 2004. www.crisp.nus.edu.sg/tsunami/tsunami.html, modified.)

A combination of side-scan sonar and multibeam echo sounder data indicates that the large elongated areas of fine sediment are situated at the steeper southern slopes of the channels. In many cases, it was not possible to distinguish between the layers of fine to medium sand in the seismic data, taken simultaneously with the side scan sonar data. When it was possible to recognize these layers in the seismic data, their thickness appeared to be on the order of a few decimetres. Small patches of the same, fine sediment are visible closer to the coastline and are commonly situated in smaller channels and depressions (Fig. 6).

The results of the grain size analysis are incorporated in Fig. 4. The elongated sediment patches are composed of fine to medium sand, while the surrounding seafloor consists of coarse sand. Both types of sediment are poorly to moderately sorted. In one grab sample, taken from about 16 m water depth a stiff mud, covered by a 3 cm thick layer of coarse, well sorted sand was found. It contained terrestrial organic remnants: grass and pieces of wood, moreover, clasts of clay were found. Additionally, side-scan sonar data revealed the presence of numerous boulders with diameters around 1 m, as determined on the basis of their acoustic shadows in the side-scan sonar images. Most of these boulders appear between the aforementioned sediment patches close to the coastline (Fig. 7). However, some boulders, located at a distance of about 4 to 6 km from the tip of Pakarang Cape, are situated within a larger channel directly north of an elongated sediment patch (Fig. 5).

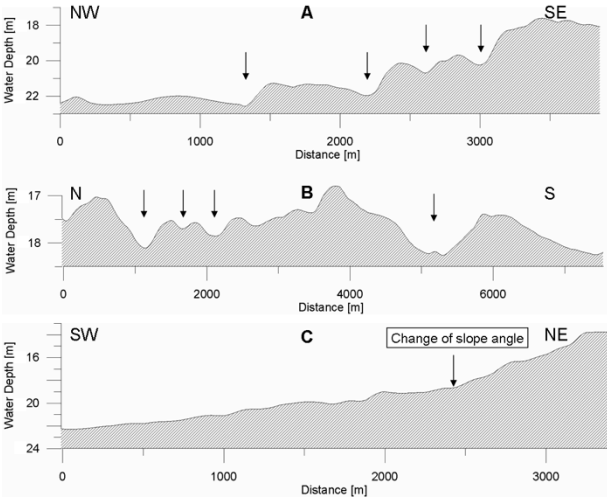

Fig. 3. Cross sections from several parts of the seafloor. Channelsare marked by arrows. For the positions, refer to Fig. 2.

5. Discussion

Although the survey took place three years after the 2004 Indian Ocean tsunami, it is likely that several of the observed features may be ascribed to this impact. For instance, the channels and elongated sediment patches observed in front of Pakarang Cape have a striking resemblance to the backwash pattern observed in the satellite images taken after the tsunami event (Fig. 4). The erosion potential of a tsunami run-up and backwash is commonly mentioned in the literature (Dawson 1994, Dawson and Shi 2000). The impacts of the backwash depend on the amount of water flowing back into the sea, which itself depends on wave height (Fagherazzi and Du 2004), and on the formation of high density hyperpycnal flows (Le Roux and Vargas 2005). High tsunami run-up heights at Pakarang Cape and the local presence of stiff mud with grass and wood found in offshore sediment samples suggest that both conditions enhancing the erosion potential of the backwash were met. Therefore, it is possible that the observed channels were formed mainly during the channelized tsunami backflow. Although due to a lack of pre-tsunami data it is not possible to exclude that the channels already existed prior to that event, several features suggest their origin or at least reshaping during the tsunami. A good correlation between the spacing of onshore incisions, interpreted to be created during run-up and backwash, and tsunami wave height is reported (Fagherazzi and Du 2004).

River mouths in the Nam Khem plain (north from Pakarang Cape) changed into wedge-shaped channels (Umitsu et al. 2007) with a width of 50-200 m, mainly due to the effect of a concentrated tsunami backwash. As the onshore return channels of the tsunami are wedge-shaped, and widening towards the coastline, it could be assumed that a connection between the onshore incisions and the wider channels, observed in shallow waters, exists. The rapid transition of these channels into the deeper, and even wider, channels in water depths of about 17 to 18 m might be caused by a change of the hydraulic behaviour of the backwash due to the changing slope angle of the seafloor (Figs. 2 and 3). The channels in deeper waters are asymmetrical in cross section. Related to this observation, it is interesting to note that regularly spaced, very shallow swales with asymmetrical profiles and filled by very fine-grained sandstones, and interpreted to be created during a paleotsunami event, have been reported (Rosetti et al. 2000).

Local erosion (adjacent to a large reef boulder where the formation of scour structures was possible) of up to 2 m during the tsunami event in a water depth of 30 m was reported (Chavanich et al. 2005). Our data suggest erosion of a lower but comparable magnitude in the channels, and less erosion of the surrounding seafloor, as indicated by well preserved tin mining holes. This observation confirms previous suggestions (Le Roux and Vargas 2005) that tsunami effects are largely related to confined channelized flows during backwash and, possibly, run-up.

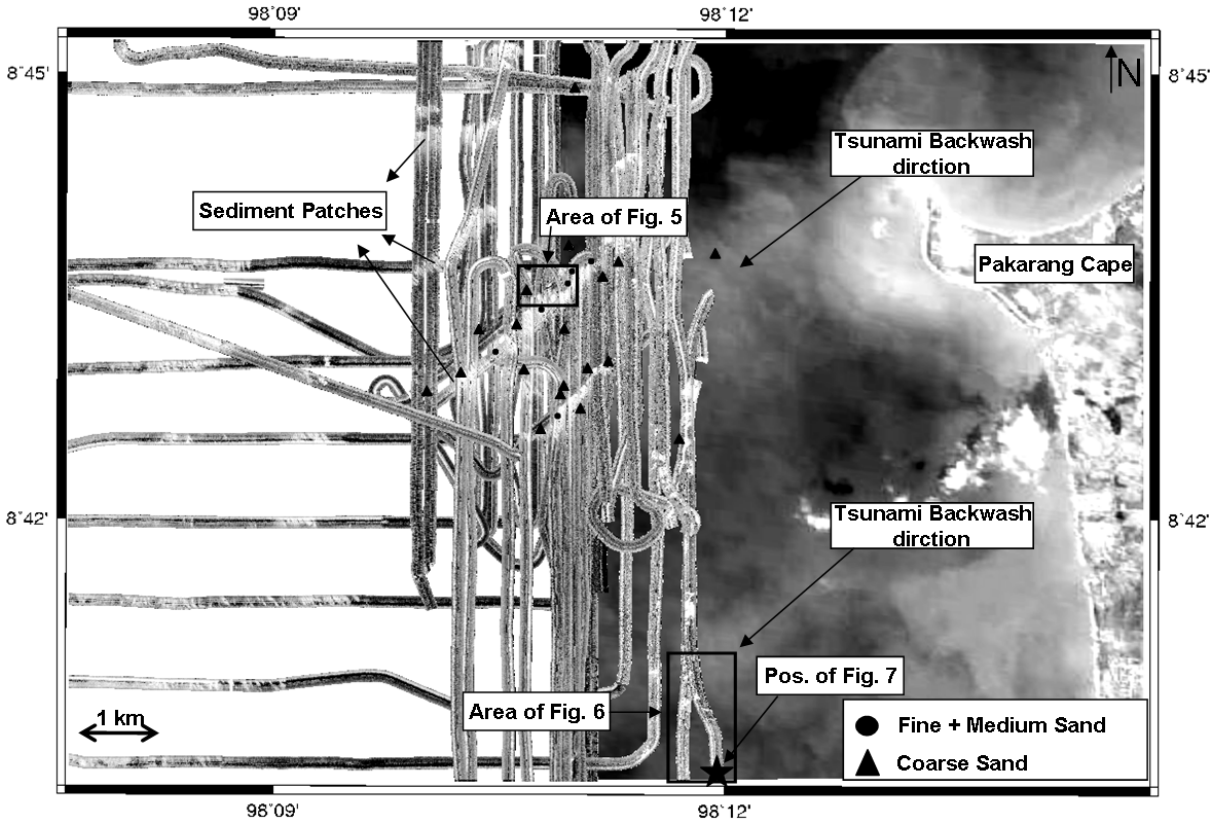

Fig. 4. Side Scan Sonar data merged with a satellite image taken shortly after the 2004 tsunami. Indicated are sediment types based on grain size analysis, as well as the locations of the following figures. (satellite image: Images acquired and processed by CRISP, National University of Singapore. IKONOS image 2004. www.crisp.nus.edu.sg/tsunami/tsunami.html, modified.)

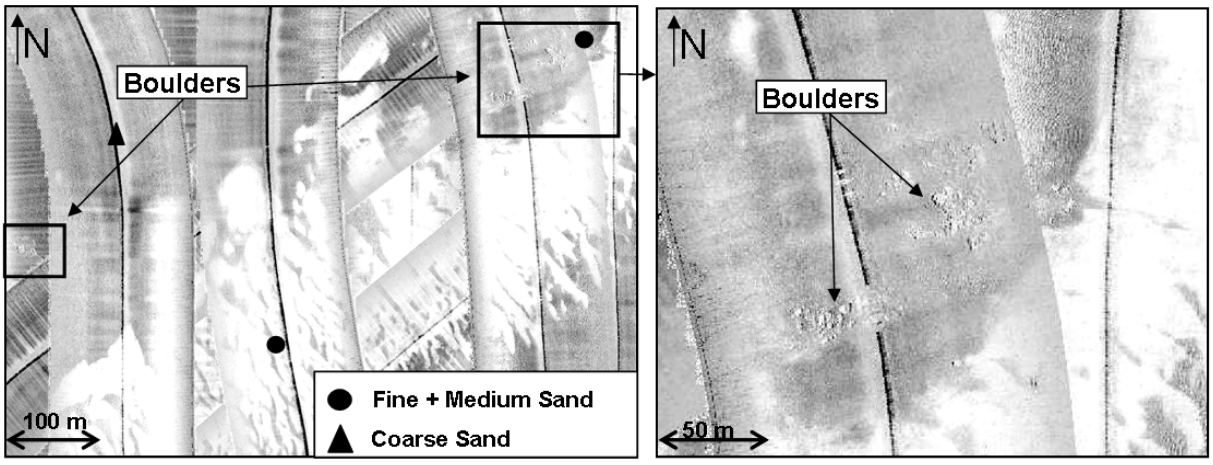

Fig. 5. Detailed view of one elongated sediment patch in front of Pakarang Cape. To the north of the patches, boulders are visible. For the location of the figure, refer to Fig. 4.

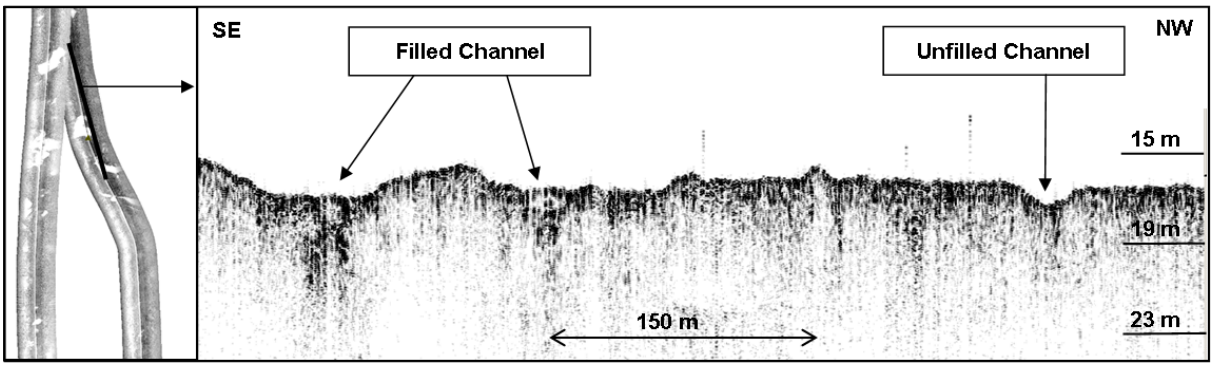

Fig. 6. Shallow seismic profiles close to the coastline with small channels. Some of these channels are filled with finer sediment, which appears white in the side scan sonar data. For the location of the figure, refer to Fig. 4.

The elongated areas and the small patches of fine and medium sand found in the channels and closer to the coastline could have been deposited during the backwash of the tsunami. If these sediments were deposited before the tsunami, one could expect that the tin mining holes would have been filled with the finer material during the past decades. However, the "flame-like" shape (indicating sediment transport) of the fine to medium sand sediment patches, as well as the presence of these sediments on the steeper southern slopes of the channels, may suggest their reworking during the post-tsunami period. In particular, their asymmetrical distribution in the channels may be a result of monsoon-related circulation and preservation of the finer sediments in relatively sheltered locations (Di Geronimo et al. 2008).

The existence of stiff muddy sediments containing pieces of grass and wood, which should be floating unless transported in a high turbidity and high density hyperpycnal flow, is strong supporting evidence of tsunami backwash and its potential erosion power. On the other hand, these deposits being covered by distinctly different coarse sand, typical for this part of the continental shelf, are already preserved in the geological record. This finding is promising for the search for paleotsunami evidence in this setting.

Interesting is the presence of boulders within the larger return channels in front of Pakarang Cape. The backwash velocity was modelled to be around 3.0 m/s at Cape Pakarang (Goto et al. 2007), slightly higher than the calculated critical velocity to move boulders. While some authors do not believe that the backwash, due to its short duration, transported boulders from the tidal flat back to the deeper waters, (Goto et al. 2007), it is very likely that boulders could easily be transported downhill from their original position on the coral reef slope during the tsunami backwash.

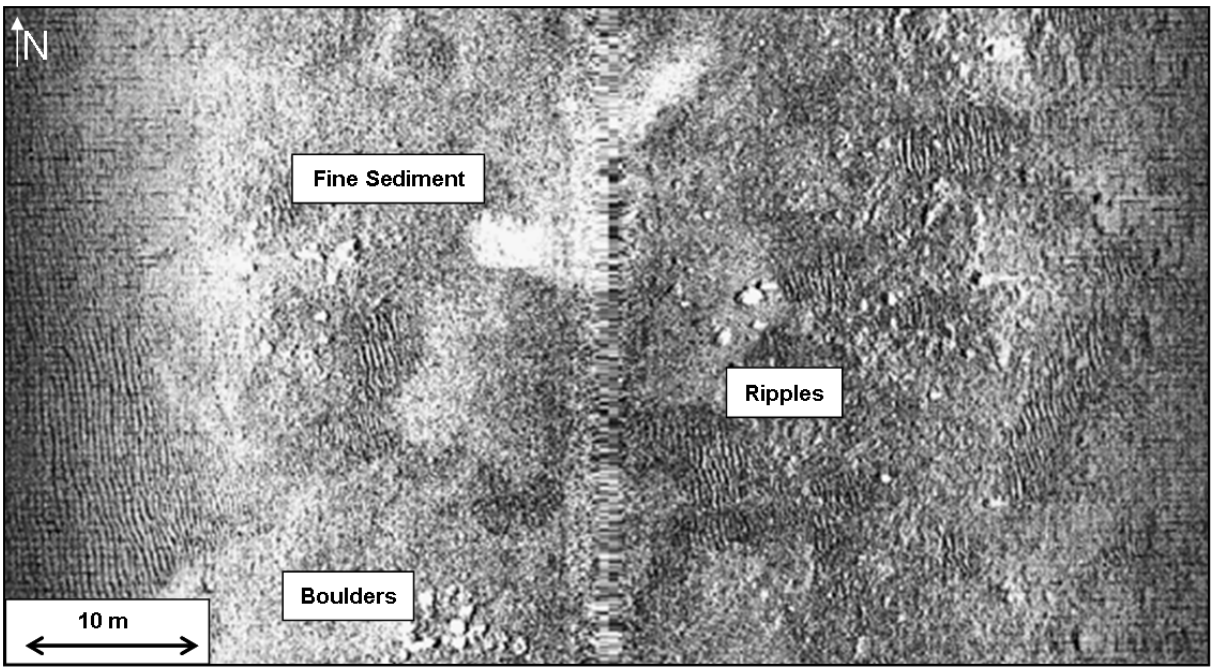

Fig. 7. Detailed view of side scan sonar data from a profile recorded close to the coastline. Different sediment types, including boulders, fine sediment and rippled sand are deposited within a distance of a few meters. The location of this figure is indicated in Fig. 4.

6. Conclusions

One of the first studies of offshore impacts of the 2004 tsunami indicates:

• Existence of a system of channels slightly oblique to the coastline, which are partly filled with finer sediments and could have been created during the backwash of the 2004 Indian Ocean tsunami.

• Variability in the channel system, which is changing with water depth and slope angle; probably as a result of changing hydrodynamic properties of the backwash (hyperpycnal flow).

• Validity of the assumptions on a channelized backwash, and maybe even run-up of the tsunami.

• Characteristic sediment deposition during the backwash, suggesting deposition from highly turbulent, high density flow.

• The backwash had enough power to transport boulders from the coral reef slope to deeper waters.

Acknowledgement

The study was supported by the DFG through research grant SCHW/11-1. W. Szczuciński was supported by a Foundation for Polish Science (FNP) fellowship. We are grateful to Phuket Marine Biological Center (PMBC) for providing us with RV CHAKRATONG TONGYAI. The help of cruise participants is greatly acknowledged.

4. Shallow water sediment structures in a tsunami-affected area (Pakarang Cape, Thailand)[4]

Peter Feldens[1], Daroonwan Sakuna[1,2], Penjai Somgpongchaiykul[3] & Klaus Schwarzer[1]

[1]Kiel University, Germany

[2]Phuket Marine Biological Centre, Thailand

[3]Biogeochemical and Environmental Change Research Unit, Prince of Songkla University, Thailand

Abstract

The influence of tsunami on the seafloor is poorly understood. Detailed hydroacoustic surveys and sediment sampling campaigns were carried out in 2007 and 2008 offshore Pakarang Cape (Thailand) to catalogue the geomarine effects of the 2004 Indian Ocean tsunami. A major problem in determining tsunami influence offshore in Thailand is the lack of pre-tsunami mappings. Starting in 15 m water depth, a system of sand ridges composed of coarse sand exists offshore Pakarang Cape. Elongated sediment transport structures on the NW-flanks of the sand ridges, slowly fading during the annual cycle, indicate the presence of a current oblique to the coastline. This current might coincide with the 2004 Indian Ocean Tsunami. A cm-thick event layer found at the base of a sand ridge is composed of silty sediment, which could be related to the tsunami backwash or strong floods during the monsoon. These event deposits are covered by coarse sand, and might enter the geological record.

1. Introduction

Tsunamis are among the largest catastrophic events in the world. They are recorded since historical times and numerous investigations have been done about their origin, wave distribution and energy release along coastlines. On December 26th, 2004 an M 9.3 submarine earthquake was generated off the northwest coast of the Indonesian island Sumatra due to a complex tectonic activity between the Indo-Australian plate and the Sunda-Plate. This generated a giant tsunami which had an impact over many SE Asian coastlines, reaching to the East-coast of Africa (Lay et al. 2005).

Compared to the influence of the 2004 Indian Ocean Tsunami to onshore areas, the impact to the offshore environment is not well understood. Only few studies document tsunami effects offshore (e.g. Van den Bergh et al. (2003), Noda et al. (2007), Abrantes et al. (2008), Feldens et al. (2009), Paris et al. (2009), but influence and physical properties of the sediment-loaded tsunami backwash are largely unknown. Dawson and Stewart (2007) propose that offshore tsunami deposits are more common in the geological record than onshore deposits. A secure identification of offshore tsunami deposits would therefore be of great value for the recognition of paleotsunamis. A major, but common problem is the missing data about pre-tsunami conditions when working on recent tsunamigenic structures on continental shelf areas. It has to be carefully considered, if observed structures have existed before a tsunami hit the area, were created during the tsunami event or were altered by the tsunami impact. We present observations and first results of selected sedimentological and morphological features, recorded during cruises in the framework of the TUNWAT project (Tsunami deposits in near-shore- and coastal waters of Thailand) offshore the tsunami impacted coastline of Khao Lak, Phang Nga Province, Thailand

[4] Reprinted with permission of "EUCC – Die Küsten Union Deutschland e.V." The original article is published in Coastline Reports 16, pages 15-25 (2010).

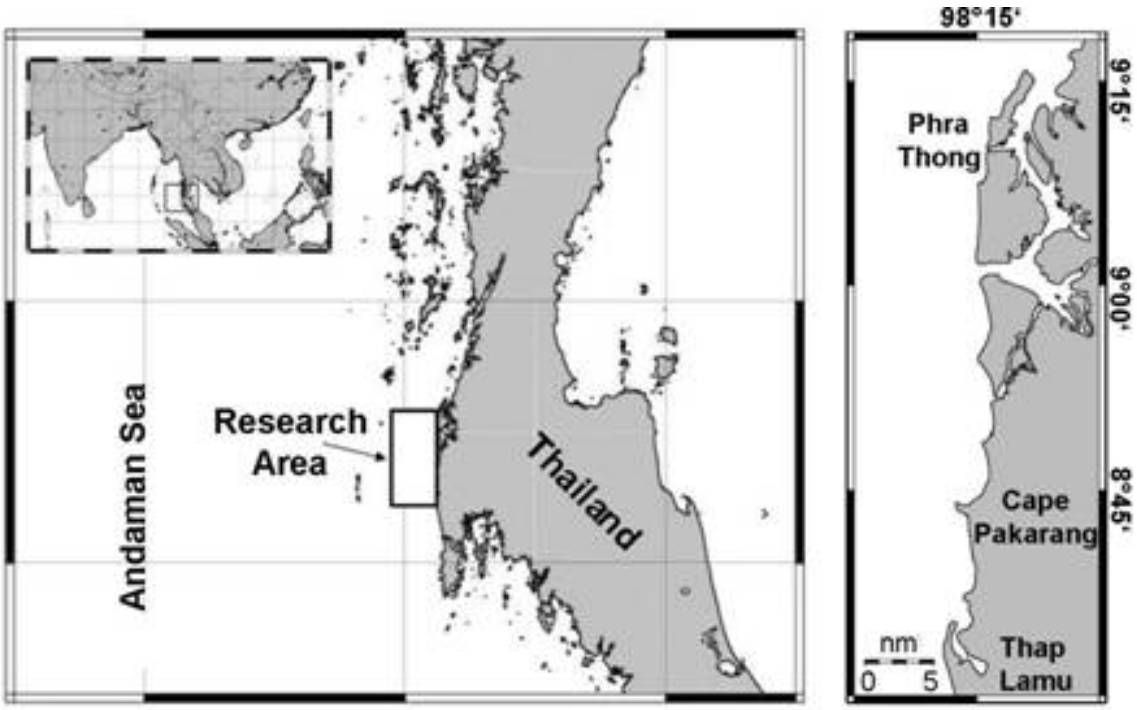

Figure 1: The research area is located in front of Khao Lak, Phang Nga province, Thailand.

2. Investigation area

The continental shelf of the Andaman Sea adjacent to the Malay Peninsula is narrow and slightly inclined; the 50 m isobaths is reached approximately 7 km offshore Phuket and about 30 km offshore Phang Nga Province located towards north. The coastal area is dominated by rocky cliffs altering with sandy lowlands and pocket beaches. From December to February the NE-monsoon dominates while the SW-monsoon is active between May and September (Khokiattiwong et al. 1991). The influence of storms and typhoons on this part of Thailand's coastline is low (Kumar et al. 2008, Jankaew et al. 2008). The tide is mixed semidiurnal, ranging between 1.1 m and 3.6 m (Thampanya et al. 2006).

The research area, between Thap Lamu and Phra Thong Island has a size of approximately 1.000 km² (figure 1). It was selected as it was hit severely by the 2004-tsunami (Bell et al. 2005, Tsuji et al. 2006). The wave run-up heights reached more than 15 m at Pakarang Cape (Siripong 2006) and up to 20 m at Phra Thong Island (Jankaew et al. 2008). At Pakarang Cape an area of about 12.500 m² was eroded by the tsunami (Synolakis & Kong 2006) and hundreds of reef rocks could be observed on the intertidal area after the event (Goto et al. 2007). For the investigation area the fluvial discharge is small, which increases the preservation potential of tsunamigenic features on the seafloor.

3. Methods

Two cruises have been carried out; a first one in Nov./Dec. 2007 with RV CHAKRATONG TONGYAI and a second with RV BOONLERT PASOOK in Nov./Dec. 2008. Both ships are operated by the Phuket Marine Biological Center (PMBC). Different side scan sonar systems were applied; a Klein 595 with digital data acquisition in 2007 and a Benthos 1624 digital side scan sonar system in 2008. Side scan sonar systems measure acoustical properties of the seafloor, which mainly depend on grain size distribution, seafloor roughness and the angle of the seafloor slope (Lurton 2002). Features protruding from the seafloor, e.g. boulders, but as well large ripples are easily recognized in side scan sonar images due to the acoustic shadow formed behind them. In this study, fine grained deposits appear in lighter colours, while

coarse grained material is represented by darker colours. For ground-truthing of the side-scan sonar data grab samples were taken on selected positions.

A shallow water multibeam echosounder (ELAC SeaBeam 1185) was used to acquire bathymetric data. Multibeam echo sounders provide many simultaneous depth measurements over a narrow section of the seafloor. The SeaBeam 1185 system is working with a frequency of 180 kHz, which is suitable for a high resolution mapping in shallow waters. The acoustic beam of the system has a fan width of 153°, giving a theoretical swath width of 8.3 times the water depths. Calibration for tidal fluctuations was done by using the software WX-Tide32 (www.wxtide32.com), as no direct water level measurements are available close to the research area.

Shallow water high resolution reflections seismics (C-Boom System), in combination with the recovery of short gravity cores, was used to obtain information about the uppermost layers of the seafloor. X-radiography images of thin slabs taken from the core surface were prepared to detect sedimentary structures that cannot be seen otherwise (Jackson et al. 1996). The database of the cruises carried out in 2007 and 2008 include about 1500 nautical miles (nm) of hydroacoustic profiles, 112 Surface sediment samples and 42 short sediment cores.

4. Results

Side scan sonar images offshore Khao Lak show several different sedimentary structures in depths from 7 to 30 m (figure 2). In water depths between 7 and 15 m, extended patches of fine grained sediments are deposited. Connected to these patches is a small scale channel system starting at 10 m water depth. Here we focus on structures appearing at 15 m water-depth. Elongated SW-NE striking morphological ridges are visible in the hydroacoustic data (Figure 2). These structures are common along the whole coastline between Thap Lamu and Pakarang Cape, and up to Phra Thong Island towards north. The continuation of the ridges into deeper waters is yet unknown. The ridges, with a steep NW- and a gently dipping SE flank reach heights of about 2 m, while their length exceeds several kilometres. The distance between two ridge crests varies from several hundred meters to several kilometres. In front of the steep north-eastern side of these ridges, small channels with incision depths of approximately 1 m are sometimes cut into the seafloor. According to seismic data, the ridges are not connected to subsurface structures, but are clearly separated from the sedimentological structures below by an unconformity (figure 5).

For one ridge, a side scan sonar mosaic was draped over the bathymetric data (figure 3) to correlate sedimentology and morphology. Grab samples taken around the ridge (figure 3) reveal the presence of different sediment properties in a small area: Generally, the south-western, landward flank of the ridge and the surface of the seafloor surrounding the ridge are composed of coarse sand. Bright elongated sediment structures are deposited on the seaward flank of the ridge and are composed of well sorted fine to medium sand. The patches are separated from each other by thin bands of coarser sediment. From their appearance in the side scan sonar image, the structures resemble large-scale flaser beddings. However, as the genesis of the observed features is different to flaser beddings, which are formed due to tidal activities, the term will not be used.

The sediment patches are commonly observed on the seaward, northern flank of sand ridges along the coastline. Rarely, they are found on the flat seafloor. Boulders are sometimes exposed in close vicinity (figure 3, figure 4). At the base of the ridge flank shown in figure 3, grab samples contain muddy material just a few centimetres below the seafloor.

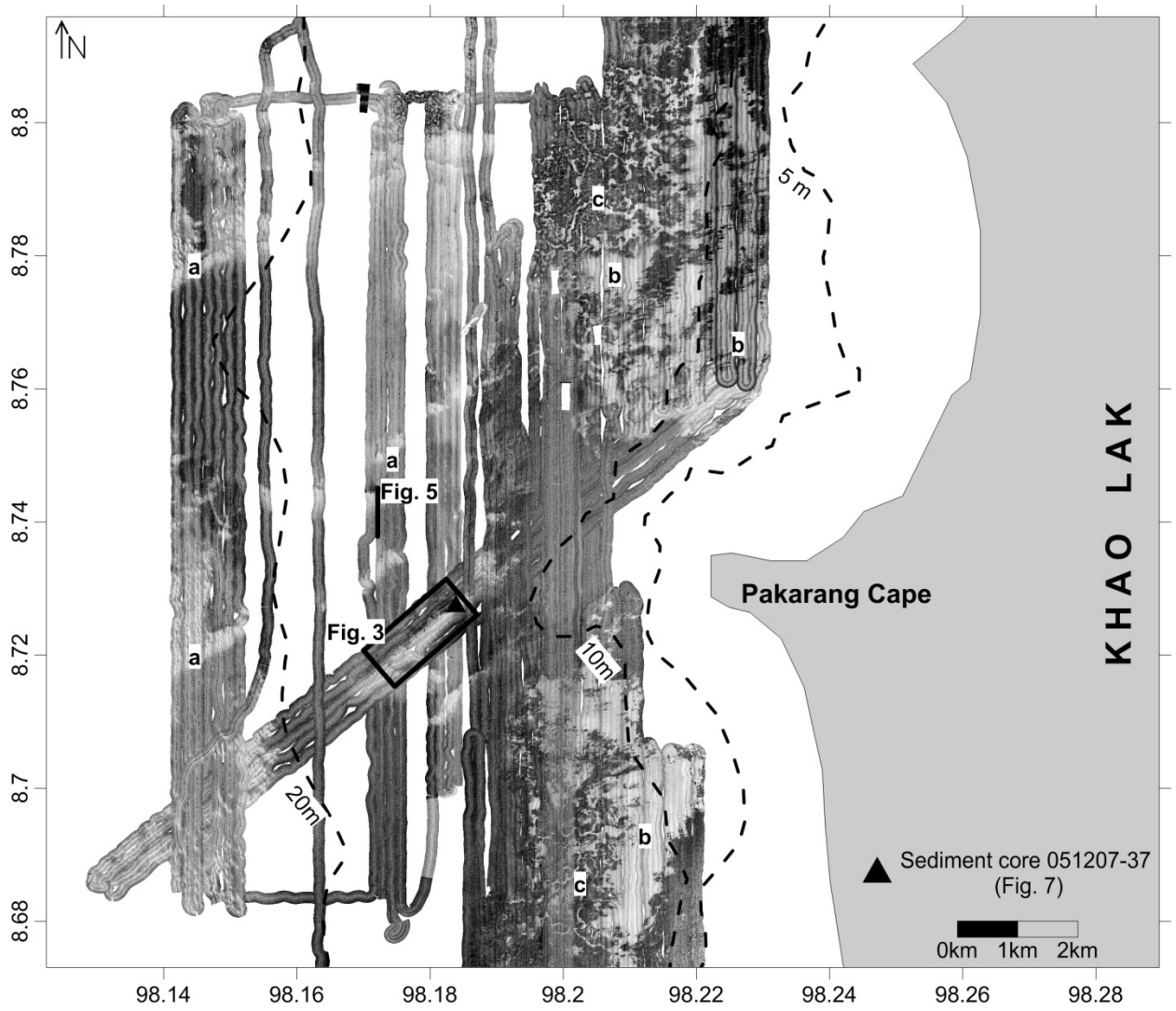

Figure 2: Side scan sonar data around Pakarang Cape. Sampling stations and the positions of fig. 3 and fig. 4 are indicated. Sediment core 051207-37 is shown in fig. 7. This article is focusing on SW-NE striking sediment structures visible as lighter-coloured bands in the side-scan sonar image (a). Closer to the coastline, extended areas of fine grained sediment (b) and a small scale channels (c) are visible.

Core 051207-37 (figure 7) is divided in four sedimentary units. Unit 1 (0-8 cm core depth) is mainly composed of brown sand, including some shell fragments. Between app. 8 and 11 cm, a layer composed of silt, containing no sand, is deposited (unit 2). The lower boundary of unit 2 is sharp, while its upper boundary is not well defined. Between app. 11 to 12 cm core depth, unit 3A is composed of well sorted sand. Below, unit 3B (12 to 20 cm core depth) contains higher amounts of clay and silt. Various shell fragments are abundant in unit 3B. From 20cm to the base of the core, unit 4 is composed of sandy silt, and includes some shell fragments. Partly, layers containing higher amounts of sediments in the sand fraction are recognized in the x-ray images.

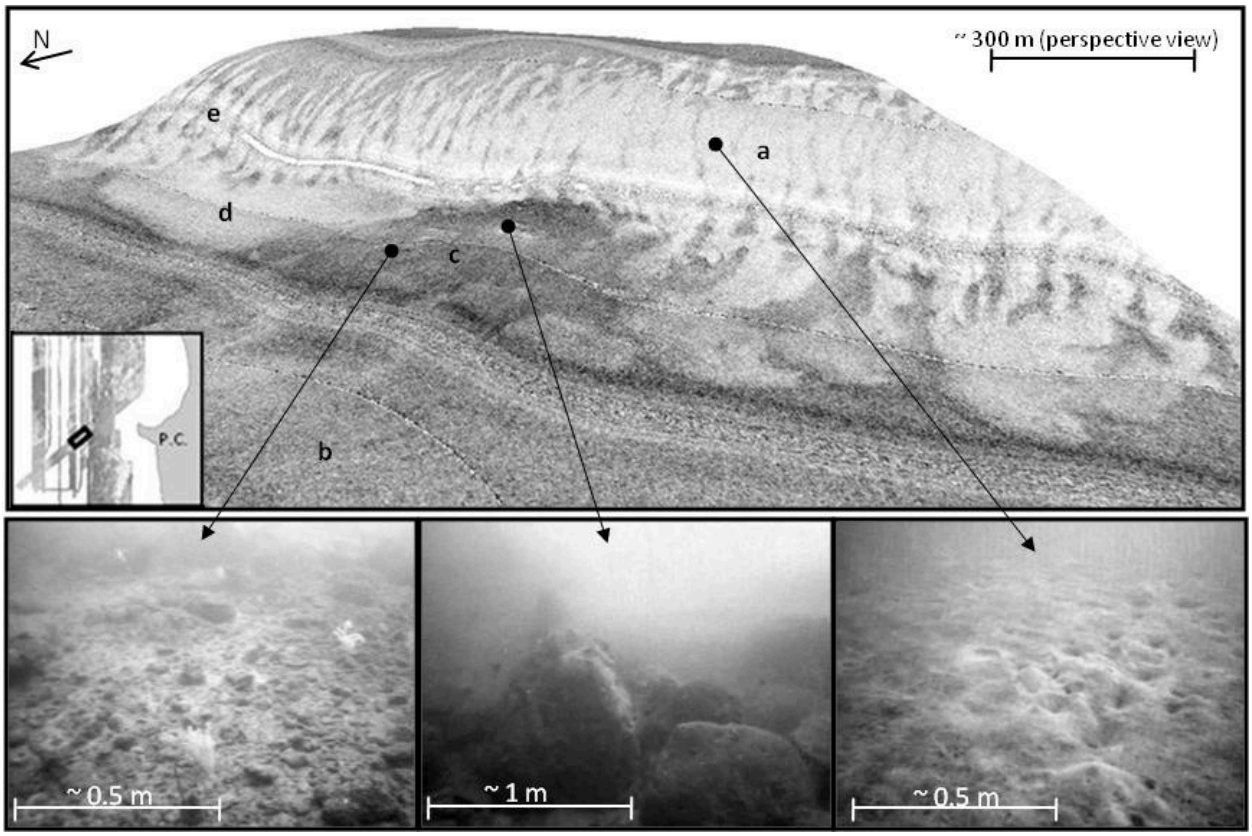

Figure 3: Side scan sonar draped over the bathymetric dataset. For position see figure 2. The length of the ridge is approx. 1500 m (perspective view). a) elongated sediment patches, consisting of fine to medium sand b) coarse sand c) carbonatic gravel and boulders (notice video image) d) sand at the surface, muddy material below e) position of short core (051207-37, fig. 7), composed of sandy material on top and a fine grained layer at 10 cm depth.

5. Discussion

Sand ridges are formed due to regular hydrodynamic processes, e.g. tidal currents in inlets, ocean currents at the shelf margin or during storms (Ernstsen et al. 2006, Flemming 1978, Holland and Elmore 2008), although moribund ridges as remnants from times with a lower sea level are known (Dyer and Huntley 1999). Goff et al. (1999) report that sand ridges on the northeast US Atlantic shelf are asymmetric, having steeper seaward flanks. Holland & Elmore (2008) report that grain sizes across sand ridges typically range from coarse to fine sand. The typical height of storm generated sand ridges is given with 3 to 12 m (van de Meene and van Rijn 2000). Commonly, sand ridges are oblique to the coastline, with the acute angle opening into the prevailing flow direction (Swift et al. 1978, Holland and Elmoore 2008). Most of these features are found in the observed ridge system. The strike direction of the ridges indicates an approximately south-north directed current that was responsible for their formation. This was not the main current direction observed during the tsunami (images of the IKONOS satellite, Goto et al. 2007). Therefore, the ridge system existed prior to the tsunami, although the definite process responsible for its formation has not yet been identified.

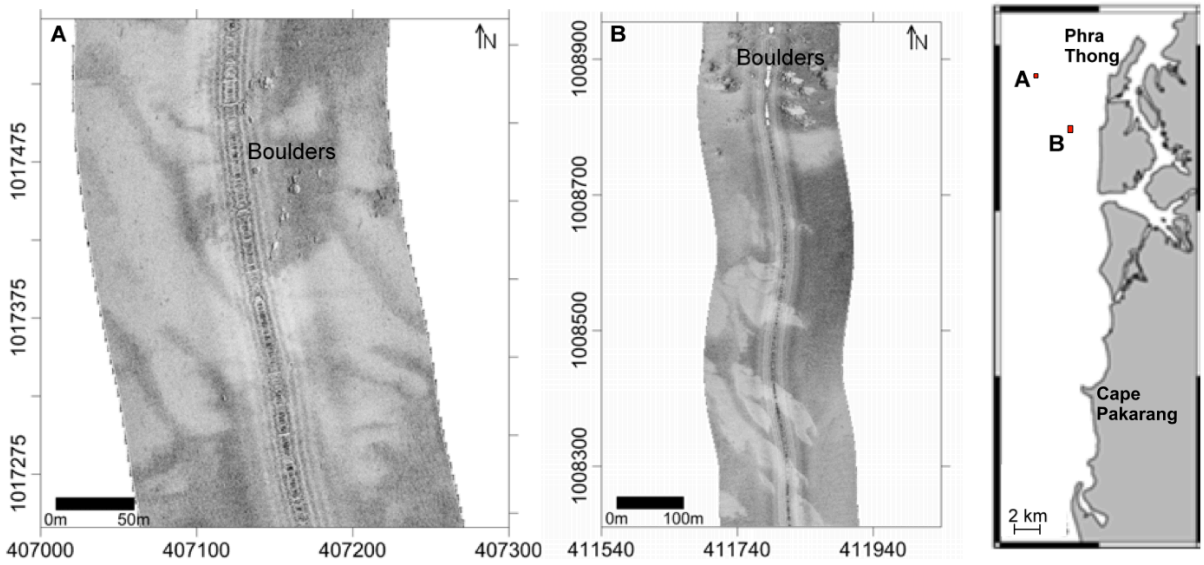

Figure 4: Elongated sedimentary structures offshore Phra Thong. Frequently, boulders are exposed in close vicinity to these structures. Water depth at A: 27 m. Water depth at B: 21 m.

Notable are the elongated sediment patches commonly found on the northern flanks of the sand ridges. While finer sediment on the steeper slope of asymmetrical sand ridges is common on sand ridges in front of storm dominated coasts (Holland and Elmore 2008), in this case it is not visible over the entire length of the flank, but instead is deposited in small patches separated by coarser sediment. Similar bedforms on the continental shelf offshore Brazil have been formed due to storm events (Moscon and Bastos 2010). The comparison of side scan sonar images from 2007 and 2008 (figure 6) show that the general shape of the patches is preserved, but smaller details begin to fade during one annual cycle, indicating an out-of-equilibrium event based deposition and ongoing reworking of the sediment. Additionally, the existence of identical sediment structures on the flat seafloor further indicates that their formation is not connected with the formation of the sand ridges. Therefore these elongated patches of fine grained sediment have to be interpreted as bedforms created by currents along the north-east to south-west direction. The general stability of these bedforms, combined with the slow fading of delicate structures suggests that no frequently occurring event is responsible for their formation. Since strong storms are rare in the area, and none occurred between the 2004 tsunami and our measurements (based on tracks published by the Regional Specialised Meteorological Centre – Tropical Cyclones (RMSC), New Delhi), it is reasonable to assume that the observed sediment pattern was influenced by the 2004 tsunami, either during the run-up or the backwash.

It is assumed that the muddy material frequently found in grab samples at the base of the sand ridge corresponds to unit 2 in core 051207-37. Therefore, such material is present over a larger area at the base of the sand ridge, and not only locally in one core. Considering the silt separating two units of coarse sand, its deposition likely corresponds to a single event. Similar deposits in cores offshore the Eel River have been described by Crocket & Nittrouer (2004) as flood deposits, which could be generated in the research area by strong monsoon events. But also a tsunami backwash transports large amounts of fine-grained material seawards (Shi & Smith 2003). The process responsible for the formation cannot be determined with certainty. However, a deposition of this material during the monsoon is unlikely, as more regularly occurring structures would be expected. Regardless of the origin of their formation, these event deposits were preserved in the comparably sheltered environments at the base of the sand ridges. They are covered by coarse sand (unit 1), typical for this area of the shelf, which

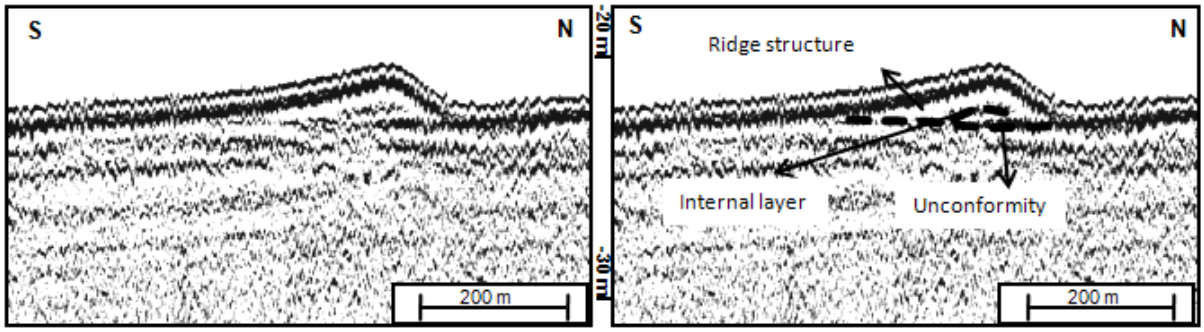

Figure 5: Seismic profile crossing a sand ridge (for position see Figure 2). Clearly visible is the asymmetric form of the ridge which is indicating a transport direction from South to North. Additionally, the ridge is separated from the older surface below by an unconformity.

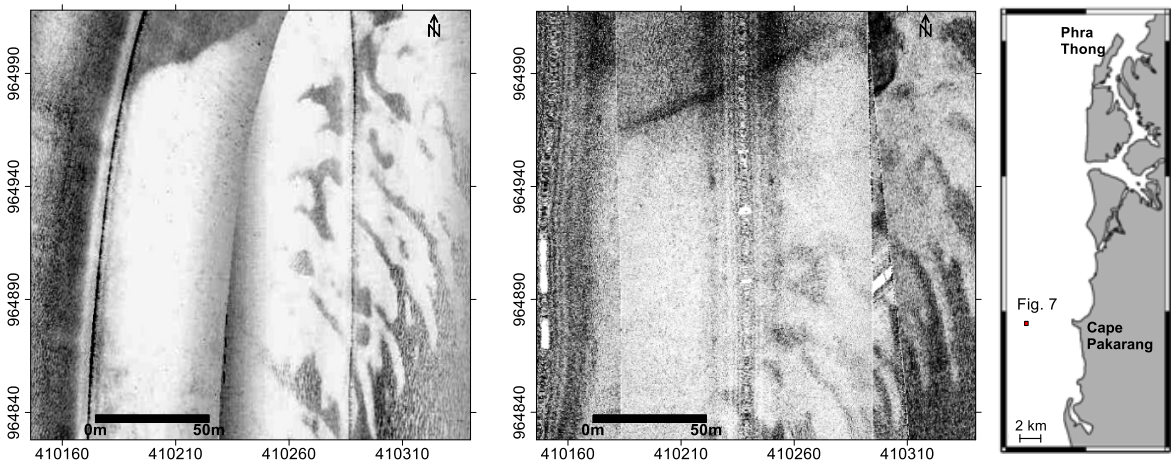

Figure 6: Two side-scan sonar images showing a comparison of a detail of the sand ridge shown in figure 3 The left image was recorded in 2007, the right image in 2008. Small differences are visible, and the contours of the elongated sedimentary structures are more pronounced in 2007.

indicates some sediment dynamic in the area. This agrees to the change of sedimentological boundaries observed in side scan sonar mosaics between 2007 and 2008 (figure 6). A potential deposition of the sediments beneath unit 2 during an event, indicated for instance by the marked change in sand content of unit 3A compared to unit 3B, or the abundance of shell fragments in unit 3B, is uncertain. Further analysis is needed to identify the origin and the spatial extension of these potential tsunami deposits, especially closer towards the shoreline.

Interesting are frequent observations of boulders close to the elongated patches deposited at the seaward flank of the sand ridges. Many of these boulders show no connection to structures in the subsurface, and must have been transported to their current position. Potentially, this could have happened during the tsunami, either during the run-up from source areas in deeper waters, or during the backwash (compare Paris et al. 2009)

During the tsunami run-up, many boulders were transported towards the intertidal area on Pakarang Cape (Goto et al. 2007). The backwash at Pakarang Cape was modelled by Goto et al. (2007). The authors show that the current speed of the backwash was in the order of 3m/s. This is strong enough to move the observed boulders (Goto et al. 2007, Imamura et al. 2008), which have a diameter of less than 1 meter according to underwater images. Taking into account a channelized backwash (Le Roux and Vargas 2005, Fagherazzi and Du 2007), it is possible that in some areas the current speed was strong enough to transport boulders downslope from the reef platform fringing Pakarang Cape back towards the sea. However, this cannot explain the presence of boulders found several kilometers in front of the coastline (Fig. 4).

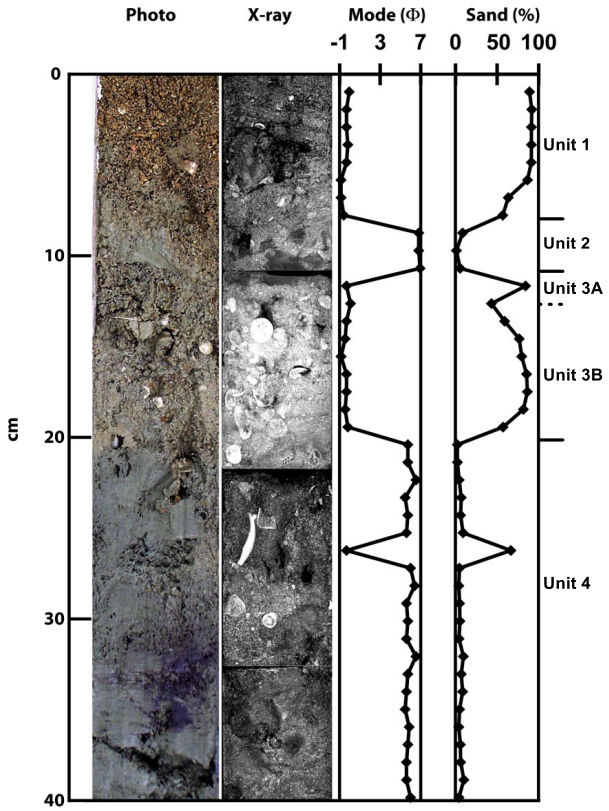

Figure 7: Properties of core 051207-37. From left to right, photo, x-ray image, first mode in phi-degrees, sand content and sedimentary units are presented. For position, refer to Fig. 2.

6. Conclusion

Detailed hydroacoustic surveys have been carried out offshore Phang Nga province (Thailand) in 2007 and 2008 and sediment samples have been collected. Starting at 15 m water depth, a system of sand ridges, formed by coarse sand, was discovered. The sand ridges existed prior to the 2004 Indian Ocean Tsunami. Elongated sediment patches on the seaward flank of the sand ridges consist of fine to medium sand, and indicate a current oblique to the coastline. They fade slowly during the annual cycle, and were potentially reworked during the 2004 Indian Ocean Tsunami. An event layer found at the base of a sand ridge is composed of silty sediment, which could be related to the tsunami backwash or floods during the monsoon. These event deposits are covered by coarse sand, and might enter the geological record.

Acknowledgement

We are grateful to NRCT (National Research Council Thailand) and PMBC (Phuket Marine Biological Center) for providing us with the research vessels CHAKRATONG TONGAI and BOONLERT SOOK. We thank masters and crew of both vessels for their outstanding support during the cruise. The German part of this study was supported by DFG through research grant SCHW/11-1. Many thanks go to Witold Sczcuciński and Karl Stattegger for good discussions.

5. Sediment distribution on the inner continental shelf off Khao Lak (Thailand) after the 2004 Indian Ocean Tsunami[5]

P. Feldens[1], K. Schwarzer[1], D. Sakuna[1,2], W. Szczuciński[3], P. Sompongchaiyakul[4]

[1]Institute of Geosciences, Kiel University, Otto-Hahn-Platz 1, 24118 Kiel, Germany.

[2]Oceanography and Environment Unit, Phuket Marine Biological Center, P.O. Box 60, Phuket 83000, Thailand.

[3]Institute of Geology, Adam Mickiewicz University, Maków Polnych 16, 61-606 Poznań, Poland.

[4] Department of Marine Science, Faculty of Science, Chulalongkorn University, Bangkok 10330, Thailand.

Abstract

The coastline of Khao Lak (Thailand) was heavily damaged by the 2004 Indian Ocean tsunami. Onshore tsunami deposits and satellite images, which show large amounts of sediment transported offshore, indicate that the seafloor was impacted by tsunami run-up and backwash. In this study, high-resolution maps of sediment distribution patterns and the geological development of the seafloor are presented. These maps are based on multibeam, side-scan sonar and seismic profiling surveys offshore Khao Lak. Paleoreefs with associated boulder fields and sandy sediment dominate the inner continental shelf. Patches of fine-grained (silt to fine sand) sediments exist in water depths of less than 15 m. The sediment distribution pattern is stable between 2008 and 2010, apart from small shifts regarding the boundaries of the fine-grained sediment patches. In one sediment core and several grab samples an event layer was documented, situated below a cover of modern sediments which is only a few cm thick. The event-layer is traced down to 18 m water depth. It consists mostly of sand and contains compounds of terrigenous origin. It is interpreted as a 2004 Indian Ocean tsunami deposit. However, on wide areas of the study-site an impact of the tsunami is hardly identifiable by seafloor morphology or sediment distribution.

Keywords: 2004 Indian Ocean tsunami, offshore tsunami deposits, continental shelf, nearshore deposits, Andaman Sea

1. Introduction

Tsunami waves may cause erosion and sedimentation in various environments including coastal lowlands, lakes, lagoons, tidal flats, beaches, continental shelves but also the deep sea (e.g. Shiki et al. 2008, Bourgeois 2009). Among these environments, the tsunami impacts in the marine realm are the least known, although, as discussed by Dawson and Stewart (2007), theoretically offshore tsunami deposits may comprise a large percentage of tsunami records in geological history.

In contrast to onshore tsunami deposits with a relatively well-established set of diagnostic features, based on many studies of recent tsunami events (e.g. Dawson and Shi 2000, Goff et al. 2001, Shiki et al. 2008, Bourgeois 2009, Chagué-Goff 2010, Goto et al. 2010a), offshore tsunami deposits are poorly known. They were investigated only in a few cases (e.g. van den Bergh et al. 2003, Noda et al. 2007, Abrantes et al. 2008, Goodman-Tchernov et al. 2009, Paris et al. 2010). The existing data are far from sufficient to establish universal key criteria

[5] This article will be published in a special volume of "Earth Planets Space". A preliminary version of the article is reprinted with permission of TERRAPUB (Terra Scientific Publishing Company).

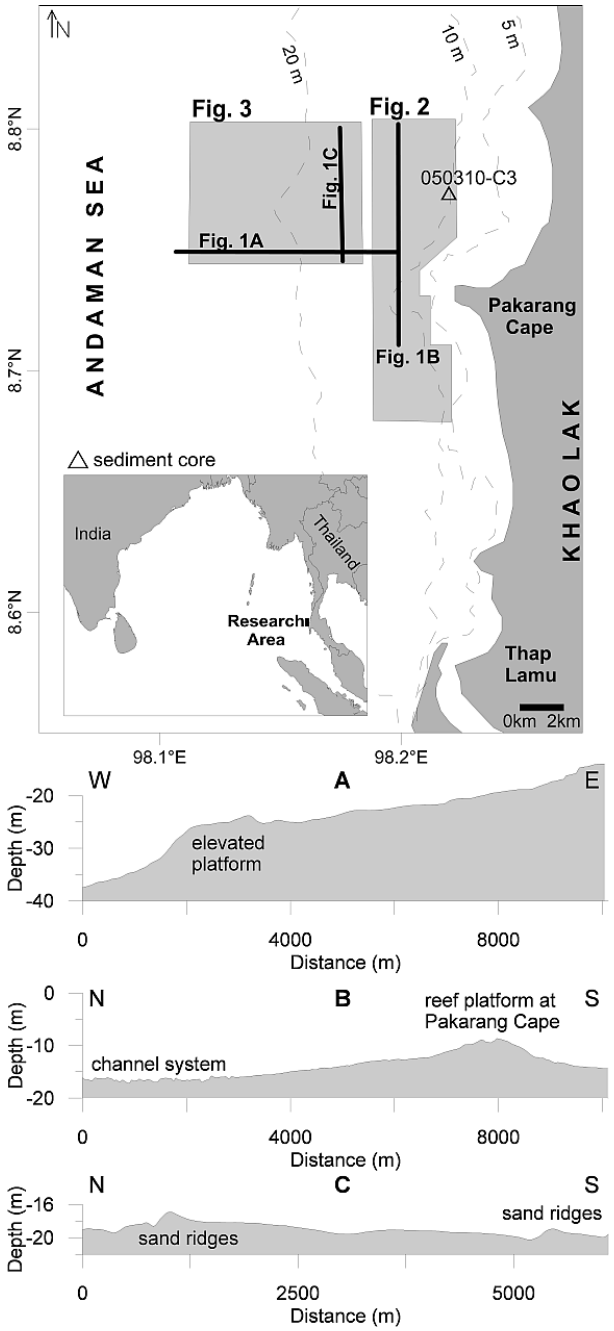

Fig. 1: Overview of the research area offshore Khao Lak and location of bathymetric profiles (A-C, vertical exaggeration ≈ 100x). Areas shown in subsequent figures, and the position of core 050310-C3 are indicated.

for identification of offshore tsunami deposits and to understand the controlling processes of deposition associated with tsunami wave passages. Even less is known about erosion of the seafloor due to tsunami waves. Most information about seafloor erosion derives from studies of onshore deposits containing marine microfossils like foraminifera (e.g. Nanayama and Shigeno 2006, Uchida et al. 2010) or diatoms (e.g. Dawson 2007, Sawai et al. 2009).

The geological impacts of the 2004 Indian Ocean tsunami are likely to present the most detailed investigation in the history of tsunami research. Regardless, limited literature exists regarding the offshore effects of this. Offshore effects were found to be variable: For instance Paris et al. (2010), applying side scan sonar mapping nearby Banda Aceh (Sumatra), documented a large boulder field deposited in water depth from 5 to 25 m mainly by the tsunami backwash flow. In the nearshore zone off India and Sri Lanka a change in bathymetry was observed after the tsunami, caused by both erosion and deposition (Narayana et al. 2007, Anandan and Sasidhar 2008, Goto et al. 2011). Local erosion in a water depth of approximately 30 m on the continental shelf of the Andaman Sea, adjacent to the coast of Thailand, was reported by Chavanich et al. (2005). Post-tsunami change in shallow water sediment distribution was documented by Kendall et al. (2009). Meanwhile, tsunami backwash deposits were reported from few sites on the inner continental shelf (Feldens et al. 2009, Sugawara et al. 2009, Sakuna et al., this volume).

Most of the evidence for offshore effects is based on a few scattered observations or sampling sites and does not allow an overall assessment of the tsunami impact on the seafloor of the inner shelf. Topographical variations lead to changes in the tsunami runup height and impacts onshore (e.g. Szczuciński et al. 2006). Therefore, it is reasonable to expect the submarine effects of tsunami to vary spatially as a result of different bathymetry. Moreover, satellite images show large amounts of suspended load transported offshore in plumes due to the commonly channelized tsunami backwash flow (Umitsu et al. 2007, Fagherazzi and Du 2008, Yan and Tang 2009).

Consequently, the local variations in runup and backwash may cause the characteristics and distribution of the resulting erosion and deposition caused by the tsunami to vary. A further issue is the potential of preservation and recognition of an offshore tsunami impact. Potential offshore tsunami deposits are subjected to several processes, which may remove or alter the deposits. These processes are for instance waves, currents, tides, and bioturbation. After the 2004 tsunami, the beaches along the Thai coastline, which had been heavily eroded, were rebuilt naturally. The coastal systems returned to equilibrium conditions within only a few years (e.g. Choowong et al. 2009, Grzelak et al. 2009). One may expect similar transformation to occur also in the shallow marine areas.

The assessment of tsunami effects on the seafloor of the inner shelf, without detailed information about pre-tsunami conditions, requires repeated high-resolution seafloor mappings. This is due to the variability of tsunami impacts and dynamics of post-tsunami processes. Seafloor mapping helps to identify modern sediment distribution patterns and annual dynamics, and particularly to locate sheltered environments where offshore tsunami deposits could be preserved. Offshore tsunami deposits identified in such environments may supplement the paleo-record already established from onshore deposits (e.g. Jankaew et al. 2008).

The present study focuses on the inner continental shelf offshore of Khao Lak (Thailand), an area which was strongly impacted by the 2004 Indian Ocean tsunami. The major objectives are:

1. to map geological structures, to document seafloor morphology and to elaborate sediment distribution patterns;

2. to identify the interannual seabed sediment dynamics by reinvestigation of the same areas;

3. to identify sediments, deposited by the 2004 Indian Ocean tsunami, and to gain information about their preservation potential.

2. Investigation area

The presented study area offshore of Khao Lak (Thailand) covers about 105 km^2 ranging from 5 to 35 m water depth. Here, the coastline consists of beaches adjacent to coastal lowlands alternating with rocky cliffs. The tides are mixed semidiurnal and range from 1.1 to 3.6 m (Thampanya et al. 2006). From December to February the NE-monsoon dominates weather patterns, while the SW-monsoon is active from May to September (Khokiattiwong et al. 1991); calm conditions prevail in between. Offshore wave heights during the SW-monsoon can reach up to 5 m (Choowong et al. 2009). During the NE-monsoon wave influence is negligible, yet strong typhoons can occur in this part of Thailand, although they are generally rare (Kumar et al. 2008, Brand 2009, Phantuwongraj and Choowong 2011). No such events occurred between the 2004 Indian Ocean tsunami and the period of our measurements (data by the Regional Specialized Meteorological Centre - Tropical Cyclones, RMSC, New Delhi).

There are no large rivers discharging into the investigation area. Meanwhile, longshore currents and sediment transport are commonly directed from south to north (Di Geronimo et al. 2009, Choowong et al. 2009), leading to the formation of common coastal figures such as sand spits. Offshore of Khao Lak, carbonate and granitic outcrops are common on the seafloor (Di Geronimo et al. 2009). In the past, extensive tin mining activities took place in Phuket-, Ranong- and Phang Nga province on land and offshore down to 50 m water depth (Suwanwerakamtorn et al. 1990). Mining pits, up to 100 m in diameter and 7 m in depth still exist offshore (e.g. Feldens et al. 2009).

The 2004 Indian Ocean Tsunami had a strong impact on the coastal areas along the Andaman Sea (Bell at al. 2005, Tsuji et al. 2006, Thanawood et al. 2006, Szczuciński et al. 2006). The maximum tsunami run-up height in the study area reached 15 m at Pakarang Cape (Siripong 2006). About 12500 m^2 of Pakarang Cape were eroded by the tsunami and a large amount of boulders were transported from an offshore reef platform into the intertidal zone (Goto et al. 2007). Onshore tsunami deposits contained numerous indicators of marine origin. Microfossils suggest seafloor erosion by the tsunami in the intertidal, nearshore and open marine (continental shelf) environments occurred (Hawkes et al. 2007, Kokociński et al. 2009, Sawai et al. 2009).

3. Methods

Full coverage side scan sonar mapping, supported by multibeam echosounding and shallow reflection seismic soundings, were performed during three cruises (Nov.-Dec. 2007, Nov.-Dec. 2008, Jan.-Feb. 2010). In 2008 and 2010 selected areas were reinvestigated to obtain information about interannual sediment dynamics. The available dataset comprises about 2000 nautical miles (nm) of hydroacoustic profiles, ranging from 5 to 90 m along the coastline off Khao Lak. Approximately 105 km^2 of full-coverage side scan sonar images taken offshore from Pakarang Cape in water depths ranging from 5 to 35 m are presented in this article.

Bathymetric data were collected using a SeaBeam 1185 multibeam system (180 kHz, ELAC Nautic GmbH). Seismic data were collected using an EG&G boomer (2007) system and a low voltage boomer device (C-Boom, 2008 and 2010) combined with an 8-element single channel streamer for signal recording. A high- and low pass filter (0.3 kHz and 7 kHz) was applied to remove acoustic disturbances. A Klein 595 side scan sonar (384 kHz) with digital data acquisition and a Benthos 1624 side scan sonar (100 and 400 kHz) were used to obtain information about sediment distribution patterns on the seafloor. The data were mosaiced and resulting images were improved by adjusting white and black values in order to better display the contrast of the side scan sonar data. In this study, low backscatter values are displayed in light grey, while high backscatter values appear in darker grey.

Grab samples were taken in order to ground-truth and calibrate the side scan sonar data. Sediment cores were collected using a Rumohr type gravity corer (7 cm internal diameter). In the laboratory, cores were cut in two halves, photographed and sampled for x-ray analysis (1 cm thick slabs) as well as for grain size analysis. Depending on the sediment composition, grab samples from the sediment surface were either sieved or analyzed using a Mastersizer 2000 laser diffraction device. Samples from the sediment core discussed in this paper were analyzed with the Mastersizer 2000.

For the grain size analysis by laser diffraction, carbonate and organic material were removed by acidification with HCl and H_2O_2 prior to analyses. Moreover $Na_4P_2O_7$ was added to avoid aggregation of fine particles during the measuring process. Grains exceeding 1.7 mm in diameter can not be analyzed with this method. This is an important restriction as the sediment core contained layers of coarser material. It was not possible to combine sieving and laser diffraction measurements for the analysis of core material as no representative sieving results could be obtained due to the limited amount of available sediment. Therefore, the obtained grain size distributions do not fully represent the grain size distributions of the sediment, when grains with a diameter > 1.7mm are present.

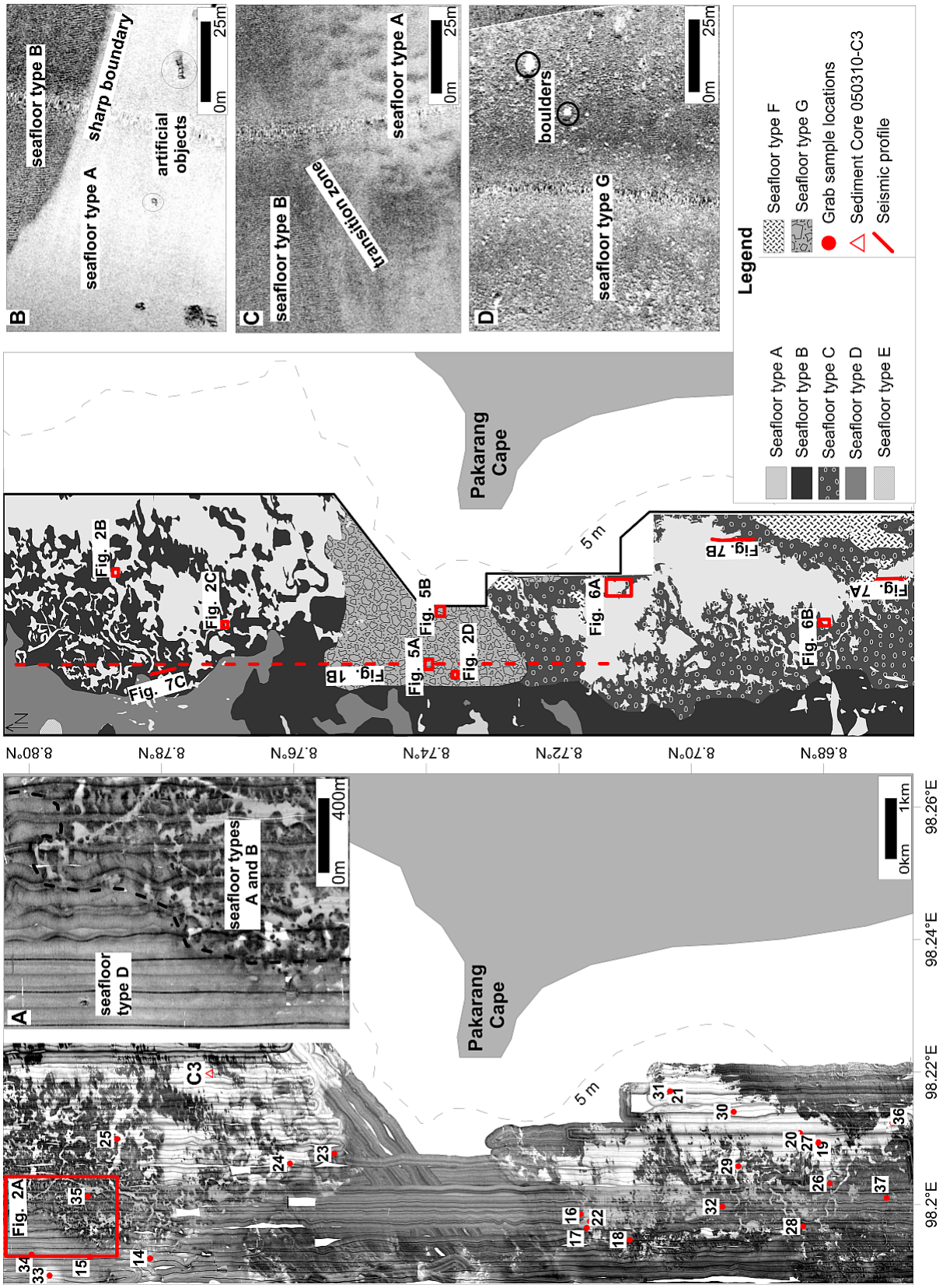

Fig. 2. Side scan sonar image (left) and the interpretation as map of different types of seafloor (right), down to app. 15 m water depth. The seafloor types is determined on the classification of side scan sonar data and is verified by surface sediment samples Insets A, B, C and D show details discussed in the text.

Grain sizes are presented in the Phi (Φ) scale with $\Phi=-\log_2 d$, with d=grain size in mm (Krumbein 1938). The mode of the grain size distribution was chosen as a central statistical parameter because it is not affected by removing coarse (laser diffraction based method) or fine (sieving) parts from the grain size distribution. Modes can also be used for bimodal sediments. Sorting values, based on unimodal samples, are given using the geometric method of moments (calculation with the software Gradistat, Blott and Pye 2001).

4. Results

4.1 Seafloor bathymetry

A dead fringing reef complex near Pakarang Cape (Sanfilippo et al. 2010) forms a platform that extends down to approximately 10 m water depth (Figs. 1 and 2). Seaward from this reef platform, the seafloor gently declines by 0.1° down to 25 m water depth, which is the depth reached about 10 km offshore of the tip of Pakarang Cape (Fig. 1A). North and south of Pakarang Cape, in water depths between 5 and 10 m, a system of small channels, up to 2 m deep and generally between 30 and 100 m in width, is incised into the seafloor (Figs. 1B and 2).

Further offshore, SW-NE striking sand ridges are present (Fig. 1C). Their height above the seafloor reaches up to 2 m. The distance between two sand ridge crests varies from several hundred meters to several kilometers. The length of the ridges exceeds 5 km. These sand ridges are asymmetric, with a steeper flank exposed to the NW and with a slope of up to 1.2°. They are also marked by a gently dipping flank exposed towards the SE. In some areas small incisions up to 1 m deep exist in front of the northwestern flanks. Most of the sand ridges can be easily recognized in the side scan sonar images; sediment with lower backscatter intensity is exposed on the steep northwestern flanks (seafloor type E, Fig. 3). The sand ridges are no longer found in approximately 25 m water depth, meanwhile a slightly elevated platform is observed in the bathymetry (Fig. 1A). Seaward of the platform, the morphological gradient of the seafloor is increasing, reaching an average descent angle of 0.5° down to 35 m water depth.

4.2 Seafloor sediment distribution patterns and their interannual dynamics

Side scan sonar mosaics based on backscatter intensities and the sedimentary composition of grab sample material identified eight major types of seafloor (named A-H) (see. Figs. 2 and 3): A) silt to fine sand, B) coarse sand with coral fragments, C) coarse sand, coral fragments and boulders, D) medium and coarse sand, E) medium sand, F) bedrock outcrops, G) boulders (reef platform), and H) fine and medium sand.

Sediments composed of silt to fine sand (type A), are common north and south of the reef fringing Pakarang Cape. This sediment type extends down to 15 m water depth (Fig. 2). The landward limit of seafloor type A is above the 5 m water depth contour. It is recognized by patches of low backscatter intensity, displayed in light grey colors in the side scan sonar mosaics. The offshore boundaries of the patches of sediment type A are irregular, and in some places extend seaward filling in shallow channels. The grain size analyses revealed these sediments to be poorly to very poorly sorted. Samples close to the coastline are partly bimodal, with modes situated in the range of medium to coarse silt (4.6 to 5.4Φ, Fig. 4A), and partly in the fine sand fraction (3.7 to 4.0Φ). The first mode generally decreases with increasing water depth (Fig. 4A). Notable exceptions include a coarser sample collected from a channel (sample 26 in Fig. 4A) and a finer sample found in a sheltered environment next to a bedrock outcrop (sample 36 in Fig. 4A).

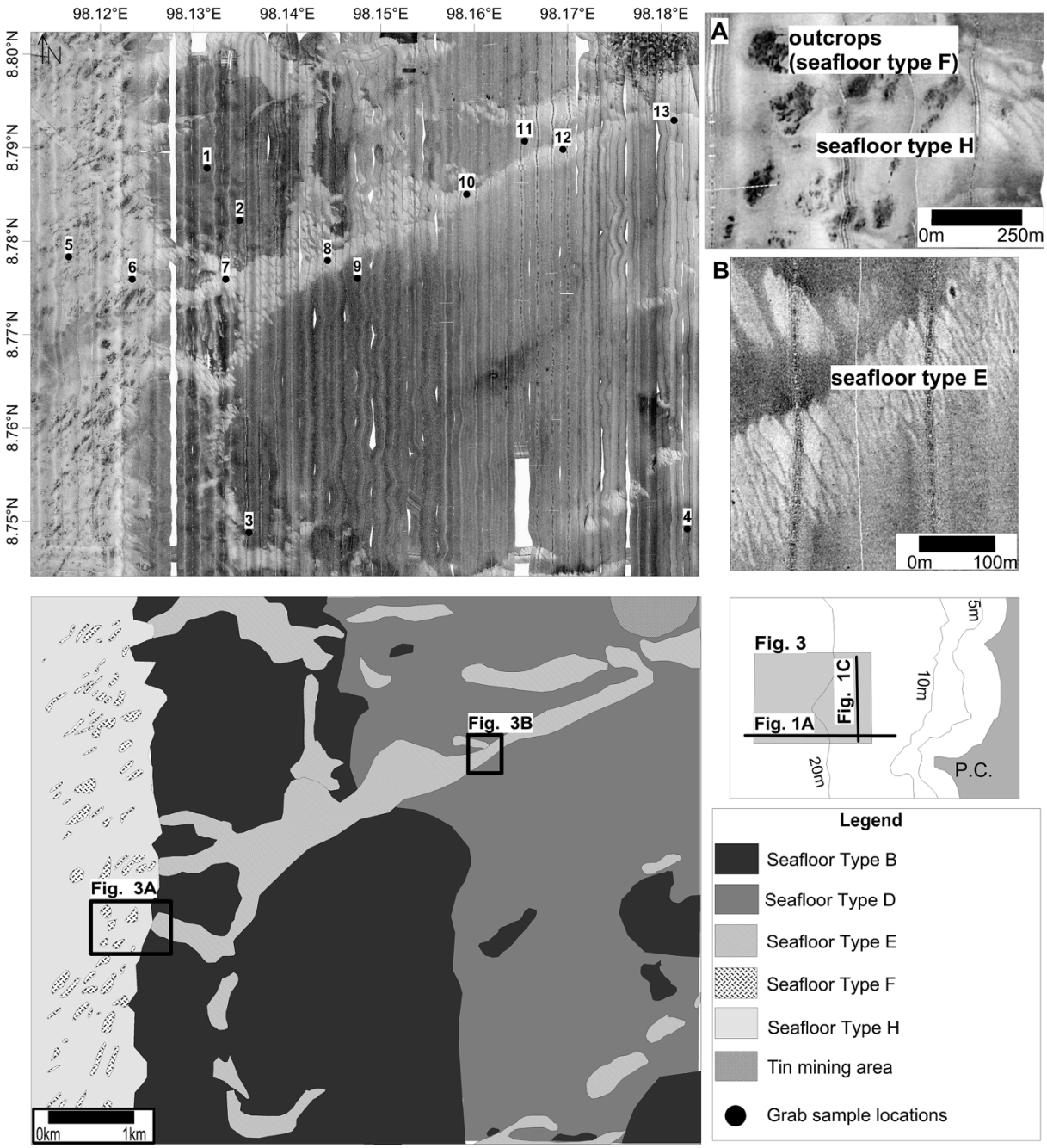

Fig. 3: Side scan sonar image (top) and seafloor type map (bottom) offshore Khao Lak, down to app. 35 m water depth. The seafloor type map is based primary on the classification of side scan sonar data and is verified by surface sediment samples analyses. The insets A and B show details on the seafloor types borders and peculiar features of the seafloor, which are discussed in detail in the text.

Patches of seafloor type A are separated by seafloor type B (coarse sand, including coral fragments) north of Pakarang Cape and seafloor type C (coarse sand with coral fragments as well as boulders) south of the Cape. Boulders are only observed in water depths less than 15 m. Seafloor types B and C are characterized by high backscatter values, displayed in dark grey colors. Boundaries separating seafloor types A and B, or A and C can be either sharp (Fig. 2B) or transitional (Fig. 2C). The modes of the poorly sorted sediments representing seafloor types B and C are within the coarse sand fraction (-0.9 to 0.4Φ).

The landward limit of seafloor type B and C is situated above the 5m depth contour. Offshore, a transitional boundary separates seafloor type B and C. A sharp boundary exists between seafloor type B sediments and seafloor type D in a depth of 16 to 18 m (Fig. 2A). However,

sediments classified as seafloor type B reappear further offshore and extend down to approximately 27 m (Fig. 3). No correlation between the first mode and water depth is recognized in samples retrieved from seafloor types B and C (Fig. 4B).

Seafloor type D is composed of medium to coarse sand, which covers the seafloor between 15 and 22 m water depth. Only a few coral fragments are found within these sediments; therefore, they are recognized by intermediate backscatter values. The sediments are moderately to poorly sorted due to mixing with some coral pieces of various sizes. Their first mode varies between 1.1 to 1.4Φ. Moderately well-sorted medium (first mode of 2.4Φ) sand is found in water depths from 15 to 25 m. These sediments are classified as seafloor type E (Figs. 2 and 3). They commonly occur on the northwestern flanks of the sand ridges (Fig. 3B). These type E - sediments are easily recognized due to their elongated form, sharp boundaries with adjacent seafloor types and low backscatter intensity (Fig. 3B). The mode of samples retrieved from seafloor type E is independent of the water depth.

Bedrock outcrops form parts of the seafloor. These areas are classified as seafloor type F, which occurs south of Pakarang Cape in water depths less than 10 m (Fig. 2), and further offshore in depths greater than 25 m (Fig. 3). The interface with other sediment types is very sharp (Fig. 3A). The appearance of the bedrock outcrops is variable in side scan sonar mosaics, depending on the inclination angle of the outcrop surfaces in relation to the position of the side scan sonar towfish.

The seaward boundary of the dead reef fringing Pakarang Cape is covered by a field of boulders (seafloor type G, Fig. 2D). This type extends down to 10 - 12 m water depth. It is marked by a transitional boundary with other sediment types.

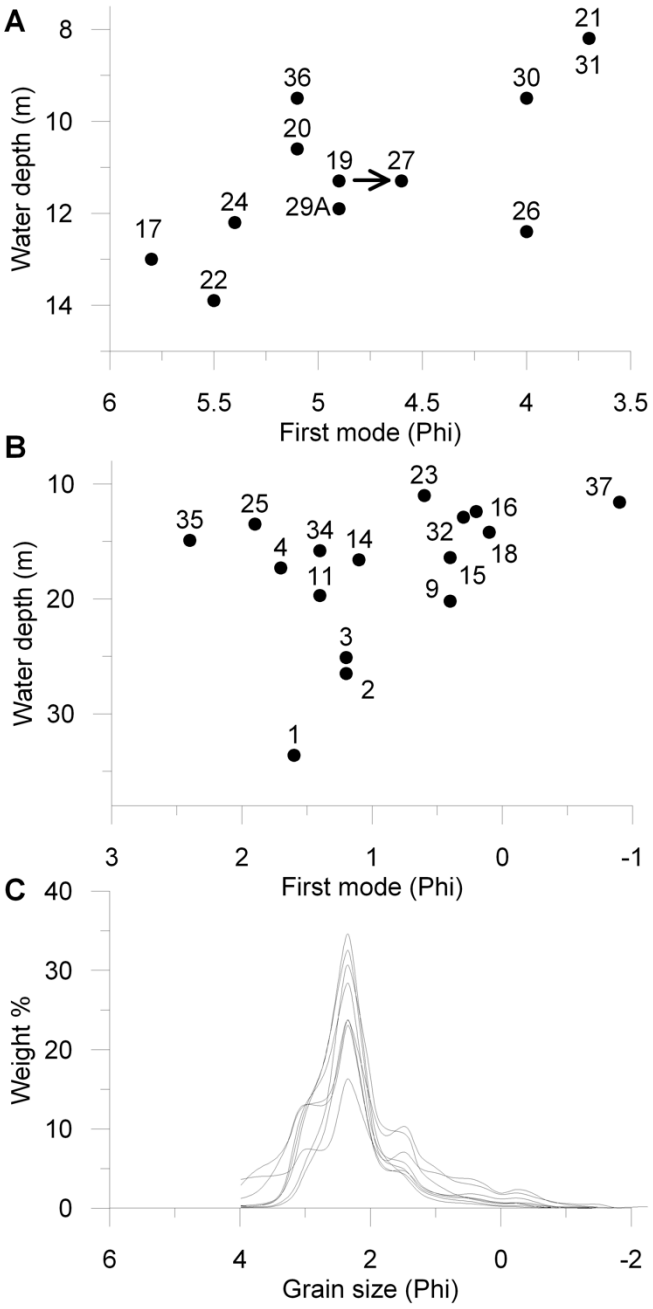

Fig. 4: Grain size data of surface sediment samples. For sampling positions see Figs. 2 and 3. A) Grain size mode versus water depth, based on samples retrieved from seafloor type A, showing a decreasing first mode with increasing water depth. Samples 19 and 27, and 21 and 31 were taken at the same positions in 2008 and 2010, respectively. B) Grain size mode versus water depth based on samples from seafloor types B, C and D show no correlation. C) The grain size distribution of samples 5, 6, 7, 10, 12, 33 obtained from seafloor type A and H. All samples have a first mode of 2.4 Φ.

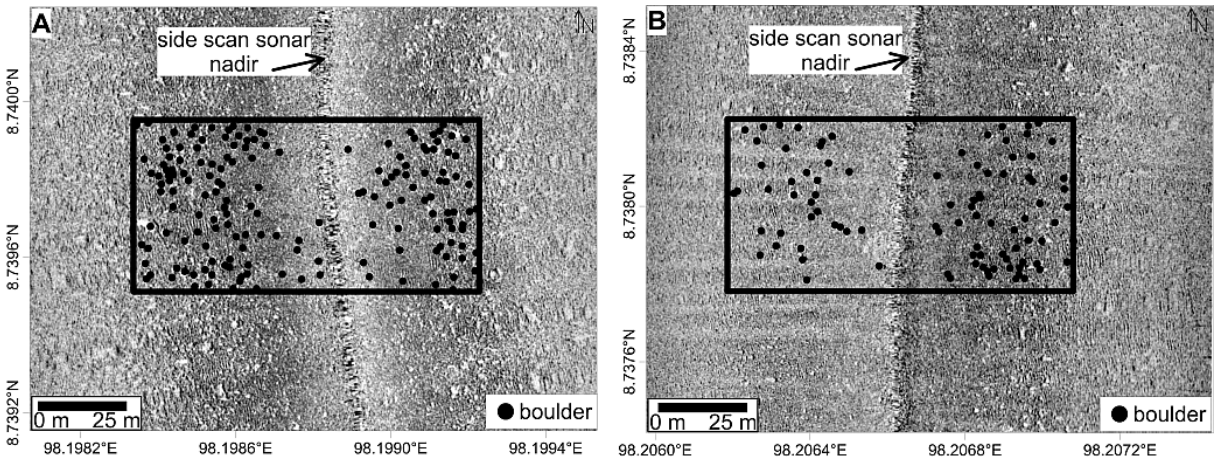

Fig. 5: The boulder density on the reef fringing Pakarang Cape (seafloor type G) is higher towards its offshore boundary (A, app. 11 m water depth), compared to the landward boundary (B, app. 9 m water depth). For positions, refer to Fig. 2.

The boulders are numerous and their diameter often exceeds 1 m and they are recognized as black dots with a bright acoustic shadow behind. The boulder density on the fringing reef is higher towards the offshore boundary of the reef platform (Fig. 5A) compared to the boulder density on its landward boundary (Fig. 5B).

Fine and medium sand below 25 m water-depth is classified as seafloor type H. This sediment has a composition very similar to the sediments of type E (poorly to moderately sorted). However, type H sediment does not show specific bedforms (Fig. 3A). Modes of sediment comprising seafloor type H do not correlate with water depth, which is similar to samples from seafloor type E, (Fig. 4C).

Repeated side scan sonar surveys of the selected areas reveal variation in the boundaries of seafloor type A. Between 2008 – 2010 they change on the order of several tens of meters, either increasing or decreasing the size of the area covered by type A sediments (Fig. 6A). The grain size composition of surface sediment changes not only at sedimentary boundaries, but also in the center of seafloor type A. Here sediment changes from a sandy to a silty composition (e.g. Fig. 6A), or vice versa (Fig. 6B). Repeated grab sampling from the same position show a slight coarsening of the first mode of the surface sediment in the center of a seafloor type A patch south of Pakarang Cape (samples 19 and 27, Fig. 4A), and no change in the first mode of two samples located close to Pakarang Cape (samples 21 and 31, Fig. 4A).

4.3 Structure of the subsurface sediments

Data concerning the subsurface sediments and the geological structure derive from three sources: reflection seismic (boomer system), grab samples and sediment cores. The seismic data provide information down to 8 m below the seafloor. Information about the development of the sub-bottom structure was mainly available from areas covered by seafloor type A sediments. Analysis of grab samples not only gave information about the sediments deposited directly at the seafloor, but also about sediments in 10 to 15 centimeters depth. In several cases, sediments different to those at the seafloor surfaces were found in these depths. Moreover, results of the analysis of a 55 cm long core, taken from the area of seafloor type A, are presented.

According to the seismic records, the silty sediments comprising seafloor type A form a thin cover, usually less than 1m thick (seismic unit 3, Figs. 7A and 7B). Within the channel system, or in areas where patches cover deeper incisions, the thickness of these deposits can reach several meters. In those cases, two sediment layers (seismic units 2 and 3), separated by an unconformity, are observed. Towards the seaward boundaries of the seafloor type A, the

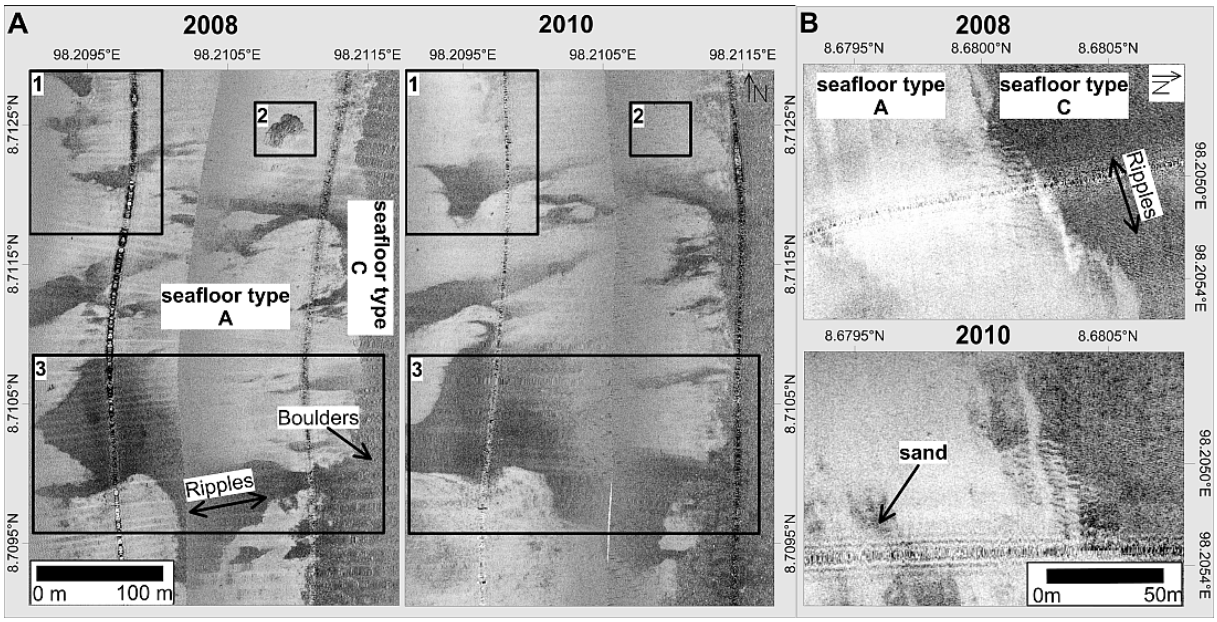

Fig. 6: Examples of repeated side scan sonar surveys. The results focus on the sediment dynamics along a boundary of seafloor type A sediment patches (for positions see Fig. 2. A) Close to the coastline (water depths down to 10 m) the boundaries between the different seafloor types change in the order of tens of meters and are increasing (1) or decreasing (3) the area covered with type A sediments. Changes are observed also within the sediment patch (2). B) Further offshore, observed changes are smaller. Change from silt to sand in the center of a type A sediment patch is marked with an arrow).

thickness of seismic unit 3 decreases below the resolution of the boomer system. Silty sediments still appear in the side scan sonar images, but they can no longer be distinguished in the seismic data as a distinct layer. The surface of the cover of silty deposits is generally on the same or a slightly lower morphological level as the surface of the surrounding sand (Fig. 7B), and distinctly lower situated close to hard-rock outcrops (Fig. 7A). Partly, the appearance of seismic unit 3 is homogenous, however, internal reflectors indicating layering can be observed as well. Seismic unit 2 is separated from units 1 and 3 by a distinct reflector. Moreover, internal reflectors terminating against this boundary are apparent. In some areas the sediments forming seafloor type B can be identified in the seismic record situated above the acoustic basement (seismic unit 4, Fig. 7C). The achieved penetration depth is generally poor, and the acoustic basement is situated close to the surface.

Sediments samples retrieved from seafloor type A occasionally contain, at depth, material different from the surface sediment. These sediments at the base of the grab sample include oval shaped patches of dark sand (first mode of 3.7 to 4.0Φ, samples 29 and 31). They are found close to the coastline and in the channel system at the seaward boundary of seafloor type A. The subsurface sediments from grab samples, retrieved close to the coastline, also contain irregular clasts composed of coarse sand with a first mode at 0.8Φ. Gravel-sized pieces of granite (sample 21) are included as well. The latter are also frequently embedded in grab samples retrieved seawards of bedrock outcrops (e.g. sample 36). At the seaward boundary of seafloor type A, lateritic fragments are found in the lower part of grab samples (sample 22). Seaward of the boundary of seafloor type A, plant material, embedded in mud and covered by sand, was found in grab samples retrieved from sediments of seafloor type D.

Sediment core 050310-C3 (11.2 m water depth, Fig. 8) provides insight into the composition of seismic unit 3 (covered by seafloor type A). It is composed of variable grain sizes ranging from silt, silty sand to sandy silt, sand and intercalations of gravels. The sediments in the core are composed of four major units which can be further divided into subunits. The uppermost

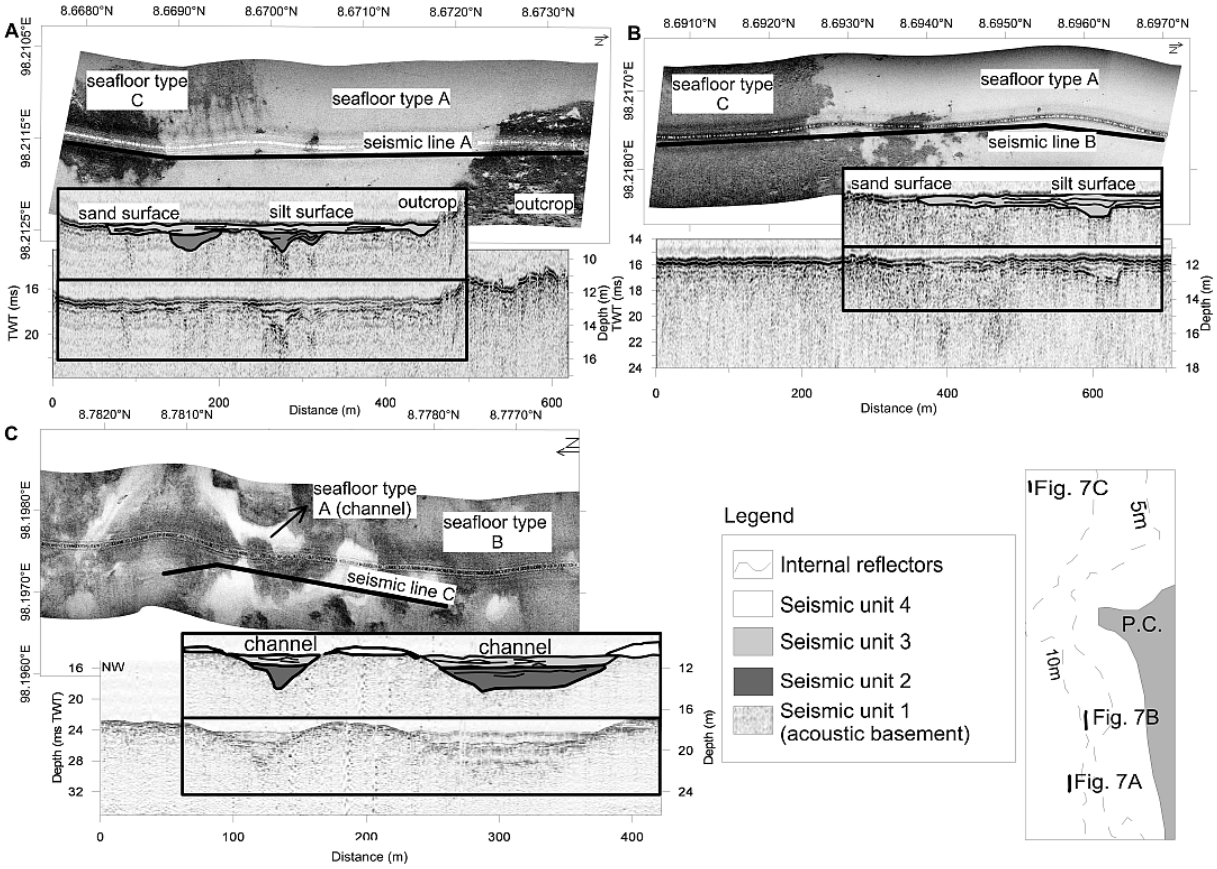

Fig. 7: Shallow water reflection seismic profiles and side scan sonar images in the area of seafloor type A, B and C (Fig. 2). Four seismic units are identified. The sediment of type A belongs to seismic unit 3, which forms a meter-thick cover. P.C.: Pakarang Cape

layer, unit 1 which is 5 cm in thickness, is mainly composed of upward fining silt (the first mode rises from 4.2 to 4.6Φ). Grain size analysis reveals that the sediments of the upper 1 cm show a second mode in the sand fraction (0.9Φ). Therefore, it is identified as a separate subunit (1A). Unit 1 does not reveal well-preserved laminations. This is likely due to bioturbation; traces of which can be recognized in the X-ray image.

Unit 1 conformably covers a 1 cm thick laminated, layer composed of coarse sand, although this layer contains more fine-grained material towards the surface. (mode 0.3Φ) This layer forms the uppermost part of unit 2 and is defined as subunit 2A. The lower boundary,separating units 2A and 2B, is sharp and likely erosional. From 5 to 18 cm, the sediment comprises poorly sorted deposits with bimodal grain size distributions ranging from silt to gravel (unit 2B). This subunit contains reworked shells and coral debris. The sorting is slightly improving towards the top of the unit. There is also an upward decrease in size and number of gravel-sized components, and an associated decrease in clay and silt content towards the top of the unit. The first and second modes in the analyzed samples range from 0.8 to 1.1Φ, and 4.0 to 5.1Φ, respectively. Unit 2 is separated from the underlying unit 3 by an erosional unconformity at 18 cm depth (Fig. 8). Small amounts of the older sediments are incorporated into the basal part of unit 2.

Compared to unit 2, sediments of unit 3 are characterized by a higher percentage of silt. The structure of unit 3 shows distinct horizontal, and cross, stratification. The first mode in the grain size distribution ranges from 0.8 to 1.4Φ. A second mode is observed only in the upper and lower parts of the unit (subunits 3A and 3C) and ranges between 5.1 and 6.0Φ. This unit may be divided into the two silty sand subunits 3A and 3C, separated by a sand layer (3B). Subunit 3A is about 9 cm thick and is composed of almost horizontally laminated sediments

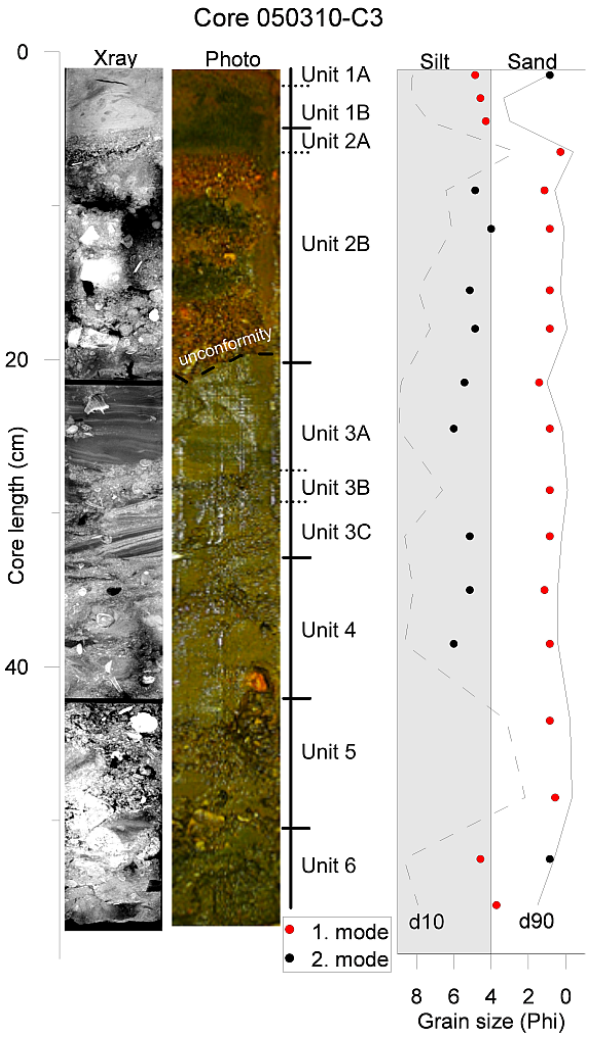

Fig. 8: Photo of sediment core 050310-C3. From left to right, x-ray image, photo, sedimentary units and grain size in form of 1st and 2nd mode, and the sedimentological parameters d10 and d90 are presented.

with several small-scale unconformities. At a depth of 24 cm a pocket containing sand and gravel interdispersed with some snail shells exists. The inclined sandy layer forming subunit 3B is situated at a depth of 26 to 28 cm. It is composed of coarse sand. The layer contains numerous shell fragments and patches of finer sediments. Its lower contact is partly erosional. The 4 cm-thick subunit 3C is composed of layered silt and sand inclined in the same direction as subunit 3B. In the upper part of this subunit, a cross lamination is preserved within an inclined silty sand layer. In general, the sediments in this subunit are coarser towards the surface. Laminae of the lower part of the unit downlap onto the upper surface of unit 4, situated at 33 cm depth. Unit 4 is composed of similar types of sediments as the above units – bimodal silty sand with the first modes ranging from 0.8 to 1.1Φ. However, the sedimentary structure of this unit is chaotic. It reveals remnants of horizontal laminations and patches of finer sediments with shells scattered throughout. Its lower boundary is sharp. Sediment between 42 and 52 cm depth is defined as unit 5 and consists of coarse sand with unimodal grain size distribution (mode between 0.8 and 1.0Φ). Shell fragments and coral debris are abundant. In some parts it reveals a faintly visible lamination, however, in general it has a massive structure with chaotic distribution of sediment patches containing finer material between sand grains. The lower boundary of this unit is uneven and erosional. The lowermost part of the core consists of poorly sorted sandy silt to silty sand (unit 6), with the first mode between 3.7 and 4.7Φ. No clear sedimentary structures can be recognized in this unit.

5. Discussion

5.1 Geological features of the inner continental shelf off Khao Lak

The obtained data indicate three seabed facies offshore of Khao Lak in water depths ranging from 5 to 35 m, which are differentiated by seafloor morphology and sediment composition. They are related to a) the fringing reef at Pakarang Cape and potential paleoreefs nearby, b) the dominating sandy inner shelf environment and c) shallow water patches of fine-grained sediments.

The fringing reef offshore Pakarang Cape is covered with boulders (sediment type G, Fig. 2). This reef terminates abruptly offshore (Fig. 2). Only a few coral boulders are observed seaward of the reef slope. In contrast high amounts of coral debris, including boulders, are located north and south of the reef (seafloor types B and C, Fig. 2). Cobbles from this area, which are covered by colonies of

organisms indicating a stable environment, were recently reported by Sanfilippo et al. (2010). Additionally, the acoustic base is situated just beneath the surface north and south of Pakarang Cape (Fig. 7), which suggests the presence of hard rock and/or very coarse material close to the seafloor. This can be seen below seismic unit 4, which is composed of coarse sand (Fig. 7C). It is likely that the areas directly north and south to Pakarang Cape are remnants of old reef platforms. The channel system at a depth of 15 m (Fig. 2) is incised into the surface of this old platform. The elevated morphological platform found in approximately 25 m water depth (Fig. 1A) is interpreted as a paleoreef as well. This interpretation is based on its morphological appearance, which is typical for a drowned reef platform (e.g. Finkl et al. 2005). The dominant seafloor type on the shelf is composed of sandy sediments, which form a smoothly inclined seafloor. Several km long sand ridges occur on the surface of the seafloor (Fig. 1C). These ridge structures are frequently observed in sandy inner continental shelf settings. They can be formed both by storm events and by regular hydrodynamic processes, for instance tidal currents or ocean currents (Holland and Elmoore 2008). Relict ridges, so-called moribund ridges, formed during lower sea levels stages also exist (Dyer and Huntley 1999). The sand ridges in the investigation area have no connection to the underlying sedimentological strata, and were eventually influenced by the 2004 Tsunami (Feldens et al. 2010). With the applied methods, no movement of the sand ridges was observed between 2008 and 2010. However, it is not possible to explicitly conclude that these ridges represent a relict form. The presence of fine sands (seafloor type E) on the leeward side of the ridges may suggest that these structures are actively being shaped.

A remarkable feature within the research area is the fine-grained (mainly silt) sediment cover observed close to the coastline (seafloor type A, Fig. 2). This material is deposited in depressions of the inferred paleoreef platform and in the channel system north and south of Pakarang Cape (Fig. 7). The mechanisms responsible for the deposition and preservation of such fine-grained material in the inner shelf environment are still poorly understood (e.g. Hill et al. 2007). However, it was found that once deposited (for example during large floods) mud deposits can be retained even in wave-dominated, highly-energetic, inner shelf environments (Scully et al. 2002, Crockett and Nittrouer 2004). Since large rivers are absent in the investigation area, the source of these sediments may be associated with recent anthropogenic activities (tin mining, deforestation, earth works), or local small river and creek flooding during the rainy season.

5.2 Mud deposits on the inner continental shelf

Accumulation of mud is observed on various continental shelves, normally due to the discharge of large rivers supplying significant amounts of fine grained sediments (e.g. Walsh and Nittrouer 2009). However, such a sediment source is missing in the study area. From other studies it is known that the mud supply to the shelf has increased in historical times due to direct or indirect anthropogenic impact (Wolanski and Spagnol 2000, Sommerfield and Wheatcroft 2007, Szczuciński et al. 2009). An increased supply of fine sediment during the last century may also be expected in the investigation area offshore Khao Lak, due to intensive tin mining activities, agriculture and tourism and related land-use change (e.g. deforestation).

The thickness of the fine-grained sediments offshore Pakarang Cape (sediment type A, Fig. 2, seismic unit 3, Fig. 7) decrease from a local maximum of 2 m to only a few cm, with distance from the shore, increasing water depth, and from fine sand to silt-sized particles. This suggests an onshore source of these sediments, and the deposition of coarse grained particles closer to the coastline. Available data indicate that most of these sediments were deposited during the last hundred years: The rates of sediment accumulation are very high, reaching more than 1 cm per year according to Pb210-dating of a sediment core taken from a mud

patch at 9.6 m water depth. (Sakuna et al., this volume). This is in agreement with an estimation of the sediment accumulation rate for the presented core 050310-C3 (11 m water depth, Fig. 8). Here, the uppermost 5 cm of mud (unit 1) lie above sediments interpreted as 2004 tsunami event deposits (see section 5.3 for the discussion). As the core was retrieved slightly more than 5 years after the tsunami occurred, the estimated accumulation rate is 0.95 cm/year.

The presented assessments of mud accumulation refer to normal conditions without strong event-influence. However, muddy sediments were also transported offshore during the tsunami, which is the most recent extraordinary event influencing the sediment distribution in this area. Observation by eyewitness, videos and satellite images show large amounts of fine-grained material transported offshore by the 2004 Indian Ocean tsunami (Umitsu et al. 2007; Fagherazzi and Du 2008, Mård Karlsson et al. 2009, Yan and Tang 2009). The suspended load extended more than 10 km offshore (IKONOS satellite images) and could be recognized for several days after the event. Therefore a large layer of mud, transported and deposited offshore due to the tsunami, would be expected. Several post-tsunami sediment sampling surveys have been performed in the present study area or nearby, but the expected widespread layer of tsunami fine grained deposits was never detected (Szczuciński et al. 2006, Di Geronimo et al. 2009, Feldens et al. 2009, Sugawara et al 2009, present study). Since all of these surveys were done at least one year after the tsunami, it is possible that these tsunami deposits were mostly redeposited and dispersed over a larger area by hydrodynamic activity due to the SE-monsoon. Di Geronimo et al. (2009) identified areas covered with mud deposits in some parts of the inner shelf off Khao Lak. They interpreted these layers as tsunami deposits due to their unusual location in shallow water. However, these muds are in the same area as seafloor type A fine-grained sediments, which, as discussed above, seem to be the result of normal sedimentation.

Repeated side scan sonar surveys in 2008 and 2010 allow for the assessment of the annual dynamics of seafloor type A sediments. The magnitude of change of the boundaries between seafloor type A and the surrounding seabottom is greater closer to the coastline (Fig. 6A), and can reach several tens of meters. The change of the extent of type A includes both increase and decrease in area. The decrease may be either due to erosion or cover by surrounding sediments. The available data do not allow for the determination of which situation takes place. However, change of the surface sediment type is also observed in the center of type A sediment patches (Figs. 6A and B). Therefore, it can be assumed that the sediments of type A are at least partially reworked during the annual cycle.

The evidence gathered on shallow water areas covered by fine-grained sediments (seafloor type A) imply that these regions might be affected by some kind of specific local circulation pattern, generating preferential conditions for good preservation of the fine-grained deposits in specific, slightly lowered areas. These areas may also be preferential for the preservation of event deposits; the 2004 offshore tsunami deposits were mostly found in these regions (present study – see chapter 5.3, Sakuna et al., this volume).

5.3 Identification of offshore tsunami impact

The results obtained on seafloor morphology and surface sediment distribution do not show widespread features, which could be directly related to the tsunami event. The only, probable results are that offshore tsunami deposits with the form of event deposits are restricted to specific areas. They are documented as unit 2 (Fig. 8) in sediment core 050310-C3. Large storm and typhoon events are generally rare in the investigation area (e.g. Phantuwongraj and Choowong 2011) with a return period in the range of decades. Their influence is generally minor (Kumar et al. 2008, Brand 2009). No severe storm event affected the area between the 2004 tsunami and the end of our sampling campaigns. Therefore, unit 2, being the most recent

event layer, is interpreted as an offshore tsunami deposit: Several characteristics reported as typical for such deposits (e.g. van den Bergh et al. 2003, Goodman-Tchernov et al. 2009, Sakuna et al. this volume) can be found in this unit. It is deposited above an erosional unconformity, contains abundant shell fragments, and is generally poorly sorted and unique in the sedimentary sequence. Material forming unit 2 derives partly from the nearby vicinity where similar sediments can be found both further onshore and offshore (seafloor type B, Fig. 2). The unit is composed of two subunits - 2A and 2B - separated by a sharp, erosional boundary. The subunits may reflect various phases of the tsunami event, but further differentiation into run-up and/or backwash is still not possible. Macroscopic terrigenous material, which would point towards backwash influence, is not found, and the observed sedimentological structures could be formed during both tsunami phases. However, a lack of terrigenous components cannot be used to exclude a tsunami origin of unit 2. Erosion on land was observed to be limited (e.g. Szczuciński et al. 2006, Umitsu et al. 2007, Fagherazzi and Du 2008), and minor in comparison with beach and nearshore zone erosion. Due to the channeled nature of the backwash (Le Roux and Vargas 2005), it cannot be expected to that land-derived material was distributed evenly throughout the inner shelf. It is also difficult to exclude explicitly the tsunami origin of unit 3, however, the laminations in its fine-grained part (units 3A and 3C) indicate recurring, more regular events (Palinkas et al. 2006) in the past. Therefore, we assume that unit 3 was likely deposited before the tsunami event.

The inferred tsunami deposits of unit 2 were covered by only 5 cm of muddy material since 2004. For this reason the tsunami deposits could also be traced by grab samples, as a penetration of up to 10 cm is possible. Indeed, several grab samples were marked by different sediments at their base than on the surface. The subsurface sediments contain pockets of fine sand, gravel, pieces of laterites and plant materials. Such deposits are found down to a depth of 18 m, approximately 8 km offshore. The composition of these subsurface sediments varies greatly between grab samples retrieved from different locations. It is assumed that their different compositions reflect both difference in sediments locally available for erosion and deposition, as well as varying spatial impact of the tsunami run-up and backwash at different positions. This is further supported by the varied internal appearance of seismic unit 3 (Fig. 7), which indicates a different composition of the first few decimeters of the seafloor beneath sediment type A. As laterites and plant material are of terrigenous origin, parts of the material were transported offshore during the backwash.

It is interesting to note that most inferred tsunami deposits are present below the seafloor of type A. The most likely explanation is that these sediment depocenters allow for a better preservation of tsunami deposits. It is also possible that the major tsunami influence during both run-up and backwash was focused spatially due to small-scale morphological variations both on- and offshore (Le Roux and Vargas 2005, Umitsu et al. 2007, MacInnes et al. 2009).

No influence of the 2004 Indian Ocean tsunami is found within sediments of seafloor types B and C. This supports the findings of Sanfilippo et al. (2010), who reported minor influence on corals living on cobbles in these areas. These areas seem to be mostly unaffected by the tsunami event. No direct traces of tsunami impact below 18 m water depth were found in hydroacoustic data or sediment samples. Seafloor type E (Fig. 2), deposited on northwestern flanks of the sand ridge system, indicates a SW-NE directed current. In incisions at the base of the sand ridges, event deposits composed of silty material covered by coarse sand were found (Feldens et al. 2010). However, it is uncertain whether these features can be attributed to the 2004 Indian Ocean tsunami.

Due to sediment dynamics in the investigation area, it is likely that existing tsunami deposits are subject to erosion and reworking processes. Tsunami deposits were not found directly at the surface, but are only covered with about 5 cm of sediment deposited after the tsunami

(unit 1, Fig. 8). Therefore, we assume that deposits of the 2004 Indian Ocean tsunami are preserved only in sheltered environments offshore Khao Lak, for instance in the channel system and in depressions seawards of granitic outcrops where post-tsunami deposition of mud or sand has taken place. This is supported by findings of Sakuna et al. (this volume).

The occurrence of tsunami deposits only in specific areas is in contrast to onshore tsunami deposits, which commonly form a continuous sand layer covering the inundation zone directly following flooding by the tsunami wave (Shiki et al. 2008). Although offshore tsunami deposits were speculated to be more common than onshore deposits (Dawson and Stewart 2007), their actual deposition and subsequent preservation depends strongly on the local geomorphological configuration of the shelf and nearshore area and onshore conditions. It is proposed that in coastal environments similar to our study area a higher amount of tsunamigenic material is deposited and preserved onshore than offshore.

Frequently reported and more easily preserved onshore and offshore tsunami deposits are boulders (e.g. Goto et al. 2007, Scheffers 2008, Goff et al. 2010). On the seafloor off Sumatra movement of boulders, which are several meters in diameter, in water depths down to 25 m has been described and modelled by Paris (2010). Goto et al. (2007) describe that the transport of hundreds of boulders towards the intertidal zone of Pakarang Cape is due to the 2004 Indian Ocean tsunami. They explained this transport through a numerical model showing that the majority of these boulders were transported onshore from a water depth of less than 10 m. In fact, the boulder density at the offshore boundary (10 – 12 m water depth) of the boulder-covered reef platform is higher than in the shallower part (indicated in Fig. 5). This supports the boulder transport model developed by Goto et al. (2010b), as the lower density in the shallower water depth might be due to removal of some of the boulders towards the shoreline during the runup phase.

6. Conclusion

The objectives of this study included the documentation of seafloor morphology, geological features as well as sediment distribution and its interannual changes in order to support the identification of the 2004 Indian Ocean tsunami impact to the seafloor offshore Khao Lak (Thailand). Wide areas of the seafloor are dominated by coarse sediments including sand and boulders, associated with fringing reefs. Moreover, in depressions and in a small channel system, which is incised in a palaeoreef platform, a layer of silt to fine sand is deposited down to 15 m water depth. These sediments were found to be mobile.

An impact of the tsunami could not be identified over wide areas of the study site in the seafloor morphology, the sediment distribution pattern, grain size composition or specific morphological features. Offshore tsunami deposits could be identified only in a limited area down to 18 m water depth. Typical features of these event deposits include layers composed of coarse sand and gravelly silty sand with a basal erosional contact. The event deposits are sandwiched by modern muddy sediments. Terrigenous compounds (laterites and plant remnants) indicate the influence of the tsunami backwash. The deposits with terrigenous constituents were already covered with few cm of sediments. They were found in local sediment depocenters likely created by the local water circulation pattern. Although onshore tsunami deposits and satellite images indicate that the seafloor was impacted by tsunami run-up and backwash, 5 years after the tsunami the lasting impact offshore Khao Lak was found to be minor.

Acknowledgements

This research was funded by DFG (grant SCHW 572/11) and NRCT. We are grateful to Phuket Marine Biological Center (PMBC) for providing ship time and other facilities, and to Somkiat Khokiattiwong and Karl Stattegger for helpful advice, two anonymous reviewers for very helpful comments which improved this manuscript and John Rappaglia for helpful comments regarding the language. We wish to thank masters and crews of RV Chakratong Tongyai, RV Boolert Pasook and MS Fahsai for their support during our research cruises.

6. Tsunami effects offshore Thailand: Conclusion and Outlook

The main objective of this study was to increase knowledge about offshore impacts of the 2004 Indian Ocean Tsunami; specifically to identify sediments deposited by the tsunami and to obtain information about their preservation potential.

In summary, it could be shown that the lasting influence of tsunami on seafloor morphology was generally minor in the study area, an open, wave-dominated coastline five years after the tsunami. Still, sediments deposited by the 2004 Indian Ocean Tsunami were recognized down to 18 m water depth. The source area of these tsunamigenic deposits comprises both reworked local material and onshore material transported seawards during the tsunami backwash. Below 18 m water depth, indications for minor tsunami influence on sediment bedforms, including erosion as well as deposition of material have been found. Several indications for offshore, downslope boulder movement during the tsunami backwash were observed, but could not be finally proofed. The deposits left by the 2004 Tsunami are commonly covered by only a few centimetres of modern sediment. As some sediment dynamics has been observed over the annual cycle, a large percentage of the tsunami deposits are expected to be reworked.

The surprisingly minor lasting influence of the tsunami on the seafloor, and the rapid return of coastlines to pre-tsunami conditions (Choowong et al. 2009, Goto et al. 2011) has several implications for further tsunami research. In the inner shelf area, evidence of tsunami events will only be preserved locally in sediment depocenters, with the potential exception of boulder fields deposited during a tsunami event (Goto et al. 2011). Tsunami influence in the mid-shelf area, however, could not be identified even a few years after the tsunami took place, based on results of this study and preliminary results by Szczuciński (2010). Therefore, it might be speculated that tsunami influence on mid-shelf areas is generally minor, with the exception of special bathymetric settings (Chavanich et al. 2009), which can cause erosion in deeper waters depths. The search for paleo-tsunamis should therefore focus on inner-shelf areas.

This restraint to shallow water depths poses several challenges for the identification of paleo-tsunami. Even if potentially small sediment depocenters preserving a sedimentary record of tsunami events can be identified and subsequently sampled, the major problem to discriminate between tsunami and storm deposits remains - all tsunami deposits identified in this study were situated in water depths also strongly affected during storms. Many of the criteria developed for onshore tsunami deposits are not applicable in the offshore environment (this study, Sakuna et al. 2011). The presented identification of tsunami deposits therefore strongly relied on information about the occurrence of events since 2004. Naturally, such information is not available in the search for paleo-tsunamis.

It might be concluded that the search for paleo-tsunamis in shallow marine environments comparable to the setting of the research area will be difficult with the available methods. Therefore, further studies should built upon the results presented here and use identified offshore 2004 Indian Ocean Tsunamis deposits to develop further sedimentological and geochemical proxies for their identification. Such work is already in progess (Sakuna et al. 2011). New geochemical proxies might also be useful to determine the still uncertain, but minor tsunami influence below 18 m water depth (Pongpiachan et al. submitted).

Next to the identification of tsunami effects, extensive silt deposits on the seafloor could be attributed to anthropogenic activities. Changing land use, e.g. deforestation and tin mining, during the last decades, supposedly triggered the deposition of these sediments. These results might be interesting regarding the environmental impact of a planned resume of tin mining operations offshore Khao Lak

Acknowledgment

I wish to thank Dr. Klaus Schwarzer for the initiation of this thesis, for insightful discussions throughout the last years and proof-reading of the articles. I am further grateful to Prof. Dr. Karl Stattegger for taking on the supervision, and to Prof. Dr. Sebastian Krastel for taking on the co-supervision.

Of course, this thesis would not have been possible without the help from many other persons and organizations. Some are already mentioned in the acknowledgments throughout this thesis.

Special thanks go to Daroonwan Sakuna. Without her last-minute efforts to charter some kind of research vessel, the 2010 cruise in Thailand - which delivered the essential results - would have been cancelled. The two previous cruises relied on her logistical skills as well. Furthermore, she helped with my core-work, and we had many inspiring discussions about tsunami impact.

Further, I wish to thank Witold Szczuciński for insightful discussions about everything tsunami-related, especially during the nights prior to the deadline of the Earth Planets Space article, and during the nights prior to talks I gave on conferences.

I thank Helmut Beese and Erik Steen for dealing with all kinds of technical problems. Daniel Unverricht gave me a crash course in using the Mastersizer 2000.

Many thanks go to Aradea Hakim and Agata Szczygielski for their indispensable help in dealing with the grain size analysis of literally hundreds of sediment samples and subsamples.

Without the support of masters and crews of FS Alkor , FS Poseidon and Boonlert Pasook, this work would have been impossible. Special thanks go to the crew of FK Littorina and master Helmut Christoph, now retired, for their outstanding support during the 27 cruises I took part in since 2006.

Not to forget, many thanks go to all members of the working group for support and discussions, and a very nice working atmosphere. In this regard, I had two great office mates with Sören Themann and Tobias Dolch.

Last, but not least, I have to apologize to Janne and many friends, for being rarely available during the last months.

References

ABRANTES, F., ALT-EPPING, U., LEBREIRO, S., VOELKER, A. AND R. SCHNEIDER (2008), Sedimentological record of tsunamis on shallow-shelf areas: The case of the 1969 AD and 1755 AD tsunamis on the Portugese Shelf off Lisbon, Marine Geology, 249, 283–293.

ANANDAN, C. AND P. SASIDHAR (2008), Assessment of the impact of the tsunami of December 26, 2004 on the near-shore bathymetry of the Kalpakkam coast, east coast of India. Science of Tsunami Hazards, 27, 26-35.

ANDRÉN, E., ANDRÉN, T. AND G. SOHLENIUS (2000), The Holocene history of the southwestern Baltic as reflected in a sediment core from the Bornholm Basin. Boreas 29, 233-250.

ASHLEY, G. M. (1990), Classification of large-scale subaqueous bedforms: a new look at an old problem. J. Sediment. Petrol. 60, 160-172.

BARTHOLDY, J., BARTHOLOMAE, A. AND B.W. FLEMMING (2002), Grain-size control of large compound flow-transverse bedforms in a tidal inlet of the Danish Wadden Sea. Marine Geology 188, 391-413.

BEHRE, K.E. (2003), Eine neue Meeresspiegelkurve für die südliche Nordsee. Probleme der Küstenforschung im südlichen Nordseegebiet 28, 9-63.

BELL, R., COWAN, H., DALZIELL, E., EVANS, N., O'LEARY, M., RUSH, B., AND L. YULE (2005), Survey of impacts on the Andaman Coast, Southern Thailand following the great Sumatra-Andaman earthquake and tsunami of December 26, 2004. Bull. NZ Soc. Earthquake Eng., 38(3), 123-148.

BENNIKE, O. AND J.B. JENSEN (1998), Late- and postglacial shore-level changes in the south-western Baltic Sea. Bulletin of the Geological Society of Denmark 45, 27-38.

BENNIKE, O., JENSEN, J.B., LEMKE, W., KUIJPERS, A. AND S. LOMHOLT (2004), Late- and postglacial history of the Great Belt, Denmark. Boreas, 33, 18-33.

BERGLUND, B.E., SANDGREN, P., BARNEKOW, L., HANNON, G., JIANG, H., SKOG, G. AND S.-Y. YU (2005), Early Holocene history of the Baltic Sea, as reflected in coastal sediments in Blekinge, southeastern Sweden. Quaternary International, 130, 111-139.

BJÖRCK, S. (1995), A review of the history of the Baltic Sea, 13.0-8.0 ka BP. Quaternary International, 27, 19-40.

BJÖRCK, S., ANDRÉN, T. AND J.B. JENSEN (2008), An attempt to resolve the partly conflicting data and ideas on the Ancylus-Littorina transition. Polish Geological Institute Special Papers, 23, 21-26.

BJØRLYKKE, K. (2010), Petroleum Geosciences. From Sedimentary Environments to Rock Physics. Springer. 508 p.

BLONDEL, P. (2009), The Handbook of Sidescan Sonar. Springer. 316 p.

BLOTT, S.J., AND K. PYE (2001), Gradistat: A grain size distribution and statistics package for the analysis of unconsolidated sediments, Earth Surface Processes and Landforms, 26, 1237-1248.

BOBERTZ, B. AND J. HARFF (2004), Sediment facies and hydrodynamic setting: a study in the south-western Baltic Sea. Ocean Dynamics 54, 39-48.

BOURGEOIS, J. (2009), Geologic effects and records of tsunamis, in: The Sea, Volume 15: Tsunamis, Edited by Robinson, A.R., Bernard, E.N., Harvard University Press.

BRAND, S. (2009), Typhoon havens handbook, http://www.nrlmry.navy.mil/~cannon/thh-nc/0start.htm.

BUNGENSTOCK, F. AND H.J.T. WEERTS (201), The high-resolution Holocene sea-level curve for Northwest Germany: global signals, local effects or data-artefacts? Int. J. Earth Sci. (Geol. Rundschau) 99, 1687-1706.

BRYANT, E. (2009), Tsunami: The Underrated Hazard (Second Edition): Springer & Praxis Publishing.

BUX, H. (1982), Geologisch-Sedimentologische Kartierung im Küstengebiet vor der Nordküste Fehmarns. Unveröff. Diplomarbeit. Mathematisch-Naturwissenschaftliche Fakultät der Christian-Albrechts-Universität zu Kiel.

CHAGUÉ-GOFF, C. (2010), Chemical signatures of paleotsunamis: A forgotten proxy?, Marine Geology, 271, 67–71.

CHAVANICH S., SIRIPONG A., SOJISUPORN P. AND P. MENASVETA (2005), Impact of Tsunami on the seafloor and corals in Thailand, Coral Reefs, 24, 535.

CHOOWONG M., MURAKOSHI N., HISADA K., CHARUSIRI P., DAORERK V., CHAROENTITIRAT T., CHUTAKOSITKANON V., JANKAEW K. AND P. KANJANAPAYONT (2007), Erosion and deposition by the 2004 Indian Ocean tsunami in Phuket and Phang-Nga Provinces, Thailand. J. Coast. Res. 23, 1270.

CHOOWONG, M., PHANTUWONGRAJ, S., CHAROENTITIRAT, T., CHUTAKOSITKANON, V., YUMUANG, S. AND P. CHARUSIRI (2009), Beach recovery after 2004 Indian ocean tsunami from Phang-nga, Thailand, Geomorphology, 104, 134–142.

CROCKETT, J.S. AND C.A. NITTROUER (2004), The sandy inner shelf as a repository for muddy sediment: an example from Northern California, Continental Shelf Research, 24, 55-73.

CURRIE, L.A. (2004), The Remarkable Metrological History of Radiocarbon Dating [II] J. Res. Natl. Inst. Stand. Technol. 109, 185-217.

DAHANAYAKE K. AND N. KULASENA (2008), Recognition of diagnostic criteria for recent- and paleo-tsunami sediments from Sri Lanka. Mar. Geol. 254, 180.

DAIL, M.B., CORBETT, D.R. AND J.P. WALSH (2007), Assessing the importance of tropical cyclones on continental margin sedimentation in the Mississippi delta region, Continental Shelf Research, 27, 1857-1874.

DAWSON A. G. (1994), Geomorphological effects of tsunami runup and backwash. Geomorphology 10, 83-94.

DAWSON S. (2007), Diatom biostratigraphy of tsunami deposits: Examples from the 1998 Papua New Guinea tsunami, Sedimentary Geology, 200, 328-335.

DAWSON, A.G. AND I. STEWART (2007), Tsunami deposits in the geological record, Sedimentary Geology, 200, 166–183.

DAWSON, A.G. AND S. SHI (2000), Tsunami deposits, Pure and Appl. Geophys., 157, 875–897.

DI GERONIMO I., ROBBA E., CHARUSIRI P., CHOOWONG M., AGOSTINO I., MARTINO C., DI GERONIMO R. AND S. PHANTUWONGRAJ (2008), Marine modern sediments and rocky bottoms of Khao Lak coastal area, Changwat Phang Nga, Andaman Sea, SW Thailand. Color Map, 1:30.000, Catania, Bangkok.

DI GERONIMO, I., CHOOWONG, M. AND S. PHANTUWONGRAJ (2009), Geomorphology and Superficial Bottom Sediments of Khao Lak Coastal Area (SW Thailand), Polish J. of Environ. Stud., 18(1), 111-121.

DIETRICH, R. AND G. LIEBSCH (2000), Zur Variabilität des Meeresspiegels an der Küste von Mecklenburg-Vorpommern. Zeitschrift für Geologische Wissenschaften, 28, 615-624.

DUPHORN, K., KLIEWE, H., NIEDERMEYER, R-O., JANKE, W. AND F. WERNER (1995), Die deutsche Ostseeküste: Sammlung geologischer Führer Bd. 88. 281 p.

DYER, K.R. AND D.A. HUNTLEY (1999), The origin, classification and modelling of sand banks and ridges, Continental Shelf Research, 19, 1285-1330.

EINSELE, G., CHOUGH, S.K. AND T. SHIKI (1996), Depositional events and their records – an introduction. Sedimentary Geology, 104, 1-9.

ERNSTSEN, V. B., NOORMETS, R., HEBBELN, D., BARTHOLOMÄ, A. AND B. W. FLEMMING (2006), Precision of high-resolution multibeam echo sounding coupled with high-accuracy positioning in a shallow water coastal environment. Geo-Mar Lett., 26, 141-149.

ERNSTSEN, V.B., R. NOORMETS, C. WINTER, D. HEBBELN, A. BARTHOLOMÄ, B.W. FLEMMING AND J. BARTHOLDY (2006), Quantification of dune dynamics during a tidle cycle in an inlet channel of the Danish Wadden Sea. In: Geo-Mar Lett., 26(3), 151–163.

FAGHERAZZI, S. AND X. DU (2008), Tsunamigenc incisions produced by the December 2004 earthquake along the coast of Thailand, Indonesia and Sri Lanka, Geomorphology, 99(1-4), 120-129.

FELDENS, P. (2008), Genese und Sedimentdynamik eines Riesenrippelfeldes im Fehmarn Belt. Unveröffentlichte Diplomarbeit. Mathematische-Naturwissenschaftliche Fakultät, Universität Kiel.

FELDENS, P., SCHWARZER, K., HÜBSCHER, C. AND M. DIESING (2009), Genesis and sediment dynamics of a subaqueous dune field in Fehmarn Belt (south-western Baltic Sea). Marburger Geographische Schriften, 145, 80-97.

FELDENS, P., SCHWARZER, K., SZCZUCIŃSKI, STATTEGGER, K., SAKUNA, D., AND P. SOMGPONGCHAIYAKUL (2009), Impact of 2004 Tsunami on Seafloor Morphology and Offshore Sediments, Pakarang Cape, Thailand, Polish J. of Environ. Stud., 18(1), 63-68.

FELDENS, P., SAKUNA, D., SCHWARZER, K. AND P. SOMGPONGCHAIYAKUL (2010), Shallow water sediment structures in a tsunami-affected area (Pakarang Cape, Thailand), Coastline Reports, 16, 15-25.

FELDENS, P. SCHWARZER, K., SAKUNA, D., SZCZUCIŃSKI, W. AND P. SOMPONGCHAIYAKUL, Sediment distribution on the inner continental shelf off Khao Lak (Thailand) after the 2004 Indian Ocean Tsunami, Earth Planets Space, submitted.

FINKL, C.W., BENEDET, L. AND J.L. ANDREWS (2005), Submarine Geomorphology of the Continental Shelf off Southeast Florida Based on Interpretation of Airborne Laser Bathymetry, Journal of Coastal Research, 21(6), 1178-1190.

FISH, J.P. AND CARR, H.A (2001), Sound Reflections – Advanced Applications of Side Scan Sonar. Lower Cape Publishing. 272 p.

FLEMMING, B.W. (1978), Underwater sand dunes along the southeast African continental margin – observations and implications. Mar. Geol., 26, 177–198.

FLEMMING, B.W. (1988), Zur Klassifikation subaquatischer, strömungstransversaler Transportkörper. Boch. Geol. Geotech. Arb., 29, 44-47

FUJINO, S., MASUDA, F., TAGOMORI, S. AND D. MATSUMOTO (2006), Structure and depositional processes of a gravelly tsunami deposit in a shallow marine setting: Lower Cretaceous Miyako Group, Japan, Sedimentary Geology, 187, 127-138.

FUJIWARA, O. AND T. KAMATAKI (2007), Identification of tsunami deposits considering the tsunami waveform: An example of subaqueous tsunami deposits in Holocene shallow bay on southern Boso Peninsula, Central Japan. Sedimentary Geology, 200, 295-313.

GERONIMO, I.D., M. CHOOWONG AND S. PHANTUWONGRAJ (2009), Geomorphology and superficial bottom sediments of Khao Lak coastal area (SW Thailand). Polish J. of Environ. Stud. 18(1), 111–121.

GOFF, J., WEISS, R. AND D. DOMINEY-HOWES (2010), Testing the hypothesis for tsunami boulder deposition from suspension, Marine Geology, 277(1-4), 73-77.

GOFF, J.A., D.J.P. SWIFT, C.S. DUNCAN, L.A. MAYER AND J. HUGHES-CLARKE (1999). High-resolution swath sonar investigation of sand ridge, dune and ribbon morphology in the offshore environment of the New Jersey margin. Marine Geology, 161, 307–337.

GOFF, J.C., CHAGUE-GOFF, C. AND S. NICHOL (2001), Paleotsunami deposits; a New Zealand Perspective, Sedimentary Geology, 143, 1– 6.

GOODMAN-TCHERNOV, B.N., DEY, H.W., REINHARD, E.G., MCCOY, F. AND Y. MART (2009), Tsunami waves generated by the Santorini eruption reached Eastern Mediterranean shores, Geology, 37, 943-946.

GOTO, K., CHAVANICH, S.A., IMAMURA, F., KUNTHASAP, P., MATSUI, T., MINOURA, K., SUGAWARA, D. AND H. YANAGISAWA (2007), Distribution, origin and transport process of boulders deposited by the 2004 Indian Ocean tsunami at Pakarang Cape, Thailand, Sedimentary Geology, 202, 821-837.

GOTO K., IMAMURA F., KEERTHI N., KUNTHASAP P., MATSUI T., MINOURA K., RUANGRASSAMEE A., SUGAWARA D. AND S. SUPHARATID (2008), Distribution and significance of the 2004 Indian Ocean tsunami deposits: initial results from Thailand and Sri Lanka. In: Tsunamiites – Features and Implications. Shiki et al. (eds.) Elsevier, pp. 105-122.

GOTO, K., KAWANA, T. AND F. IMAMURA (2010a), Historical and geological evidence of boulders deposited by tsunamis, southern Ryukyu Islands, Japan, Earth-Science Reviews, 102(1-2), 77-99.

GOTO, K., OKADA, K., AND F. IMAMURA (2010b), Numerical analysis of boulder transport by the 2004 Indian Ocean tsunami at Pakarang Cape, Thailand, Marine Geology, 268(1-4), 97-105.

GOTO, K., TAKAHASHI, J., OIE, T. AND F. IMAMURA (2011), Remarkable bathymetric change in the nearshore zone by the 2004 Indian Ocean tsunami: Kirinda Harbor, Sri Lanka, Geomorphology, 127, 107-116.

GRZELAK, K., KOTWICKI, L. AND W. SZCZUCIŃSKI (2009), Monitoring of Sandy Beach Meiofaunal Assemblages and Sediments after the 2004 Tsunami in Thailand, Polish J. of Environ. Stud., 18(1), 43-51.

HAWKES, A.D., M. BIRD, S. COWIE, C. GRUNDY-WARR, B.P. HORTON, A.T. SHAU HWAI, L. LAW, C. MACGREGOR, J. NOTT, J.E. ONG, J. RIGG, R. ROBINSON, M. TAN-MULLINS, T.T. SA, Z. YASIN AND L.W. AIK (2007), Sediments deposited by the 2004 Indian Ocean tsunami along the Malaysia-Thailand peninsula, Marine Geology, 242, 169-190.

HILL, P.S., FOX, J.M., CROCKETT, J.S., CURRAN, K.J., FRIEDRICHS, C.T., GEYER, W.R., MILLIGAN, T.G., OGSTON, A.S., PUIG, P., SCULLY, M.E., TRAYKOVSKI, P.A. AND R.A. WHEATCROFT (2007), Sediment delivery to the seabed on continental margins, in Continental Margin Sedimentation: From Sediment Transport to Sequence Stratigraphy, Edited by Nittrouer, C.A., Austin, J.A., Field, M.E., Kravitz, J.H., Syvitski, J.P.M. and P.L. Wiberg, Blackwell Publishing.

HOLLAND, K.T. AND P.A. ELMORE (2008), A review of heterogeneous sediments in coastal environments, Earth-Science Reviews, 89, 116-134.

HORI K., KUZUMOTO R., HIROUCHI D., UMITSU M., JANJIRAWUTTIKUL N. AND B. PATANAKANOG(2007), Horizontal and vertical variation of 2004 Indian tsunami deposits: An example of two transects along the western coast of Thailand. Mar. Geol. 239, 163.

IMAMURA, F., K. GOTO AND S. OHKUBO (2008), A numerical model for the transport of a boulder by tsunami. Journal of Geophysical Research 113, C01008, doi:10.1029/2007JC004170.

JACKSON, P.D., K.B. BRIGGS AND R.C. FLINT (1996), Evaluation of sediment heterogeneity using microresistivity imaging and X-radiography. Geo-Marine Latters 16, 219–225.

JANKAEW, K., ATWATER, B.F., SAWAI, Y., CHOOWONG, M., CHROENTITIRAT, T., MARTIN, M.E. AND A. PRENDERGAST (2008), Medieval forewarning of the 2004 Indian Ocean tsunami in Thailand, Nature, 455, 1228-1231.

JENSEN, J.B. (1995), A Baltic Ice Lake transgression in the southwestern Baltic: Evidence from Fakse Bugt, Denmark. Quaternary International, 27, 59-68.

JENSEN, J.B. AND W. LEMKE (1996), Geologische Karte von Dänemark 1:200000. Blatt Fehmarn Belt – Arkonabecken. Geological Survey of Denmark and Greenland.

JENSEN, J.B., BENNIKE, O., WITKOWSKI, A., LEMKE, W. AND A. KUIJPERS (1997). The Baltic Ice Lake in the southwestern Baltic: sequence-, chrono- and biostratigraphy. Boreas, 26, 217-236.

JENSEN, J.B., BENNIKE, O., WITKOWSKI, A., LEMKE, W. AND A. KUIJPERS, (1999), Early Holocene history of the southwestern Baltic Sea: the Ancylus Lake stage. Boreas, 28, 437-453.

JENSEN, J.B., BENNIKE, O., LEMKE, W. AND A. KUIJPERS (2005), The Storebælt gateway to the Baltic. Geological Survey of Denmark and Greenland Bulletin, 7, 45-48.

JONES, E.J.W. (1999), Marine Geophysics. Wiley. 466p.

JØRGENSEN, F. AND P.B.E. SANDERSEN (2009), Buried valley mapping in Denmark: evaluationg mapping method constraints and the importance of data density. Z. dt. Ges. Geowiss., 160/3, 211-223.

KAUFHOLD, P. (1988) Zur Dynamik des Riesenrippelfeldes im Fehmarn Belt (Westliche Ostsee). Unveröff. Diplomarbeit. Mathematisch-Naturwissenschaftliche Fakultät der Christian-Albrechts-Universität zu Kiel.

KAUFHOLD, H. (1995), Verteilung und Zusammensetzung der quartären Oberflächensedimente im westlichen Fehmarnbelt (Ostsee). Meyniana, 47, 45-67.

KEARY, P, BROOKS, M. AND I. HILL. (2002), An introduction to Geophysical Exploration. Blackwell Science. 263p.

KELLETAT, D., S.R. SCHEFFERS AND A. SCHEFFERS (2007), Field signatures of the SE-Asian Mega-Tsunami along the West Coast of Thailand compared to Holocene Paleo-Tsunami from the Atlantic Region. Pure appl. Geophys., 164, 413–431.

KENDALL, M.A., ARYUTHAKA, C., CHIMONIDES, J., DAUNGNAMON, D., HILLS, J., JITTANOON, C., KOMWACHIRAPITAK, P., KONGKAEW, V., MITTERMEYR, A., MONTHUM, Y., NIMSANTIJAROEN, S., PATERSON, G.L.J., FOSTER-SMITH, R., FOSTER-SMITH, J. AND N. THONGSIN (2009), Post-tsunami recovery of shallow water biota and habitats on Thailand's Andaman Coast. Polish J. of Environ. Stud., 18(1), 69-75.

KESSEL, H. AND A. RAUKAS (1979), Estonia. In: Gudelis,V., Königsson, L.-K. (Eds.): The Quaternary History of the Baltic. Acta Universitatis Upsaliensis, Symposia Universitatis Upsaliensis Annum Quingentesimum Celebrantis I, Uppsala, pp. 127–146.

KLIEWE, H. AND W. JANKE (1982), Der holozäne Wasserspiegelanstieg der Ostsee im nordöstlichen Küstengebiet der DDR. Petermanns Geographische Mitteilungen 126, 65-74.

KHOKIATTIWONG, S., LIMPSAICHOL, P., PETPIROON, S., SOJISUPORN, P., AND B. KJERFVE (1991), Oceanographic variations in Phangnga Bay, Thailand under monsoonal effects, Phuket Marine Biological Center Research Bulletin, 55, 43-76.

KOKOCIŃSKI, M., W. SZCZUCIŃSKI, A. ZGRUNDO AND A. IBRAGIMOW (2009), Diatom assemblages in 26 December 2004 tsunami deposits from coastal zone of Thailand as sediment provenance indicators. Polish J. of Environ. Stud., 18(1), 93-101.

KOLP, O. (1965), Paläogeographische Ergebnisse der Kartierung des Meeresgrundes der westlichen Ostsee zwischen Fehmarn und Arkona. Beitr. Meereskunde, 12-14, 1-59.

KOLP, O. (1979), Eustatische und isostatische Veränderungen des südlichen Ostseeraumes. Petermann Geographische Mitteilungen, 123, 177-187.

KOLP, O. (1986). Entwicklungsphasen des Ancylus-Sees. Petermann Geographische Mitteilungen, 2, 79-93.

KRUMBEIN, W.C. (1938), Size frequency distribution of sediments and the normal phi-curve, J. Sed. Petr. 8,3, 84 – 90.

KUIJPERS, A. (1980), Current-induced Bedforms in the Danish Straits between Kattegat and Baltic Sea. Meyniana, 37, 97-127

KUMAR, V.S., BABU, V.R., BABU, M.T., DHINAKARAN, G. AND G.V. RAJAMANICKAM (2008), Assessment of Storm Surge Disaster Potential for the Andaman Islands, Journal of Coastal Research, 24, 171-177.

LAMPE, R. (2005), Lateglacial and Holocene water-level variations along the NE German Baltic Sea coast: review and new results. Quaternary International, 133-134, 121-136.

LARSON, G. AND R. SCHAETZL (2001), Origin and Evolution of the Great Lakes. J. Great Lakes Res., 27(4), 518-546.

LAY, T., H. KANAMORI, J.C. AMMON AND M. NETTLES (2005), The great Sumatra-Andaman earthquake of 26 December 2004. Science 306, 1127–1133.

LE ROUX, J.P. AND G. VARGAS (2005), Hydraulic behavior of tsunami backflows: insights from their modern and ancient deposits, Environ. Geol., 49, 65–75.

LEMKE, W. (1998), Sedimentation und paläogeographische Entwicklung im westlichen Ostseeraum (Mecklenburger Bucht bis Arkonabecken) vom Ende der Weichselvereisung bis zur Litorinatransgression. Marine Science Reports 31.

LEMKE, W., KUIJPERS, A., HOFFMANN, G., MILKERT, D. AND R. ATZLER (1994), The Darss Sill, hydrographic threshold in the southwestern Baltic: Late Quaternary geology and recent sediment dynamics. Continental Shelf Research, 14(7-8), 847-870.

LEMKE, W., AND A. KUIJPERS (1995), Late Pleistocene and early Holocene paleogeography of the Darss Sill area, southwestern Baltic. Quaternary International, 27, 73-81.

LEMKE, W., JENSEN, J.B., BENNIKE, O., ENDLER, R., WITKOWSKI, A. AND A. KUIJPERS (2001), Hydrographic thresholds in the western Baltic Sea: Late Quaternary geology and the Dana River concept. Marine Geology, 176, 191-201.

LEMKE, W., JENSEN, J.B., BENNIKE, O., ENDLER, R., WITKOWSKI, A. AND A. KUIJPERS (2002), Spät- und postglaziale Flüsse und Seen in der heutigen westlichen Ostsee. Greifswalder Geographische Arbeiten 26, 73-77.

LURTON, X. (2002), An introduction to underwater acoustics: principles and applications. Praxis Publishing. 347 p.

LUTZ, R., KALKA, S., GAEDICKE, C., REINHARDT, L. AND J. WINSEMANN (2009), Pleistocene tunnel valleys in the German North Sea: spatial distribution and morphology. Z. dt. Ges. Geowiss. 160(3), 225-335.

MACINNES, B.T., BOURGEOIS, J., PINEGINA, T.K. AND A. KRAVCHUNOVSKAYA (2009), Tsunami geomorphology: Erosion and deposition from the 15 November 2006 Kuril Island tsunami, Geology, 37(11), 995-998.

MÅRD KARLSSON, J., SKELTON, A., SANDÉN, M., IOUALALEN, M., KAEWBANJAK, N., POPHET, N., ASAVANANT, J. AND A. VON MATERN (2009), Reconstructions of the coastal impact of the 2004 Indian Ocean tsunami in the Khao Lak area, Thailand, Journal of Geophysical Research, 114, C10023, 1-14.

MCCAVE, I.N. AND J.P.M. SYVITSKI (1991), Principles and methods of geological particle size analysis. In: J.P.M. Syvitski (ed.) Principles, methods and Applications of Particle Size Analysis. Cambridge University Press. 369p.

MCLEAN, S. R. (1981), The role of non-uniform roughness in the formation of sand ribbons. Marine Geology, 42, 49-74

MENZIES, J. (2003), Tills and tillites. In: Middleton, G.V., et al., (Eds.), Encylopedia of Sediments and Sedimentary Rocks. Kluwer Academic Publishers, Dordrecht, The Netherlands, pp. 744–746.

MILKERT, D. AND H. M. FIEDLER (2002), Processing and mosaicking digital side scan sonar images: two examples from the western Baltic Sea. Baltica, 15, 40-48.

MÖRNER, N.-A. (1976), Eustatic changes during the last 8000 years in view of radiocarbon calibration and new information from the Kattegat region and other northwestern European coastal areas. Palaeogeography, Palaeoecology, Palaeoclimatology, 19, 63-85.

MORALES, J.A., BORREGO, J., SAN MIGUEL, E.G., LÓPEZ-GONZÁLEZ AND B. CARRO (2008), Sedimentary record of recent tsunamis in the Huelva Estuary (southwestern Spain), Quaternary Science Reviews, 27, 734-746.

MOSCON, D.M.C. AND A.C. BASTOS (2010), Occurence of storm-generated bedforms along the inner continental shelf - southeastern Brazil, Brazilian Journal of Oceanography, 58, 45-56.

MUSSETT, A.E. AND M.A. KHAN (2000), Looking into the Earth: An Introduction to Geological Geophysics. Cambridge University Press. 470p.

NANAYAMA, F. AND K. SHIGENO (2006), Inflow and outflow facies from the 1993 tsunami in southwest Hokkaido, Sedimentary Geology, 187,139-158.

NARAYANA, A.C., TATAVARTI, R., SHINU, N., AND A. SUBEER (2007), Tsunami of December 26, 2004 on the southwest coast of India: Post-tsunami geomorphic and sediment characteristics, Marine Geology, 242, 155-168.

NEWTON, R.S., SEIBOLD, E., AND F. WERNER (1973), Facies distribution patterns on the Spanish Sahara continental shelf mapped with side scan sonar. Meteor Forschungsergebnisse, C15, 55-77. Berlin.

NIEDERMEYER, R.-O., LAMPE, R., JAHNKE, W., SCHWARZER, K., DUPHORN, K., KLIEWE, H. AND F. WERNER (2011), Die deutsche Ostseeküste, 2. völlig neu bearbeitete Auflage, 370 p. (in print)

NITTROUER, C.A., AUSTIN, J.A. JR, FIELD, M.E., KRAVITZ, J.H., SYVITSKI, J.P.M. AND P.L. WIBERG (2007), Writing a Rosetta stone: insights into continental-margin sedimentary processes and data. In: Nittrouer, C.A. et al. (eds.): Continental Margin Sedimentation: from sediment transport to sequence stratigraphy. Special publication number 37 of the International Association of Sedimentologists.

NODA, A., KATAYAMA, H., SAGAYAMA, T., SUGA, K., UCHIDA, Y., SATAKE, K., ABE, K. AND Y. OKAMURA (2007), Evaluation of tsunami impacts on shallow marine sediments: An example from the tsunami caused by the 2003 Tokachi-oki earthquake, northern Japan, Sedimentary Geology, 200, 314–327.

NOVAK, B. AND S. BJÖRCK (2002), Late Pleistocene-early Holocene fluvial facies and depositional processes in the Fehmarn Belt, between Germany and Denmark, revealed by high-resolution seismic and lithofacies analysis. Sedimentology, 49, 451-465.

NOVAK, B. AND S. BJÖRCK (2004), A Late Pleistocene lacustrine transgression in the Fehmarn Belt, southwestern Baltic Sea. International Journal of Earth Sciences, 93(4), 634-644.

PÄLIKE, H., N.J. SHACKLETON AND U. RÖHL (2001), Astronomical forcing in Late Eocene marine sediments. Earth Planet. Sci. Lett. 193, 589–602.

PALINKAS, C.M., NITTROUER, C.A. AND J.P. WALSH (2006), Inner-Shelf Sedimentation in the Gulf of Papua, New Guinea: A Mud-Rich Shallow Shelf Setting, Journal of Coastal Research, 22(4), 760-772.

PARIS, R., FOURNIER, J., POIZOT, E., ETIENNE, S., MORIN, J., LAVIGNE, F., AND P. WASSMER (2010), Boulder and fine sediment transport and deposition by the 2004 tsunami in Lhok Nga (western Banda Aceh, Sumatra, Indonesia): A coupled offshore-onshore model, Marine Geology, 268, 43–54.

PHANTUWONGRAJ, S. AND M. CHOOWONG (2011), Tsunamis versus storm deposits from Thailand. Nat. Hatards. doi: 10.1007/s11069-011-9717-8.

PONGPIACHAN, S., KLYSUBUN, W., THUMANU, K., KOSITANONT, C., FELDENS, P., SCHWARZER, K., PRIETZEL, J., HO, K.F. AND J. CAO, Parameters influencing analytical reliability of sulfur speciations in environmental samples using sulfur k-edge x-ray absorption near-edge structure (XANES). Analytica Chemica Acta, submitted.

RAZZHIGAEVA N.G., GANZEI L.A., GREBENNIKOVA T.A., IVANOVA E.D. AND V.M. KAISTRENKO (2006), Sedimentation particularities during the tsunami of December 26, 2004, in northern Indonesia: Simelue Island and the Medan coast of Sumatra Island. Oceanology 46, 875, 2006.

ROSETTI D.D.F., GOLES A.M., TRUCKENBRODT W. AND J. ANAISSE JR (2000), Tsunami-induced large scale scour-and-fill structures in Late Albian to Cenomanian deposits of the Grajau Basin, northern Brazil. Sedimentology 47, 309-323.

RÖßLER, D. (2006), Reconstruction of the Littorina Transgression in the Western Baltic Sea. Marine Science Reports 67, 1-111.

SAKUNA, D., SZCZUCIŃSKI, W., FELDENS, P., SCHWARZER, K. AND S. KHOKIATTIWONG, Sedimentary deposits left by the 2004 Indian Ocean tsunami offshore Khao Lak, Andaman Sea (Thailand), Earth Planets Space, submitted.

SANFILIPPO, R., ROSSO, A., BASSO, A., VIOLANTI, D., DI GERONIMO, I., DI GERONIMO, R., BENZONI, F. AND E. ROBBA (2010), Cobbles colonization pattern from a tsunami-affected coastal area (SW Thailand, Andaman Sea), Facies, DOI:10.1007/s10347-010-0226-0.

SAWAI, Y., K. JANKAEW, M.E. MARTIN, A. PRENDERGAST, M. CHOOWONG AND T. CHAROENTITIRAT (2009), Diatom assemblages in tsunami deposits associated with the 2004 Indian Ocean tsunami at Phra Thong Island, Thailand, Marine Micropaleontology, 73,70-79.

SCHEFFERS, A. (2008), Tsunami boulder deposits, in Shiki et al. "Tsunamiites - features and implications", 299-317, Elsevier, 425p.

SCHWARZER, K. AND M. DIESING (2003), Erforschung der FFH-Lebensraumtypen Sandbank und Riff in der AWZ der deutschen Nord- und Ostsee. 2. Zwischenbericht.

SCHWARZER K. AND M. DIESING (2006), Erforschung der FFH-Lebensraumtypen Sandbank und Riff in der AWZ der deutschen Nord- und Ostsee. Abschlussbericht.

SCHWARZER, K., GAREL, E. AND M. DIESING (2007), Fortführung der geowissenschaftlichen Erforschung der FFH-Lebensraumtypen Sandbank und Riff in der AWZ der deutschen Nord- und Ostsee. Abschlussbericht.

SCULLY, M.E., FRIEDRICHS, C.T. AND L.D. WRIGHT (2002), Application of an analytical model of critically stratified gravity-driven sediment transport and deposition to observations from the Eel River continental shelf, northern California, Continental Shelf Research, 22, 1951-1974.

SEIFERT, T., TAUBER, F. AND B. KAYER (2001), A high resolution spherical grid topography oft he Baltic Sea – 2nd edition. Baltic Sea Science Congress, Stockholm

SHANMUGAM, G. (2011), Process-sedimentological challenges in distinguishing paleo-tsunami. Nat. Hazards. doi: 10.1007/s11069-011-9766-z

SHI, S. AND D.E. SMITH (2003), Coastal tsunami geomorphological impacts and sedimentation processes: Case studies of modern and prehistorical events, International conference on Estuaries and Coasts, Hangzhou, China November 9-11.

SHIKI, T., TSUJI, Y., YAMAZAKI, T., AND T.K. MINOURA (2008), Tsunamiites - Features and implications, Elsevier, 425pp.

SIRIPONG, A. (2006), Andaman Seacoast of Thailand Filed Survey after the December 2004 Indian Ocean Tsunami, Earthquake Spectra, 22, 187-202.

SOMMERFIELD, C.K. AND R.A. WHEATCROFT (2007), Late Holocene sediment accumulation on the Northern California Shelf: Oceanic, fluvial and anthropogenic influences, GSA Bulletin, 119(9-10), 1120-1134.

STACKEBRANDT, W. (2009), Subglacial channels of Northern Germany – a brief review. Z. dt. Ges. Geowiss., 160(3), 203-210.

STEPHAN, H-J. (2001), The Young Baltic Ice advance in the western Baltic depression. Geological Quarterly 45(4), 359-363.

SUGAWARA, D., MINOURA, K., NEMOTO, N., TSUKAWAKI, S., GOTO, K., AND F. IMAMURA (2009), Foraminiferal evidence of submarine transport and deposition by backwash during the 2004 Indian Ocean tsunami, Island Arc, 18, 513–525.

SUWANWERAKAMTORN, R, PAIJITPRAPAPORN, A., DOWNRESANG, D. AND P. SUWANASING (1990), Sediment dispersion from offshore Tin dredging along Andaman Sea coast using satellite data, Proc. Asian Association of Remote Sensing (ACRS).

SWIFT, D.J.P., G. PARKER, N.W. LANFREDI, G. PERILLO AND K. FIGGE (1978), Shoreface-connected Sand Ridges on American and European Shelves: A Comparison. Estuarine and Coastal Marine Science, 7, 257–271.

SYNOLAKIS, C.E. AND L. KONG (2006), Runup measurements of the December 2004 Indian Ocean Tsuanmi. In: Earthquake Spectra, 22(S3), 67–91.

SYVITSKI, J.P.M., PRATSON, L.F., WIBERG, P.L., STECKLER, M.S., GARCIA, M.H., GEYER, W.R., HARRIS, C.K., HUTTON, E.W.H., IMRAN, J., LEE, H.J., MOREHEAD, M.D. AND G. PARKER (2007), Prediction of margin stratigraphy. In: Nittrouer, C.A. et al. (eds.): Continental Margin Sedimentation: from sediment transport to sequence stratigraphy. Special publication number 37 of the International Association of Sedimentologists.

SZCZUCIŃSKI W., NIEDZIELSKI P., RACHLEWICZ G., SOBCZYŃSKI T., ZIOŁA A., KOWALSKI A., LORENC S. AND J. SIEPAK (2005), Contamination of tsunami sediments in a coastal zone inundated by the 26 December 2004 tsunami in Thailand. Environ. Geol. 49, 321.

SZCZUCIŃSKI, W., CHAIMANEE, N., NIEDZIELSKI, P., RACHLEWICZ, G., SAISUTTICHAI, D., TEPSUWAN, T., LORENC, S. AND J. SIEPAK (2006), Environmental and Geological Impacts of the 26 December 2004 Tsunami in Coastal Zone of Thailand - Overview of Short and Long-Term Effects, Polish J. of Environ. Stud., 15(5), 793-810.

SZCZUCIŃSKI, W., STATTEGGER, K. AND J. SCHOLTEN (2009), Modern sediments and sediment accumulation rates on the narrow shelf off central Vietnam, South China Sea, Geo-Mar Lett, 29, 47-59, 2009.

SZCZUCIŃSKI, W. (2010), Impacts of 2004 Indian Ocean tsunami on mid continental shelf of Andaman Sea, In: The 3rd International Tsunami Field Symposium. Program and abstracts, Sendai, Japan, 10-11 April, 2010, 57-58 pp.

THAMPANYA, U., VERMAAT, J.E., SINSAKUL, S. AND N. PANAPITUKKUL (2006), Coastal erosion and mangrove progradation of Southern Thailand, Estuarine, Coastal and Shelf Science, 68, 75-85.

THANAWOOD, C., YONGCHALERMCHAI, C. AND O. DENSRISEREEKUL (2006), Effects of the december 2004 tsunami and disaster managment in Southern Thailand, Science of Tsunami Hazards, 24(3), 206-217.

TSUJI, Y., NAMEGAYA, Y., MATSUMOTO, H., IWASAKI, S-I., KANBUA, W., SRIWICHAI, M. AND V. MEESUK (2006), The 2004 Indian tsunami in Thailand: Surveyed runup heights and tide gauge records. Earth Planets Space, 58, 223-232.

UCHIDA, J.I., FUJIWARA, O., HASEGAWA, S. AND T. KAMATAKI (2010), Sources and depositional processes of tsunami deposits: Analysis using foraminiferal tests and hydrodynamic verification, Island Arc, 19(3), 427-442.

UMITSU, M., TANAVUD, C. AND B. PATANAKANOG (2007), Effects of landforms on tsunami flow in the plains of Banda Aceh, Indonesia, and Nam Khem, Thailand, Marine Geology, 242, 141-153.

USIRIPRISAN C. CHIEMCHINDARATANA S., SHOOSUWAN S. AND Y. CHATRAPAKPONG (1987), Offshore exploration for tin and heavy minerals in the Andaman Sea. Department of Mineral Resources, Thailand, 224 p.

VAN DE MEENE, J.W.H. AND L.C. VAN RIJN (2000), The shoreface-connected ridges along the central Dutch coast – part 1: field observations. Continental Shelf Research 20, 2295–2323.

VAN DEN BERGH, G.D., BOER, W., DE HAAS, H., VAN WEERING, TH.C.E. AND R. VAN WIJHE (2003), Shallow marine tsunami deposits in Teluk Banten (NW Java, Indonesia), generated by the 1883 Krakatau eruption, Marine Geology, 197, 13–34.

VON POST, L. (1927), Svea älv: Ett Geologiskt naturminne. Sveriges Natur, 7-31.

WALSH, J.P. AND C.A. NITTROUER (2009), Understanding fine-grained river-sediment dispersal on continental margins, Marine Geology, 263, 34-45.

WEISS, R. AND H. BAHLBURG (2006), The Coast of Kenya Field Survey after the December 2004 Indian Ocean Tsunami., Earthquake Spectra 22 (S3), 235–240.

WEISS R. (2008), Sediment grains moved by passing tsunami waves: Tsunami deposits in deep water. Mar. Geol. 250, 251.

WERNER, F., ARNTZ, W. E. AND TAUCHGRUPPE KIEL (1974), Sedimentologie und Ökologie eines ruhenden Riesenrippelfeldes. Meyniana 26, 39-62.

WERNER, F. (2000), New aspects of sand waves (Fehmarn Belt, western Baltic) by using high-resolving sonography. Baltica 13, 85-87

WINN, K., AVERDICK, F.-R., ERLENKEUSER, H. AND F. WERNER (1986), Holocene sea level rise in the western Baltic and the question of isostatic subsidence. Meyniana, 38, 61-80.

WINTER, T.C. AND J.W. LABAUGH (2003), Hydrologic consideration in defining isolated wetlands. Wetlands, 23(3), 532-540.

WITTMAACK, A. (1988), Interngefüge und akustische Unterlage des Riesenrippelfeldes im Fehmarn Belt. Unveröff. Diplomarbeit. Mathematisch-Naturwissenschaftliche Fakultät der Christian-Albrechts-Universität zu Kiel.

WOHLFARTH, B., BJÖRCK, S., FUNDER, S., HOUMARK-NIELSEN, M., INGÓLFSSON, Ó., LUNKKA, J-P., MANGERUD, J., SAARNISTO, M., AND T. VORREN (2008), Quaternary of Norden. Episodes 31(1), 73-81.

WOLANSKI, E. AND SPAGNOL, S. (2000), Environmental degradation by mud in tropical estuaries, Reg. Environ. Change, 1, 152-162.

YAN, Z. AND D. TANG (2009), Changes in suspended sediments associated with 2004 Indian Ocean tsunami, Advances in Space Research, 43(1), 89-95.